Power Systems Knowledge Hub

Department of Electrical Engineering and Computer Science
University of Central Florida
Senior Design 2: Spring 2021
Dr. Samuel Richie
Dr. Lei Wei

Group #19:
Hector Collazo, CpE
Christopher Marks, EE
Ivelisse Rivera, EE
Christy Wilhite, CpE

Sponsor: Florida Power & Light Company (FPL)
Contributors: Dr. Deepal Rodrigo (FPL) and Dr. Wei Sun (UCF)

Table of Contents

List of Figures

List of Tables

1. Executive Summary

The addition of renewable energy sources to the power grid is rapidly increasing by the day. Although this is great for the environment, the grid is becoming increasingly complex to maintain. This is creating the need to develop methods that will enable better monitoring and management of the grid. Providing reliable energy to customers is a top priority for power companies. Increasing situational awareness can help in this endeavor by allowing quicker responses to disturbances. This can aid in the prevention of outages or reduce duration of current outages.

In order to maintain an increasingly complex grid, more engineers that focus on this discipline will be needed. Over the past two decades, there has been a decline in the number of students graduating with degrees that specialize in power systems. In order to attract more engineers to this field, more interactive learning methods about power systems are necessary. This project targets both of these issues. It emphasizes the importance of increasing situational awareness in the distribution grid, as well as promotes interest in power system related engineering education.

This project consists of an interactive touch table where users can learn about the power grid by interacting with a solar panel and with a real-time simulated distribution system. Solar panels are very popular types of renewable energy sources and including one in this project promotes interest in power systems. The users are able to see how the angle change of a solar panel affects its power output which can lead to the variability causing disturbances in the power system.

2. Project Description

In this section, the project will be explained at a high level. The background of WAMS will be discussed. The project's purpose and motivation will be described. The goal and objective of the project will be defined. The engineering and marketing requirements of this project will be listed and justified.

2.1 Background

With increased renewable integration, the grid-of-the-future is becoming increasingly complex to manage. Because of this, better ways to monitor and manage the complexity of the grid are required. On January 11th, 2019, a unit in TECO Energy Inc., or Tampa Electric Company, was vibrating, and it led to frequency oscillations in the entire eastern interconnect as shown in Figure 1. [47] These oscillations lasted for approximately 15 minutes. The event was solved after an operator at TECO noticed the unit's vibrations and decided to shut it off. Florida Power and Light (FPL) knew that there were frequency oscillations, but they did not have enough information to detect the source of the event or its location.

Independent System Operator New England (ISO-NE) knew within seconds that the location of the source of the frequency oscillations was outside their regions and that it was coming from the South. This is because they had WAMS, or Wide Area Management System. With the use of Phasor Measurement Units (PMUs), WAMS increases situational awareness and allows for faster diagnosis of system events. If FPL had WAMS during this event, they would have detected the location of the source of the event within seconds. FPL is currently implementing WAMS into their energy management system at transmission level.

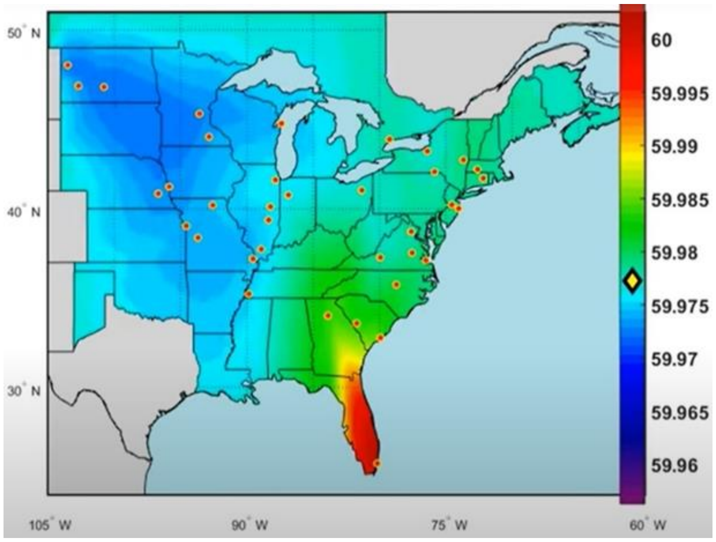

Figure 1: Frequency Oscillations on January 11th, 2019

WAMS was first created by Bonneville Power Administration in the late 80's and was first tested in the Western Interconnection of the North American power system [90]. It continued to be developed throughout the early 90's and in 1995 the US Department of Energy and the Electric Power Research Institute started the Wide Area Management System Project to stabilize and increase reliability in the Western System Dynamic Information Network (WesDINet) [90]. As PMU's became more common throughout power systems, WAMS became more commonly seen in the transmission systems of power companies throughout North America and even globally.

2.2 Motivation

Over the past two decades, the need for engineers who specialize in power systems has increased while the number of graduating engineers with specialized degrees in this area has decreased. This imbalance has affected the industry's ability to recruit engineers needed to maintain our power systems [26]. In addition, it limits the innovation that could be possible with a large pool of fresh graduates from which employers could choose.

This project is designed to promote interest in power systems at the high school and undergraduate levels by educating users on the topic and providing an interactive learning tool where they can see how the distribution system functions. The design will also promote interest in photovoltaic power with a user controlled solar panel. It is important for future engineers to see the importance of traditional grid power as well as renewable energy sources that will become increasingly important in the future.

Another important aspect in the motivation of this project is to improve the reliability of the power grid. In this case, it involves finding ways to the use of the WAMS algorithm at the distribution level. This could result in a significant reduction in the amount of time that users go without power when there is a power outage is at that level. Finding ways to get the power back on for users as quickly as possible when there is a problem is extremely important to power companies such as Florida Light and Power.

2.3 Goal and Objective

With increased penetration of edge-of-the-grid devices, such as solar panels, the distribution system is becoming highly complex to manage. After implementing WAMS into FPL's transmission system, FPL will investigate the possibility of implementing it to their distribution system.

Therefore, the project has two main objectives:

1. Promote interest in power systems related engineering education.
2. Emphasize the importance of increasing situational awareness in the distribution grid.

An easy-to-use interactive touch table was developed to demonstrate and educate students and visitors on power systems. It emphasizes the importance of increasing situational awareness and allows users to have an interactive way of learning about small-scale solar panels. Figure 2 shows the high-level view of the project.

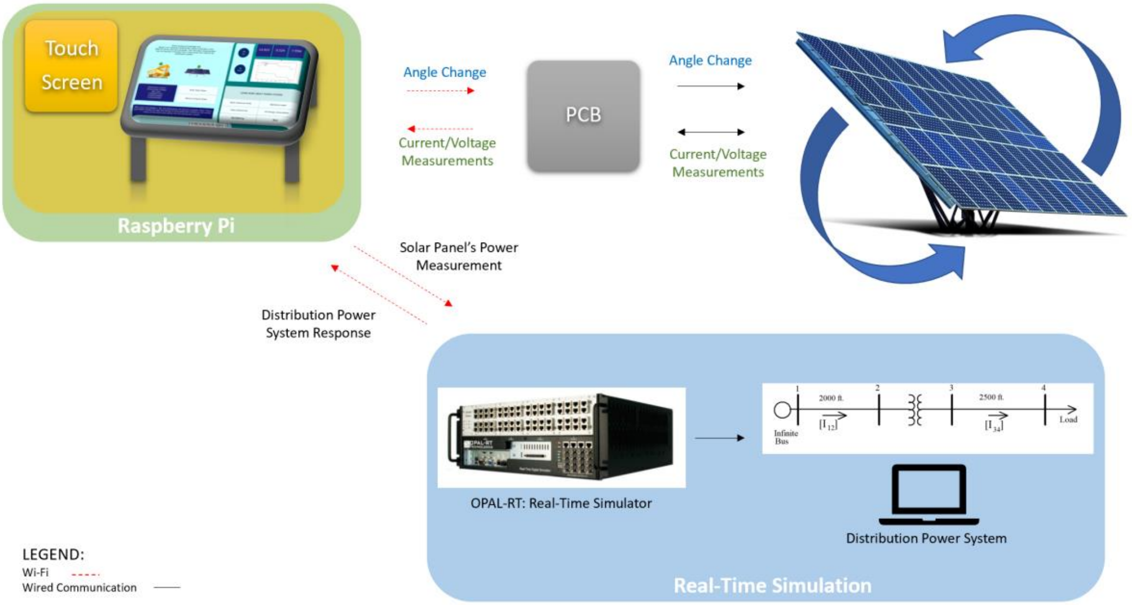
Touch Screen
Raspberry Pi
Angle Change
Current/Voltage Measurements
PCB
Angle Change
Current/Voltage Measurements
Solar Panel's Power Measurement
Distribution Power System Response
1
2000 ft.
2
3
2500 ft.
4
Infinite Bus
[I12]
[I34]
Load
OPAL-RT: Real-Time Simulator
Distribution Power System
Real-Time Simulation
LEGEND:
Wi-Fi
Wired Communication

Figure 2: Project Overview

In order to accomplish the project's objective, the goals shown in Table 1 were set. The goals were classified as basic, advanced, and stretch. We have successfully achieved the advanced goal. The stretch goal should be completed by a future senior design group.

Table 1: Goals Overview

Goal Type	Description
Basic	Interactive touch table that allows users to change the angle of the solar panel and see how that affects its power output. The table will also display educational material about power systems.
Advanced	Interactive touch table displays a simulation of a real-time distribution system with the use of OPAL-RT.
Stretch	User initiates a disturbance in the simulated distribution system and WAMS algorithm analyzes the data and determines the type of disturbance and its location.

2.4 Design Architectures and Related Diagrams

Figure 3 shows the communication architecture of the system, which is composed of five main components. 1) A Raspberry Pi (RBP) was used as the stand-alone MCU to power our graphical user interface (GUI). A touch screen monitor was chosen to provide a more interactive learning experience for the user. 2) The printed circuit board (PCB) was designed and used to measure the power output of the solar panel, send the control signals to change the angle of the solar panel, and communicate wirelessly with the RBP. 3) The PCB sends the control signals to a Stepper Motor Driver, which then 4) makes the stepper motor move. 5) The RBP processes the readings from the PCB and then sends it to OPAL-RT. OPAL-RT is a real-time simulator that was used to simulate a distribution power system.

The power measurements read from the PCB and sent through the RBP are injected into a three-phase bus in the distribution grid. This is done to show the users how the variable output power of the solar panel affects the system. It is important to note that the communication between the RBP, PCB, and OPAL-RT is through Wi-Fi, while the communication between the PCB, Stepper Motor Drive, and the Stepper Motor is wire-based communication.

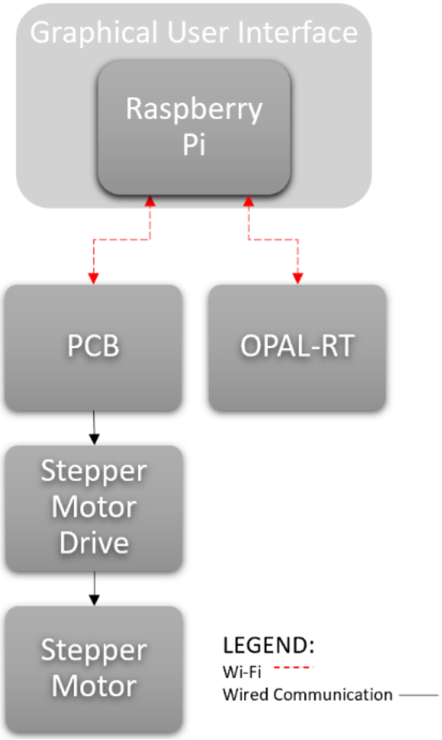

Figure 3: Communication Architecture

Figure 4 shows the system architecture. The gray block represents the PCB. The PCB is composed of a power measurement module, a 100-pin MCU, and a Wi-Fi module. The green block represents the RBP. The yellow block represents the GUI, and the blue box represents the real-time simulator.

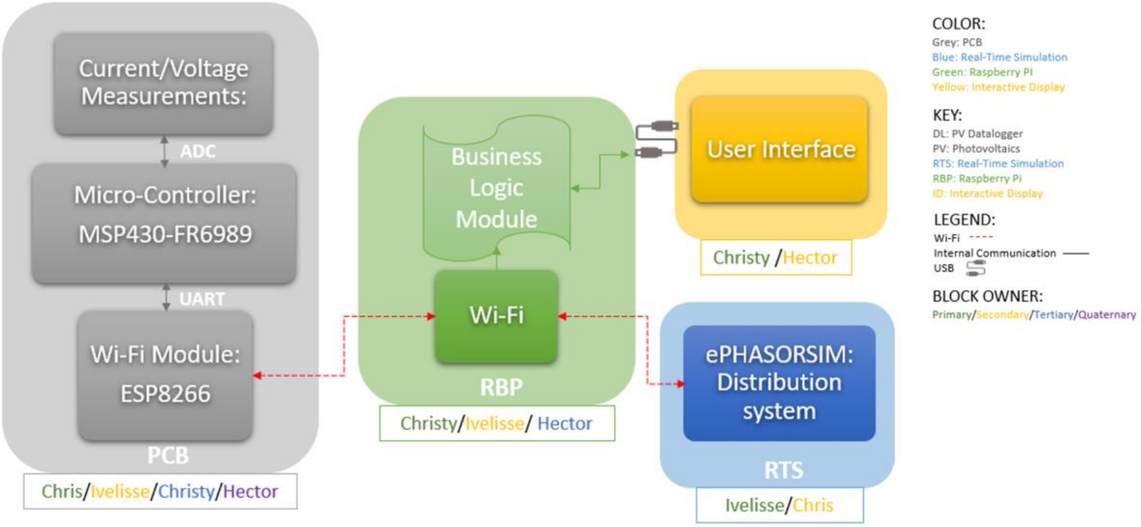

Figure 4: System Architecture

2.5 Raspberry Pi Business Logic Module

The Raspberry Pi (RBP) originally had five main functions that were planned to be implemented in the programming logic. The unit would need to connect with OPAL-RT and exchange data, and it would also to be able to decode IEEEC37.118 data which is used by OPAL-RT. It would need to exchange data with the PCB via a server and/or database. It would need to implement the WAMS algorithm and be able to output the results, and it would need to run the user interface on the touchscreen that will display the output of WAMS and allow the user to interact with the distribution simulation and solar panel as well as access educational material.

Since the stretch goal of implementing the WAMS algorithm was not reached, that function and the ability to decode the IEEEC37.118 data were not implemented in the final design. Figure 5 shows the current business logic module that has been implemented.

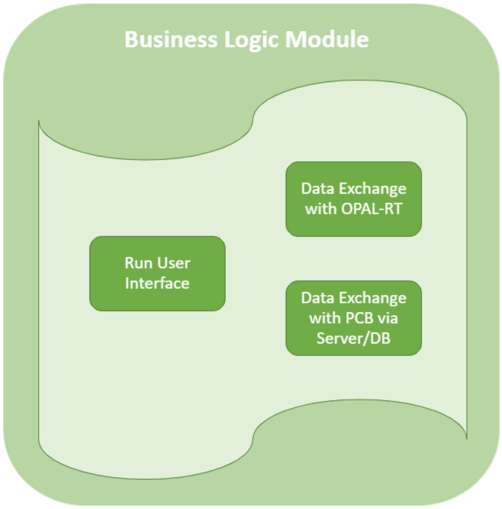
Business Logic Module
Data Exchange with OPAL-RT
Run User Interface
Data Exchange with PCB via Server/DB

Figure 5: Business Logic Module

2.6 Requirements and Specifications

Table 2 shows the engineering requirements and specifications and Table 3 shows marketing requirements that our system must satisfy to be successful and to satisfy FPL's needs. In addition, the table specifies which requirements will be demonstrated to the review panel.

Table 2: Requirements and Specifications

Marketing Requirements	Engineering Requirements	Justification	Review Panel Demo
6	1. PCB should be able to support 0- to 18-V input from the solar panel.	Since the solar panel will be connected to the solar panel, it should be able to handle voltages of up to 18 V.	✓
3, 4, 9	2. The touchscreen should be multitouch enabled. Total number of multitouch points should be at least 2. It should also support common gesture functions found on smart phones or tablets.	Multitouch touchscreen of at least two points and above is very popular and has an increasing market share because they offer excellent user experience	
8, 9	3. Solar panel capable of generating maximum power output of 100 W and at least 12 V output	Compact design/lightweight for easier motor movement, mounting, and solar tracking	
9	4. 3-phase 60 Hz power system model with at least 4 buses.	Power Systems in the United States supply 3-phase electricity and operates at 60 Hz.	
1, 4, 7	5. PCB should have wireless functionality. It should be able to connect to UCF's 2.4 GHz network.	In order to communicate with OPAL-RT, which is connected to UCF's network, the PCB should be able to connect to UCF's WPA2 Enterprise.	✓
1, 2	6. Stand-alone Micro-Controller Unit (MCU) with advanced processing capabilities to connect to the touch table.	The MCU must support the needed Linux based Operating System (OS) capable of connecting with OPAL-RT and processing real-time and simulation data. The OS must be able to support the user interface and accompanying graphics.	

Marketing Requirements	Engineering Requirements	Justification	Review Panel Demo
6, 11	7. Device capable of producing torque to move a solar panel weighing about 20 kg.	Solar panel generating 100 W at 12 V weigh around 16-20 kg.	
6	8. PCB should be able to support up to 6 A input from the solar panel.	Since the solar panel will be connected to the solar panel, it should be able to handle currents up to 6 A.	
1	9. The PCB should include status indicator light to indicate that the system is on and receiving/transmitting data	Visual status indicator on PCB allows for easier debugging.	
6	10. Current and voltage measurement accuracy should have less than 5% error.	In order to accurately show how the angle change of the solar panel affects its power output.	
1, 4, 6, 9	11. Angle change response time should be less 12 seconds.	Users expect a fast response time when making change to the system.	✓
1, 7, 9	12. Ability to transfer solar panel measurement data over Wi-Fi and display them on monitor at most 5 seconds.	Users expect accurate measurements in near real-time.	

Table 3: Marketing Requirements

Marketing Requirements
1. The system should process real-time data
2. The system should be able to process big data
3. The display should have multi-touch capabilities
4. The display should respond to user’s command quickly
5. The User Interface should be easy to use
6. The system should include solar panel and supported components
7. The system should be able to communicate wirelessly using 802.11a/b/c/n/ac standard [50]
8. The system should be low cost
9. The system should educate users about power system topics in an interactive learning style

2.7 House of Quality

The house of quality (HOQ) developed from Tables 2 and 3 is shown in Figure 6. The marketing requirements are represented in the row headings and the engineering requirements in the column headings.

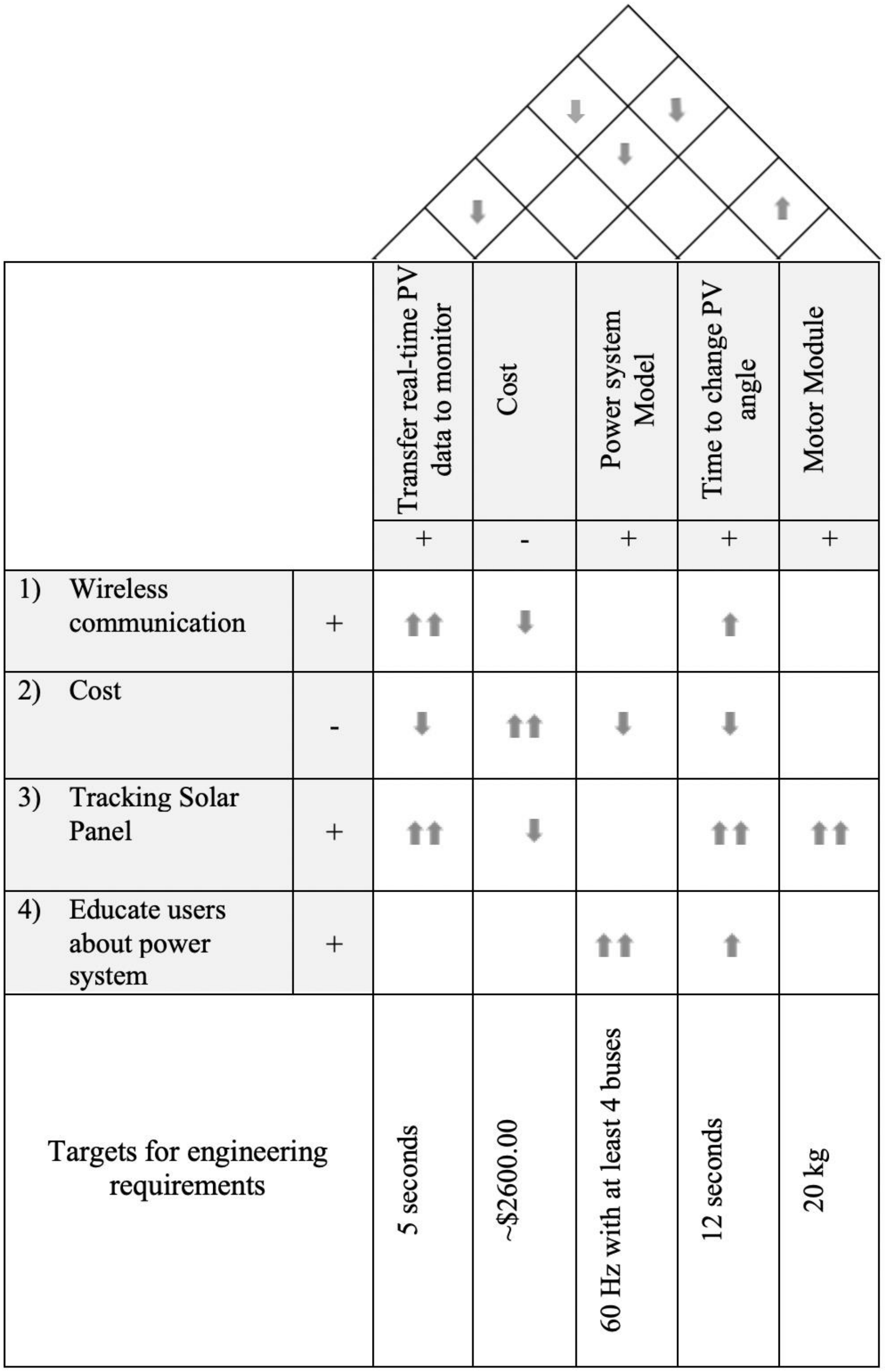

		Transfer real-time PV data to monitor	Cost	Power system Model	Time to change PV angle	Motor Module
		+	-	+	+	+
1) Wireless communication	+	⬆⬆	⬇		⬆	
2) Cost	-	⬇	⬆⬆	⬇	⬇	
3) Tracking Solar Panel	+	⬆⬆	⬇		⬆⬆	⬆⬆
4) Educate users about power system	+			⬆⬆	⬆	
Targets for engineering requirements		5 seconds	~$2600.00	60 Hz with at least 4 buses	12 seconds	20 kg

Figure 6: Engineering and Marketing Requirements HOQ

3. Research Related to Project

This section is composed of background information about specific technologies that were either used or considered to be used for the project. Comparison between such technologies is done in this section to aid in the selection process. This section also specifies which technology was chosen for the project.

3.1 Decision Matrix

Table 4 is a decision matrix for various features of the project. The matrix provides the pros and cons for these options to assist in deciding how we will implement the features mentioned in the table.

Table 4: Options Matrix

Option	Pros	Cons
Build our own distribution model	1. Experience gained	1. Extra work 2. Not tested
Use an existing distribution model	1. Tested and approved model by IEEE	
Buy a battery	1. Store energy produced from solar panels	1. Additional Cost
Buy a touch screen monitor	1. Small amount of testing needed 2. Easy setup 3. Cheaper option	1. Specific sizes make variant price points
Build our own touch screen monitor	1. Built to our specifications and needs	1. Extra work

3.2 Relevant Technologies and Part Selection

This section details the research into technologies that are relevant to this project and how the parts were compared and then selected for use.

3.2.1 Touch Table

A touch-screen table is used to display an interactive user interface that allows the user to change the angle of the solar panel and see the resulting changes in power output as well as see how injecting solar energy into a distribution system simulation affects it.

3.2.1.1 Touch Screen

Cost constraints prohibited using a premade touch table for this project, so a touch screen display was used with a table frame to house it. Constructing the touch table in this manner yielded a cost savings of over $1,500 for the project. Table 5 contains the decision matrix which led to the choice to make a touch table rather than buy a premade one [76].

Table 5: Pre-made vs building touch table frame

	Advantages	Disadvantages
Pre-made Touch Table	• Less work • Guaranteed to have appropriate dimensions • Some models can accommodate screen angle changes	• Very high cost (>$3100) • Few models available
Build a frame to hold purchased touch screen display	• **Lower cost** • **More control over table parameters**	• **Requires mechanical and carpentry knowledge** • **More work**

A set of criteria was developed to select the touch screen monitor. The display should support multi-touch functions of at least two touch points such as commonly found on smartphones and tablets. The display should also use HDMI or USB connections to connect to the stand alone micro-controller unit (MCU) and be large enough to accommodate a minimum of four people gathering around it at a time. For this reason, the display should be at least 43 inch which would have dimensions of approximately 26” H x 38” W (66.04cm H x 96.52cm W) and is also a common size for monitors. The screen resolution should be at least 780 x 1080.

Cost research and analysis on available touch screens revealed that 43 inch and larger screens cost over $1,800 with one exception which is a 55 inch Phillips 55BDL4051T touch monitor for $1,678 available from www.fullcompass.com with free shipping [32]. This monitor was selected and used since it satisfied the project requirements and was the most cost-effective solution. This monitor is a 10-point infrared multi-touch display with 1920 x 1080 resolution at 60 Hz and built-in speakers. It has a typical touch response time of 12ms and uses an HDMI connection to a computer as well as a USB connection to support the touch capabilities. This display contains its own Quad Core Cortex A9 1.8GHz CPU and an ARM Mali400 Quad Core 533 MHz GPU. It has 2GB of DDR3 memory and 16GB of storage [23].

Table 6 shows the comparison between the Phillips display that was selected, a 49inch Samsung display [73], a 49 inch LG display [74], and a 43 inch LG display [75].

Table 6: Touch Screen Comparison

	Phillips 55BDL4051T	Samsung PM49H	LG 49TA3E-B TA3E Series	LG 43TA3E-B TA3E Series
Price	$1,678.00 (no shipping or taxes are being applied)	$2,387.23 ($2,251.00 + $136.23 shipping)	$1,910.71 ($1,740.00 + $45.71 shipping + $125.00 tax)	$1,806.15 (1,508.00 + $179.99 shipping + $118.16 tax)
Diagonal Size	55 inch	49 inch	49 inch	43 inch
Dimensions	(1271.0 x 741.7 x 91.4) mm (50.04 x 29.20 x 3.60) in	(1096.9 x 629.1 x 30.5) mm (43.2 x 24.8 x 1.2) in	(1,142.2 x 672.4 x 71.4) mm (45 x 26.5 x 2.8) in	(1,009.6 x 597.8 x 71.4) mm (39.7 x 23.5 x 2.8) in
Screen Type	Not specified	HD LED BLU	FHD IPS (In-Plane Switching, a type of LED)	FHD IPS (In-Plane Switching, a type of LED)
I/O Connections	DP 1.2, USB, HDMI(2), DVI-D, VGA	HDMI 2.0(2), HDCP 2.2, USB 2.0(2)	HDMI (2), DVI-D, USB 3.0	HDMI (2), DVI-D, USB 3.0
Response Time	12ms	8ms	12ms	12ms
Processor	CPU: Quad Core Cortex A9 1.8GHz GPU: ARM Mali400 Quad Core 533 MHz	CPU: Quad Core Cortex-A12 1.3GHz	Not specified	Not specified
OS/OS compatibility	Android OS	Tizen 2.4 OS (VDLinux)	Windows 7/8/8.1/10, Mac OS X, Android, Linux	Windows 7/8/8.1/10, Mac OS X, Android, Linux
Memory	2GB DDR3	2.5GB DDR3-933	8 GB	8 GB
Storage	16GB	8GB (3.75GB Occupied by O/S, 4.25GB Available)	not specified	not specified
Weight	18.0 kg 39.68 lbs	13.17 kg 29.04 lbs	22.3 kg 49.2 lbs	17.1 kg 37.7 lbs
Power Consumption	76 W/h	47 W/h	60W/h	55W/h

3.2.1.2 Touch Table Frame

The table frame was designed to hold the touch screen parallel to the ground so that the users can gather around it from all sides. The dimensions of the Phillips display are 50.04W x 29.20H x 3.60D inches (127.10W x 74.17H x 9.14D cm) with a weight of 39.68lbs (18kg). The table frame was built out pressure treated lumber and can support over 500lbs which easily allows for the weight of the display plus any people that may casually lean on it during use. The frame provides an extra 2-4 inches (5.08-10.16 cm) of wood around the dimensions of the display and it has casters on the bottom of the legs which raise the table to 34 inches (86.36 cm) tall. The casters assist in moving the table with ease. The frame was painted in heavy-duty paint, and the blue color is a acknowledgement to our sponsor, Next Era Energy.

3.2.2 Connection to Real-Time Distribution System

In order to demonstrate the importance of increasing situational awareness most accurately in distribution systems, the connection to a power grid is needed. This way, users will better understand how actual distribution systems behave and the importance of monitoring the grid with fast and reliable methods. Currently, FPL is successfully receiving and analyzing real-time synchrophasor PMU data from the transmission grid. FPL’s next step is to implement the same methods to distribution grids. To do this, microPMUs are needed in the distribution grid to receive and analyze real-time synchrophasor data at consumer voltage level.

MicroPMUs offer higher precision than PMUs. As mentioned in the *Micro-phasor Measurement Units (µPMUs) and Its Applications in Smart Distribution Systems* paper, “Conventional PMUs in use for the transmission system have ±1° accuracy, and PMU has 0.01°.” [1] A request to connect to FPL’s microPMUs was denied because they do not have them available yet. When FPL’s microPMUs become available for connection, they will be used, but for now, other methods to connect to a real-time system that sends synchrophasor measurements from the distribution systems will be considered. All while using the protocols and standards needed for a smooth transition to FPL’s microPMUs.

3.2.2.1 OPAL-RT Real-Time Simulators

OPAL-RT TECHNOLOGIES Inc offers real-time simulation technology to allow engineers and researchers “…make their innovative ideas a reality.” [2] They are the world leader in real-time simulation testing equipment not only for power electronic systems, but for electro-mechanical systems as well. Their technology has been used in multiple successful projects. For example, the US Department of Energy Energise Project titled “Scalable/Secure Cooperative Algorithms and Framework for Extremely-high Penetration Solar Integration (SolarExPert)” used OPAL-RT’s technology. [3] University of Central Florida (UCF) was a team member of this successful project, alongside National Renewable Energy Laboratory (NREL), Hawai‘i Natural Energy Institute (HNEI), Siemens, General Electric (GE), Duke, and OPAL-RT.

3.2.2.1.1 OP5600

For the reasons mentioned above, it was decided to investigate OPAL-RT’s technology as an optimal solution for the given constraints. More specifically, OP5600 real-time digital simulator, was highly considered due to it being available for use. This simulator is located at UCF’s Harris Corporation Engineering Center (HEC) in Siemens Digital Grid Laboratory. It is important to note that our advisor Dr. Wei Sun, is the laboratory director of Siemens Digital Grid Laboratory which enables the team to have access to it. OP5600 simulator is shown in Figure 7 and its highlights listed below. [4] Table 7 shows general specifications of OP5600 simulator.

OP5600 Product Highlights:

- Powerful real-time target with up to 32 INTEL processor cores @3.0 GHz
- Real-time operating system: Linux REDHAT
- Xilinx SPARTAN-3 or VIRTEX-6 FPGA
- Up to 8 I/O boards
- 128 analog I/O or 256 digital I/O or a mix of both
- Rear DB37 connectors
- Front I/O monitoring (access to all I/Os)
- Up to 4 PCI slots
- Support for third-party I/Os
- Extensive communication protocol support
- IEEE C37.118, IEC61850, DNP3, CAN Bus, ARINC-429 and more

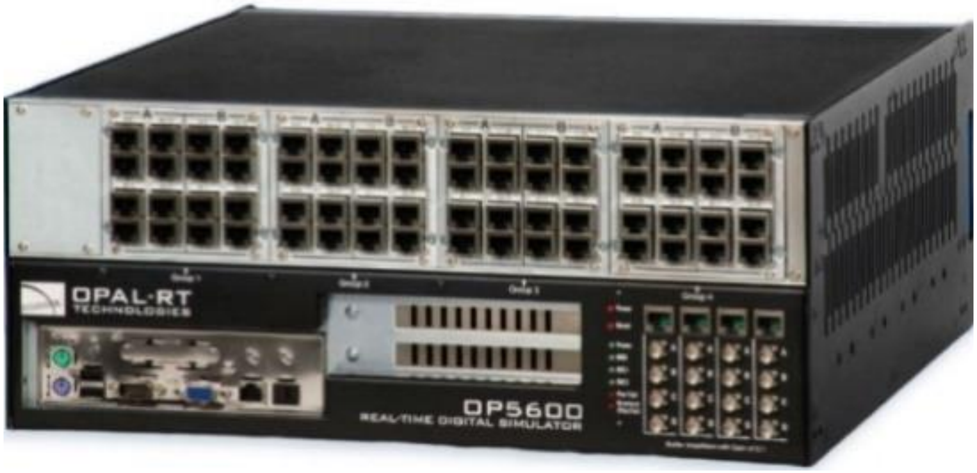

Figure 7: OP5600 Real-Time Simulator

Table 7: OP5600 Real-Time Simulator Specifications

General Specifications	
Price	~ $27,000.00
CPU	OP5650V3-8 : 8 Cores, 3.2 GHz
FPGA	Xilinx® Artix®-7 FPGA, 200T
Software Compatibility	RT-LAB and HYPERSIM suites
High speed communications	4x SFP socket, 1 to 5Gbps, duplex multi-mode optical fiber (50/125 or 65/125µm), Xilinx Aurora compatible Up to 5 PCI or PCIe interface cards
Performance	Up to 120 3-phase buses by core on 3.2 GHz CPU
Dimensions (HxWxD) & weight	17.8 x 47.7 x 49.3 cm (7'' x 18.8" x 19.4") Simulator: 9.07 - 15 Kg (20 lbs to 33 lbs) Expansion chassis: 4.54 - 5.9 Kg (10 lbs to 13 lbs)

It is important to note that OPAL-RT supports IEEEC37.118 protocol. This is important because this is the protocol used for synchrophasor measurements for power systems. This standard is used by FPL. This enables the possibility to send actual phasor measurement data from FPL's microPMUs to a model in OPAL-RT.

3.2.2.1.2 OP5700

OP5700 real-time digital simulator was also considered. This simulator is located at Research Building 1 at UCF. OP5700 is shown in Figure 8 and its highlights are listed below [6]. Table 8 shows the general specifications of OP5700 [6].

OP5700 Product Highlights:

- ATX motherboard
- Linux-based real-time operating system
- Intel Xeon E5 CPU with 4, 8, 16 and 32 processor cores, up to 3.2GHz. See Configuration Options below.
- 10MB Cache Memory per 4 cores
- up to 32GB of DRAM
- 512GB SSD disk
- 6 PCIe slots used to connect the internal FPGA board and PCIe or PCI third-party I/O and communication cards

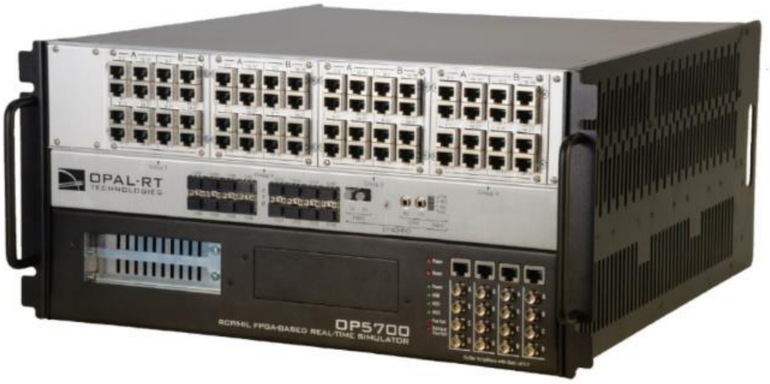

Figure 8: OP5700 Real-Time Simul

Table 8: OP5700 Real-Time Simulator Specifications

General Specifications	
Price	~ $70,000.00
CPU	Intel Xeon E5, 4 core / 3GHz to 32 cores / 2.3GHz
FPGA	Xilinx Virtex 7 FPGA on VC707 board, 485T, 485 760 Logic cells, 2 800 DSP slices
High speed communications	16 SFP sockets, up to 5GBps
Dimensions (HxWxD) & weight	22.27 x 47.7 x 49.3cm (8.75’’ x 18.8” x 19.4”) HxWxD

3.2.2.1.3 OPAL-RT Real-Time Simulator Selection

Table 9 summarizes the key points that were compared when choosing which one to use. It is important to note that UCF had granted permission for our team to use this free of cost. Therefore, the biggest factor that led to our decision was its availability. Both simulators are being used for research purposes. Therefore, choosing one that was being used less was important. Another important aspect was that the simulator had the capability of sending IEEE C37.118 streams, and OP600 can do this. For these reasons, OP5600 was chosen.

Table 9: OPAL-RT Technology Comparison

Components	OP5600	OP5700
Availability	Available	Being used for multiple research projects
Price	~ $27,000.00	~ $70,000.00
CPU	OP5650V3-8: 8 Cores, 3.2 GHz	Intel Xeon E5, 4 core / 3GHz to 32 cores / 2.3GHz

3.2.2.2 Simulation of Power Systems Method Selection

As previously mentioned, OPAL-RT TECHNOLOGIES Inc is the world leader in real-time simulation testing equipment for power electronic systems. [2] They offer multiple methods to simulate power systems. When choosing which to use, two things were considered. First, the model size, or number of nodes present in the system and second, the period (frequency) of simulated transient phenomena. The three methods offered by OPAL-RT are ePHASORSIM, eMEGASIM, and eFPGASIM. These are summarized below, in Table 10. [7]

Table 10: Different Methods to Model Power Systems

RT-LAB		
eMEGASIM	ePHASORSIM	eFPGASIM
EMT real-time simulation. Typical time step of 50 μs. Model running on CPU cores.	Phasor real-time simulation for transient stability studies. Typical time step of 10 ms. Model running on CPU cores.	EMT real-time simulation. Typical time step of 500 ns. Model running no FPGA.

One of the goals of this project is to be able to visualize how the increase of integration of renewable energy sources into distribution systems makes it more complex to operate, monitor, and control. In order to study this, it is required to simulate a distribution grid at a sub-second timestep in phasor domain mode. For this reason, ePHASORSIM was chosen. ePHASORSIM offers the ability to simulate, test, and maintain networks at a minimum sub-second time-step of 10ms. [8] This is acceptable because in order to match current mircoPMUs data rates in power systems, a time-step of at least 33.33ms, or 30 Hz, is needed. Another important consideration as to why to use ePHASORSIM is because it is available to use with UCF's OP5600.

All the methods shown in Table 10 are MATLAB/Simulink toolboxes used by RT-LAB. ePHASORSIM is one Solver block in MATLAB/Simulink. As shown in Table 7, OP5600 simulator offers software compatibility with RT-LAB. RT-LAB provides tools for running and monitoring real-time simulations. An open architecture enables RT-LAB to easily work with MATLAB/Simulink, which allows the use of ePHASORSIM. MATLAB, or MATrix LABoratory, "…combines a desktop environment tuned for iterative analysis and design processes with a programming language that expresses matrix and array mathematics directly." [5] Simulink is a block diagram environment for multidomain simulation and Model-Based Design that is integrated with MATLAB. [6]

3.2.2.2.1 EPHASORSIM in Simulink

One of the functions that the distribution table will offer is to display a distribution system that runs real-time. This is to allow users to interact with a distribution system by applying disturbances and monitoring the grid. This is the system that WAMS algorithm will use to analyze and produce the desired results. Therefore, the use of a distribution power system model that runs real-time is required. EPHASORSIM offers the ability to simulate power systems in real time.

As previously mentioned, ePHASORSIM is one Solver block in MATLAB/Simulink. It is in the Simulink Library Browser. It can run three-types of power grid input file formats: Excel, PSS/e Ver. 32, Cyme Ver. 7.x, and Power Factory. The user selects the type of file format that they will input to the solver block. Therefore, before using ePHASORSIM, the model needs to be already formatted in one of the compatible formats listed. The ePHASORSIM block requires an excel file that defines the inputs and output pins of the block. For example, if the user wants to see the voltage magnitude and angle of a certain bus, it must be defined in the excel sheet. Another example would be that the user wants to inject current into a certain bus. This would also need to be defined in the excel sheet. RT-LAB user guide documentation provides documentation on the Excel sheet format that should be followed.

EPHASORSIM block offers both the Power-flow calculation and the Dynamic simulation. The required solution is defined in ePHASORSIM solver block. If both the Power-Flow calculation and the Dynamic simulation is selected, the Power-flow calculation is always performed before the start of the dynamic simulation. Meaning that it will only run the base case of the model. Power-flow calculation functionality in ePHASORSIM solver block is a good tool when it is desired to check the initial state of the system or/and check if the results match with where the original model was modeled at. For example, if the model was initially modeled and run in PSS/e, power-flow calculation can be performed on both and then compared with each to ensure that all the values of the system are correct. Power-flow calculation in ePHASORSIM offers three initialization options: From input data, Smart Start and Flat Start. User can also set the power mismatch termination condition, and the max number of Newton Raphson iterations.

As mentioned previously, ePHASORSIM can run the dynamic simulation as well. The model time-step of the simulation needs to be defined here. This is important in respect to our project because we want our model to run real-time and produce Phasor Measurement Data at a rate of 30 Hz. Therefore, the system must have a time-step less than or equal to 33ms. This time step is allowed in ePHASORSIM.

3.2.2.3 Balanced VS Unbalanced Distribution Power System Selection

There are two types of three-phase power systems, balanced and unbalanced. In this section, we will investigate both and select which one is the best fit to our project. Table 11 summarizes the main differences between a balanced system and an unbalanced system.

The voltage and current output from the solar panel will be injected to the three-phase power distribution system modeled in ePHASORSIM. Because of this, the single-phase voltage and current output from the inverter should be converted to three-phase. This can be done by developing a simple algorithm in Simulink as shown in Figure 9 below.

Table 11: Balanced VS Unbalanced Power System [5]

Balanced	Unbalanced
Load is equally distributed in all three-phases	Load is un-equally distributed per phase
Voltage magnitude is the same in all three-phases and separated by 120°	Voltage Magnitude is different in each phase

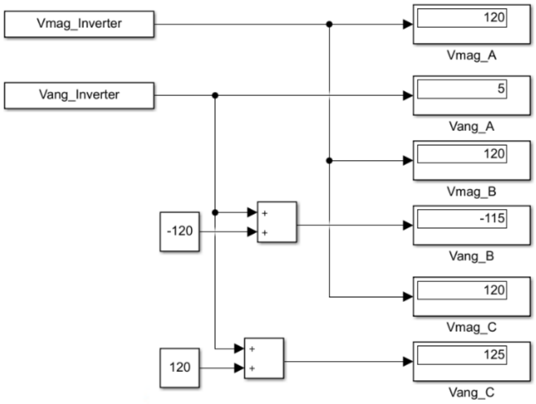

Figure 9: Three-phase algorithm

In this algorithm, the voltage magnitude received from the solar panel was kept the same for all three phases, and all the angles were separated by 120°. It is important to note that Phase B was set to lag Phase A by 120, and Phase C was set to lead Phase A by 120. This order was chosen because this is what FPL follows. The values converted will then be inputed to the three-phase bus in the ePHASORSIM model. Taking this into consideration, it is clear to see that a three-phase balanced distribution power system is needed.

3.2.2.4 IEEE Distribution Test Feeders Selection

As previously mentioned, ePHASORSIM will be used to run the models in real-time but it requires a model that has been developed in one of the compatible file formats listed in the previous section. This section investigates available models.

IEEE Distribution Test Feeders are developed for use by researchers. As mentioned in the *Analytic Considerations and Design Basis for The IEEE Distribution Test Feeders* journal article, “The purpose of these test feeders is to provide models of distribution systems that reflect the wide diversity in design and their various analytic challenges” [67]. The purpose of these test feeders is to provide a common set of data that could be tested by various purpose developers and check the correctness of the results [68]. These distribution test feeders were carefully developed and are used by many researchers. Therefore, rather than modeling our own distribution system, it was decided to use an already developed distribution system from IEEE.

Two IEEE distribution test feeders were considered, IEEE 4 and IEEE 123. Figure 10 shows the one-line diagram of IEEE 123 and Figure 11 shows the one line diagram of IEEE

4-bus system. Please, refer to Table 12 below to see the key difference of these power systems. For WAMS algorithm to work, the system should have at-least two-buses, and both systems meet this criterion. The system should also have a load, to demonstrate how a big change in demand affects the system and both systems also meet this criterion. Another important criterion is that they are available to be modeled in OPAL-RT with the use of ePHASORSIM solver block, and they both are.

The *Analytic Considerations and Design Basis for The IEEE Distribution Test Feeders* journal article provides guidance in which feeders are best suited for various types of analysis [67]. They mention the original application in which each distribution test feeder was originally developed for. Listed below are the intended applications to be performed on IEEE 4 and IEEE 123 when they were developed.

IEEE 4 Intended Applications:

- Net Power Flow Methods
- Islanded Operations
- State and Parameter Estimation
- New Control Schemes
    - New voltage regulator control methods
    - Advanced photovoltaic inverter functionality
    - Power Hardware-in-the-Loop (PHIL)
    - Control Hardware-in-the-Loop (CHIL)

IEEE 123 Intended Applications:

- Net Power Flow Methods
- Islanded Operations
- Integration studies
- State and Parameter Estimation
- New Control Schemes
    - DMS testing or control methods that respond to circuit conditions at multiple points

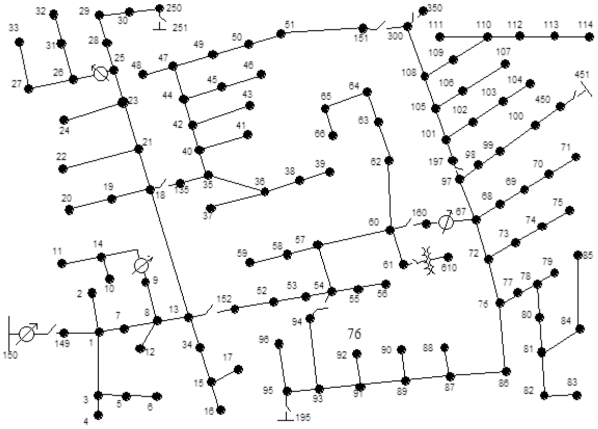

Figure 10: IEEE 123 Node Test Feeder

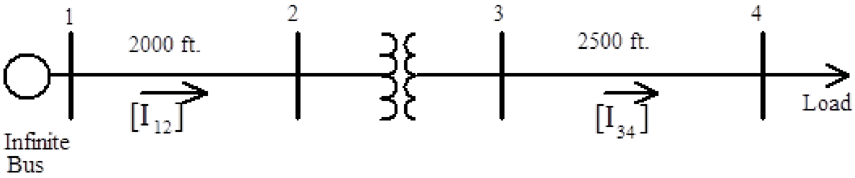

Figure 11: IEEE 4 Node Test Feeder

Table 12: IEEE Distribution Test Feeders Comparison

Component	IEEE 4	IEEE 123
Power System Type	3-Phase Distribution	3-Phase Distribution
Number of Buses	4	123
Balanced or Unbalanced	Both Available	Unbalanced Available
Loads	1 Three-Phase Load	5 Three- Phase Spot Loads 80 1-Phase Spot Loads
Transformers	1 Three-Phase Transformer	1 Three-Phase Transformer
Frequency	60 Hz	60 Hz
ePHASORSIM Model Availability	Yes	Yes
ePHASORSIM Model File Format	Excel	Cyme

Our project evaluates control schemes and the model receives power values from a physical solar panel. Therefore, our model contains Power Hardware-in-the-Loop (PHIL). A relatively small test feeder is adequate for PHIL laboratory tests [67]. The system we chose, needs to also be balanced. Therefore, IEEE 4 was chosen as our model.

3.2.2.4.1 Transformers in Simulink VS Gain Blocks

The power distribution system modeled in Simulink, with the use of ePHASORSIM, receives real-time power measurements from the RBP. The RBP is receiving those measurements from the PCB that is measuring the power output of the solar panel. As previously discussed, the power distribution grid chosen as our model is a three-phase balanced system, more specifically, IEEE 4. Bus 3 of IEEE 4 was initially chosen as the bus to inject the three-phase current measurements from the solar panel. Figure 11 was modified to demonstrate this addition of the solar panel to the system, and this is shown below in Figure 12.

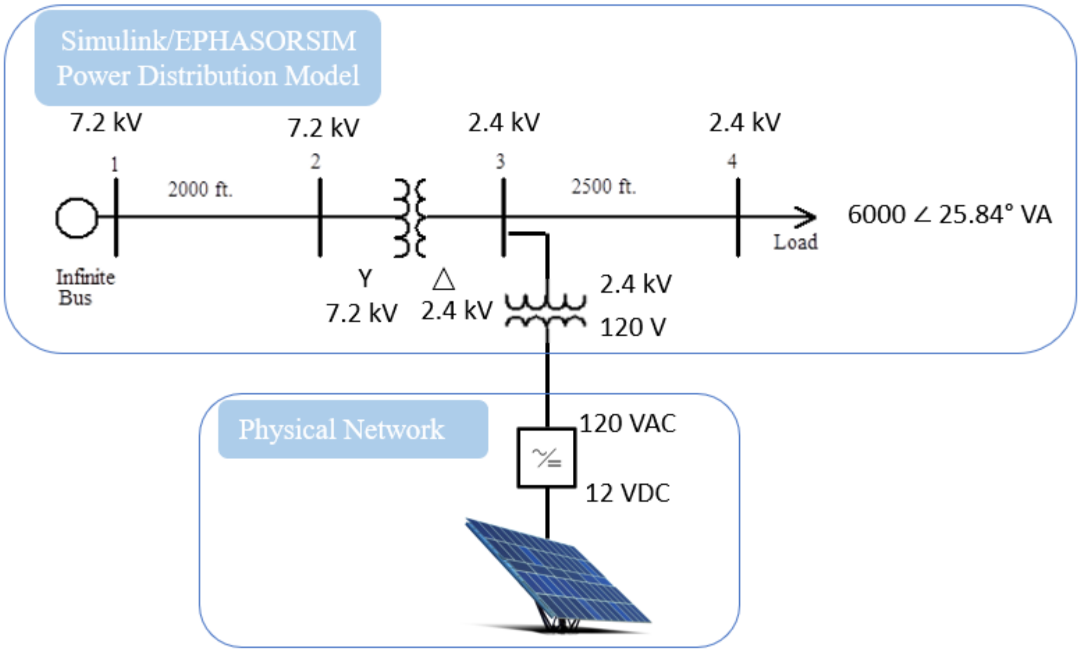

Figure 12: Hardware-In-the-Loop (HIL) Power Distribution System Model

As seen in figure 12, the output from the solar panel is 12 VDC. Therefore, the algorithm shown in figure 9 is necessary. The algorithm will convert the output of the inverter to three-phase balanced output. As shown, 120 V does not match bus 3 voltage of 2.4 kV. For this reason, a method to boost up the measurements read from the inverter is needed. Both gain blocks and transformer blocks in Simulink will be investigated in in this section. Figure 13 shows the results from designing a system that uses a transformer block to boost up the voltage measurements received from the inverter to 2.4 kV. Figure 14 demonstrates the results from using a gain block to increase the voltage to 2.4 kV. These values were injected to the distribution system at 20 seconds of simulation. It is important to note that phase C of bus 3 was outside acceptable limits at base case.

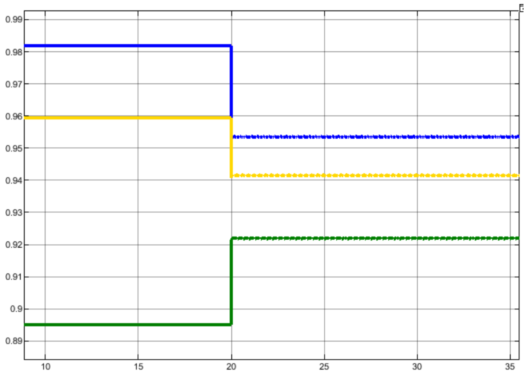

Figure 13: Bus 3 P.U. Voltage with Transformer Block Design

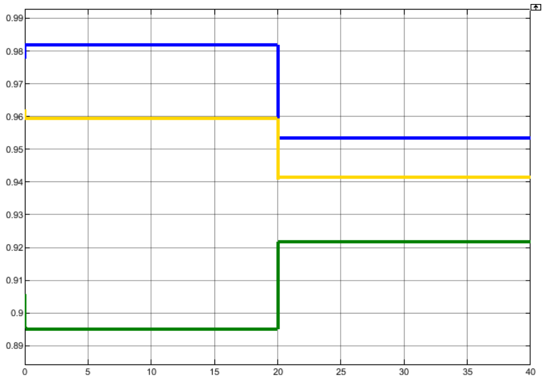

Figure 14: Bus 3 P.U. Voltage with Gain Block Design

As shown in the figures, both methods gave similar results. For both models, the voltage measurements received from the solar panel were converted to balanced three-phase measurements by using the algorithm shown in figure 9. It is important to note that the model takes in the values from the inverter as current injections. Table 13 summarizes how the transformer and the gain block were implemented to the model.

Table 13: Transformer Block VS Gain Block

Parameter	Transformer Block	Gain Block
Output	Sinusoidal Wave	Constant Value
Transformer used	Wye-ground to Delta	None
Gain Block	None	Gain Block: Voltage * 20.01481
Current Calculation	Three-Phase Measurement Block	Gain Block: Voltage / 10000 W

For the model with the transformer block, a function was created to convert the digital measurements received from the inverter to sinusoidal values. These values were then used as an input to a controlled voltage source. This was done so that the transformer could read and transform these phasor values. The outputs from the transformer were then read by using a three-phase measurement block. This is were the current was calculated. This three-phase measurement block also serves as a bus; therefore, a load was connected to it so that it would draw current. The load was set as a constant PQ load. The values of this load were set to be the same as the values of the load at bus 4 in IEEE 4, which was shown in figure 12. As shown in figure 13, the bus 3 voltages at 20 seconds of simulation changed. This is because at this time, the current injection was applied to bus 3. After 20 seconds of simulation, it is seen that the voltage is oscillating, it is behaving as a sinusoidal wave, rather than a straight line. This is because the system is receiving the analog outputs from the transformer. This is different than when using the gain block.

For the model with the gain block, the voltage values were multiplied by 20.01481. This is because 120 V times 20.01481 equals 2.4 kV, which is the base voltage value of bus 3. After the voltage was increased, the measurements were converted from to current. This was done by diving the voltage by the power that the inverter produces, more specifically, 1000 W. The current magnitude and angle were then injected to bus 3. The results were as shown in figure 14. Since the voltage was not converted to a sinusoidal value, the voltage seen in bus 3 is constant. Which is the main difference between the transformer block model and the gain block model.

The initial model did not accurately represent how the variable output power of the solar panel affects the distribution grid. Therefore, the model shown in Figure 15 was designed. In this model, the power output from the solar panel is scaled up to represent a solar farm. Then, it goes through an AC-DC inverter before being injected to bus 5. Bus 5 and the 120 V to 2.4 kV transformer were added inside the ePHASORSIM model and the gain and the inverter were modeled with Simulink blocks outside of the ePHASORSIM block.

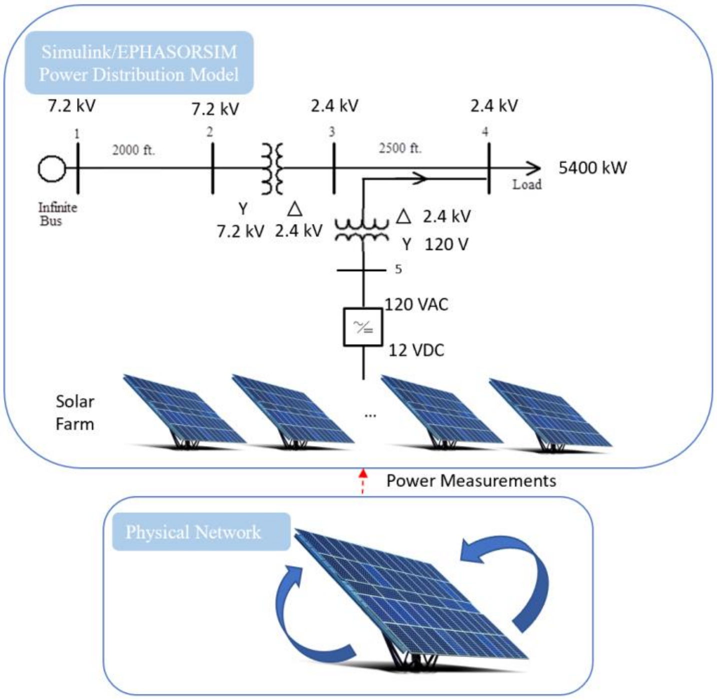

Figure 15: Distribution System Design V2.0

To verify the distribution system design, the same model was designed in OpenDSS. OpenDSS is an electric power Distribution System Simulator (DSS). This was done in order to verify the distribution system design. OpenDSS is an electric power Distribution System Simulator (DSS). The base case of both models were ran, and the results matched. As shown in Figure 16, the largest percent error found was 0.126 %. It is important to note that OpenDSS was used only to validate the models, it is not able to run real-time. Therefore, only the base case of both models were validated.

OpenDSS was also used to find which value of the current would need to be injected to bus 5 in order to completely provide power to the load of 5400 kW. After the current value needed was found, a gain of 353514 was added so that when the solar panel is producing maximum power it will be able to completely supply the power for the load. The load won’t need to get any current from the infinite bus.

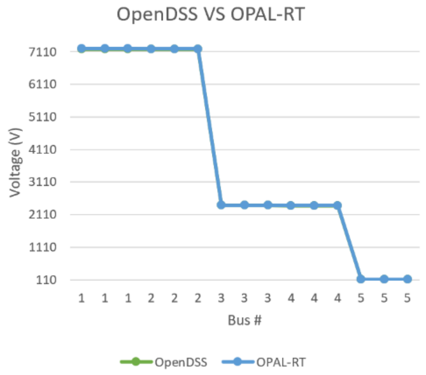

Figure 16: Model Comparison

3.2.3 Solar Panels

One of the main goals of the interactive touch table is to provide engaging methods to learn about the power grid. Therefore, the functionality of changing the angle of a solar panel was added. This allows users to learn how much the angle of the solar panel affects its power output, as well as how the variability of the power output from the solar panel affects the distribution grid stability. When discussing with FPL, it was decided to look for solar panels capable of generating maximum output of 100 W with a voltage output of at least 12 V. The reason for this is because it is a requirement that the solar panel has a compact design and is lightweight. This allows easier motor movement when changing the angle of solar panel.

3.2.3.1 Solar Panel Technology Comparison

The first solar panel considered was the Renogy 100 W 12 V Monocrystalline Solar Panel shown in Figure 17. [9] The second solar panel considered was the NewPowa 100 W 12 V polycrystalline shown in Figure 18. [10] Table 14 compares the specifications of both solar panels.

Figure 17: Renogy 100 W Monocrystalline Solar Panel

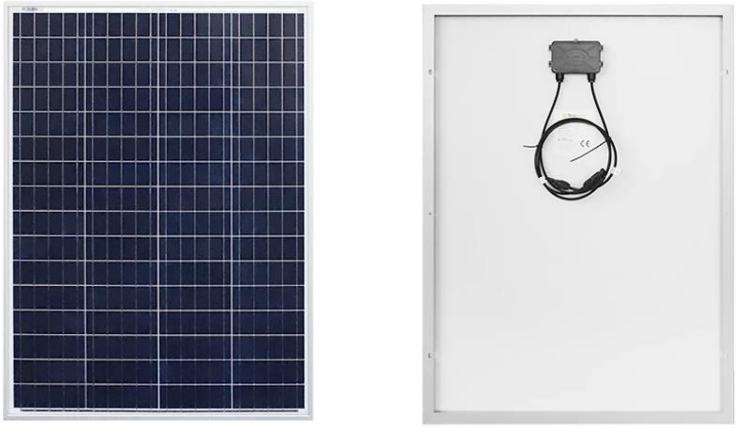

Figure 18: NewPowa 100 W 12 V polycrystalline

Table 14: Renogy VS NewPowa

	Specifications	
Type	**Renogy**	**NewPowa**
Price	$101.73	$75.00
Maximum Power	100 W	100 W
Optimum Operating Voltage	17.9V	17.2V
Optimum Operating Current	5.72A	5.81A
Operating Temperature	-40°F to 176°F	-40°F to 185°F
Solar Cell Type	Monocrystalline	Polycrystalline
Weight	14.3 lbs (6.5 kg)	15.43 lbs (7 kg)
Dimensions	42.2 x 19.6 x 1.38in (1074 x 498 x 35mm)	35.83 x 26.57 x 1.18in (910 x 675 x 30mm)
Cell Efficiency	21%	Class A High Efficiency

It is important to note that all the specifications and data described in the Table 14 were tested under Standard Test Conditions (STC). STC refers to the fixed set of laboratory conditions under which all solar panels are tested. Light sources in laboratories are calibrated to output 1000W/m^2 of solar lights on the solar module. The temperatures of the solar cells and the ambient room temperature are both set at 77 degrees Fahrenheit, or 25 degrees Celsius. [11] This means that all these values are based on ideal conditions enabling a fair comparison.

NewPowa has lower a lower price than Renogy. The maximum power output for both is 100 W. Renogy produces an operating voltage output 0.7 V higher than NewPowa. NewPowa produces an operating current of .09 A higher than Renogy. When multiplying the optimum operating voltage with the optimum operating current of each solar panel, Renogy produces 102.388 W while NewPowa produces 99.932 W. Meaning that at ideal conditions, Renogy produces 2.456 W more than NewPowa. NewPowa has a larger range of temperature at which it operates at by 9 degrees Fahrenheit.

A key difference, as seen in Table 15, is that Renogy has monocrystalline solar cells while NewPowa has polycrystalline silicon solar cells. Table 15 summarizes the differences between the two types. [12] It is clear to see that Monocrystalline is more efficient than Polycrystalline and this is due to monocrystalline silicon wafers using single-crystal silicon while polycrystalline manufactures melt multiple silicon fragments together to produce the wafers for the panels. Since monocrystal cells are constituted of a single crystal, it allows for a better electricity flow, resulting in a higher efficiency than polycrystalline solar panels.

Table 15: Comparison Chart

Parameters	Monocrystalline	Polycrystalline
Cost	High	Low
Efficiency	High	Low
Appearance	Black color panels	Blue color panels
Lifespan	Minimum 25 years	Up to 25 years
Temperature Coeff.	High	Low

As was shown in Table 14, Renogy is lighter than NewPowa by 1.13 lbs. Renogy is longer than NewPowa but NewPowa is wider. NewPowa is thinner than Renogy. They both come with 14 AWG output cables. Renogy's output cables are 1.97 ft long, or 23.6 in, while NewPowa's output cables is 2.95g ft, or 35.43 in.

3.2.3.2 Solar Panel Technology Selection

The Renogy 100 W monocrystalline solar panel shown in Figure 15 was selected. The biggest factor considered while making the decision was the type of solar cells that the solar panels had. The Renogy solar panel had monocrystalline cells. As was shown in Table 15, monocrystalline cells are more efficient. They are also usually a higher cost than polycrystalline solar panels but Renogy was selling it at a price that was very close to polycrystalline inverters, which are cheaper. Because of these reasons, the Renogy inverter was selected.

3.2.4 Motor

The use of photovoltaic principles has evolved ever since its discovery back in 1839 [55], and from this discovery emerges the use of solar cells to generate electricity using the light intensity of our sun. With our search for renewable energy, solar panels have become a huge contributor into finding a solution for the use of fossil fuels. Many solar panels, we will recognize them as PV panels or photovoltaic panels, have evolved in their construction and usage, millions of units being used worldwide. To ensure optimum performance of the PV panel, the solar cells should maintain constant contact with sunlight to generate the most electrical output. A stationary PV panel can only receive a small amount of sunlight directly thus generating a smaller electrical output. It is because of this fact that the Solar Tracking Model was invented.

A Solar Tracker is a device consisting of a motor that orients the PV panel towards the sun in order to receive the incoming sunlight directly for longer periods of time generating larger amounts of energy compared to a stationary PV panel. Most Solar Tracking designs implemented in the motorization of a PV panel have integrated the use of stepper, servo, or other types of motors to change the angle of the PV panel to receive the optimal amount of sunlight in a given point in time. Based on the needs of torque, position control, maintenance, durability, and operating voltage there are many aspects to consider when going into choosing a particular type of motor. One of those aspects choosing between Alternating Current motors vs a Direct Current motors.

3.2.4.1 Alternating Current

Alternating current, more commonly known as AC, is, according to Shawn Hymel, "the flow of charge that changes direction periodically. As a result, the voltage level also reverses along with the current." [56] We know AC to be a variable electrical current that changes with time more typically used to power buildings or houses. AC can be produced in a variety of forms if the voltage and current continue to alternate outputting as different waveforms (being sine wave, square wave and triangle wave). The most common AC waveform, this being the sine wave, can be defined using a certain equation consisting of three factors: phase, frequency, and amplitude. The sine wave can be defined using these parameters, according to Hymel, as:

$$V(t) = V_P \sin(2\pi f t + \varphi) \tag{1}$$

where V(t) is the voltage as a function of time, V_P is the amplitude, f is the frequency, t is time, and φ is the phase. 2π is our only constant in this equation that converts the frequency from cycles to angular frequency. [56]

AC is more commonly used to power homes and buildings, normally seeing this output when connecting to an outlet, since generating and transporting the electrical energy through long distances becomes easier because, according to Hymel, "At high voltages (over 110kV), less energy is lost in electrical power transmission. Higher voltages mean lower currents, and lower currents mean less heat generated in the power line due to resistance." [56] This telling us that even though the electrical energy has to travel a further distance which would normally cause an increase in temperature, the higher voltages prevent the excess heat to produce due to the lower levels of current. AC can also be seen powering electric motors of some of the more common household appliances like washers/dryers, freezers, refrigerators, etc.

3.2.4.2 Direct Current

Direct Current, more commonly known as DC, opposed to AC provides a constant current or voltage output towards a device making it a unidirectional flow of energy. According to Hymel, “Voltage and current can vary over time so long as the direction of flow does not change.” [56] This means that as long as the direction of the energy remains the same, the variation in the current or voltage being delivered is minimal. Mathematically speaking, since the variation over time is relatively zero, we can describe DC voltage/current as:

$$V(t) = V \tag{2}$$

$$i(t) = i \tag{3}$$

where V(t) is voltage as a function of time, and V is the constant delivered voltage. Similarly, i(t) is current as a function of time, and is the constant delivered current. Normally, a battery will lose its charge over time meaning that the power output will lower at some point. However, we best describe DC as a constant voltage throughout.

DC is most commonly seen in electronics and smaller devices that run on battery, AC adapters that connect to outlets on the wall, or use a cable (USB being the most common) for drawing power like our mobile devices, TVs, small motors, electric and hybrid cars, etc.

3.2.4.3 AC vs DC

In Table 16 we go over the advantages and disadvantages of utilizing AC or DC motors to operate the PV Panel movement.

Table 16: AC vs DC Decision Matrix

Motor	Advantages	Disadvantages
DC	• Higher Starting Torque • Easily Control Speed • Easy to Promptly Control • Fewer Rectification and Electronics Needs	• High maintenance due to low brush life • Significant power loss on full wave rectified voltage • High starting torque can damage reducers
AC	• Low Cost • Better Speed Variation • High Power Factor • Reliable Operation	• Inability to operate at low speeds • Poor Positioning Control • produce eddy currents due to the production of a back emf • Speed control is difficult to attain

After further review and much consideration, the best option for our work will be using a DC source to power the motor that performs the PV panel movement. This is due to the more reliable control speed, higher starting torque and the constant voltage output needed to perform the solar tracking.

3.2.4.4 Stepper Motor

The stepper motor, according to Bill Earl, “Stepper motors are DC motors that move in discrete steps. They have multiple coils that are organized in groups called phases. By energizing each phase in sequence, the motor will rotate, one step at a time. With a computer controlled stepping you can achieve very precise positioning and/or speed control. For this reason, stepper motors are the motor of choice for many precision motion control applications.” [57] Opposed to servo motors, stepper motors are inherently open-looped devices meaning that it has no feedback sensors or any mechanisms that work towards minimizing error, this meaning it doesn’t possess a dedicated system that verifies if the system reached its goal or desired output. Instead, open-looped systems rely on accuracy and repeatability to achieve a certain output.

Based on previous projects seen, we have determined that there are two stepper motors that could best fit our work needs: the Nema 23 Bipolar Stepper Motor, and the Nema 17 Bipolar Geared Stepper Motor. The Nema 23 Bipolar Stepper Motor is shown in Figures 19 and 20 while Table 17 shows the specifications of the motor. The Nema 17 Bipolar Geared Stepper Motor is shown in Figures 21 and 22 while Table 18 shows the specifications of the motor.

Figure 19: Nema 23 Bipolar Stepper Motor

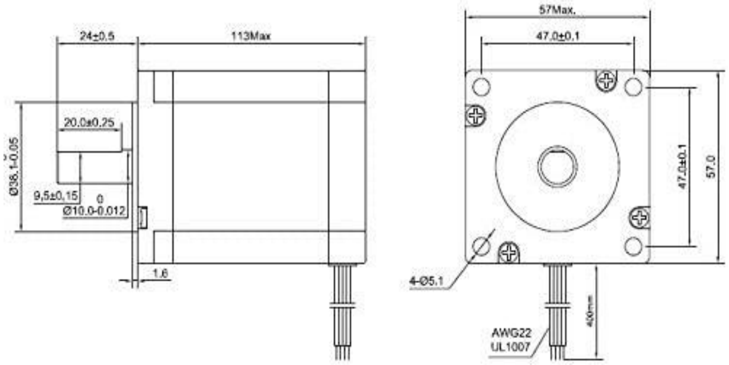

Figure 20: Nema 23 Bipolar Stepper Motor Dimensions

Table 17: Nema 23 Bipolar Stepper Motor Specifications

Item	Specification
Operating Temperature	-10℃～50℃
Step Angle	1.8˚
Holding Torque	30.5 kg/cm
Rated Current	4.2A
Rated Voltage	3.78V
Step Accuracy	+/- 5.00%
Motor Type	DC Bipolar Stepper Motor

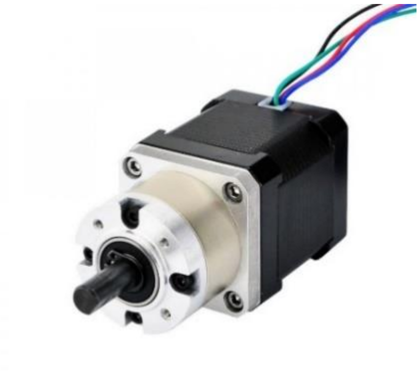

Figure 21: Nema 17 Bipolar Geared Stepper Motor

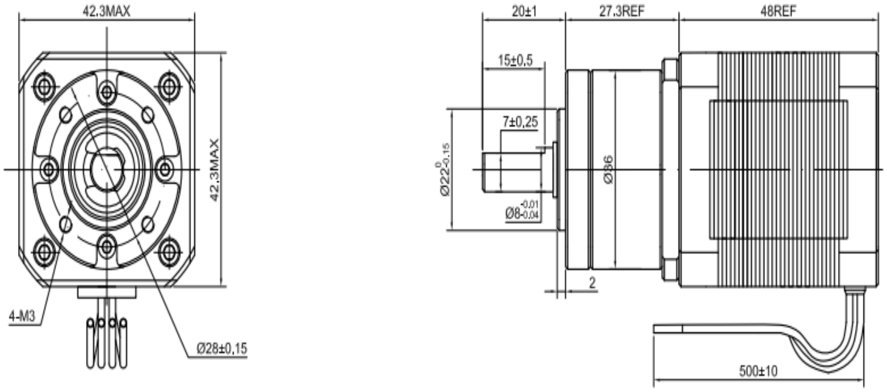

Figure 22: Nema 17 Bipolar Geared Stepper Motor Dimensions

Table 18: Nema 17 Bipolar Geared Stepper Motor Specifications

Item	Specification
Operating Temperature	-10℃～50℃
Step Angle	1.8˚
Holding Torque	20.3 kg/cm
Rated Current	1.68A
Rated Voltage	2.8V
Step Accuracy	90%
Motor Type	DC Bipolar Stepper Motor

Due to its better holding torque and does not need the use of an external gearbox, the Nema23 Bipolar Stepper Motor would be the better option of the two.

3.2.4.5 Servo Motor

The servo motor, according to Automation Engineer Wally Gastreich, “is a closed-loop mechanism that incorporates positional feedback in order to control the rotational or linear speed and position. The motor is controlled with an electric signal which determines the amount of movement which represents the final command position for the shaft.” [58]

When we mention that the Servo motor is a closed-loop mechanism we mean that it’s a device that can automatically regulate a given process variable without human interaction which can be completed when using the various feedback sensors like encoders and potentiometers in order to correct itself on its own without the assistance of a person. Utilizing these feedback sensors, Servo motors can show a better accuracy when reading position and managing speeds to meet the desired goal.

Based on previous projects seen, we have determined that there are two servo motors that could best fit our work needs: the DS3218MG ANNIMOS Digital Servo Motor, and the MG996R Digital Servo Motor. The DS3218MG ANNIMOS Digital Servo Motor is shown in Figures 23 and 24 while Table 19 shows the specifications of the motor. The MG996R Digital Servo Motor is shown in Figures 25 and 26 while Table 20 shows the specifications of the motor.

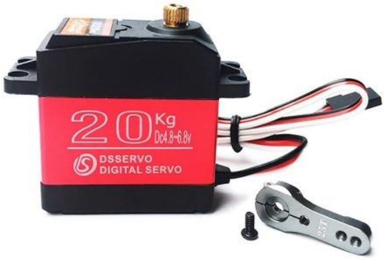

Figure 23: DS3218MG ANNIMOS Digital Servo Motor

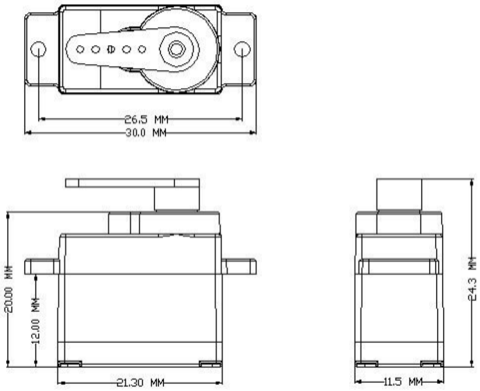

Figure 24: DS3218MG ANNIMOS Digital Servo Motor Dimensions

Table 19: DS3218MG ANNIMOS Digital Servo Motor Specifications

Item	Specification
Operating Temperature Range	-10℃～50℃
Operating Voltage Range	4.8V～6.8V
Dead band width	3µs
Working Frequency	1520µs / 333hz
Stall Torque	/cm (at 5V) 19kg and 21.5kg/cm (at 6.8V)
Speed	0.16sec/60˚ (at 5V) and 0.14sec/60˚ (at 6.8V)
Weight	60g
Limit Angle	270˚
Motor Type	DC Servo Motor

Figure 25: MG996R Digital Servo Motor

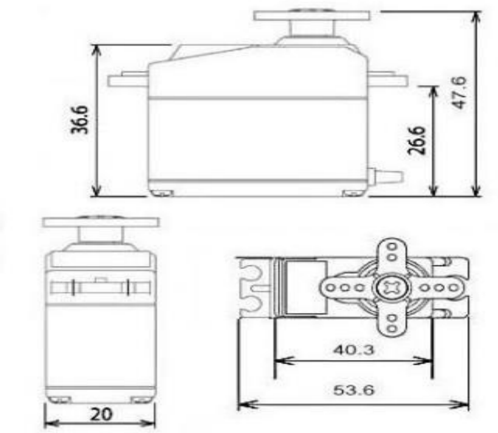

Figure 26: MG996R Digital Servo Motor Dimensions

Table 20: MG996R Digital Servo Motor Specifications

Item	Specification
Operating Temperature Range	0℃～55℃
Operating Voltage Range	4.8V～7.2V
Dead band width	5μs
Stall Torque	9.4kg/cm (at 4.8V) and 11kg/cm (at 6V)
Speed	0.17sec/60˚ (at 4.8V) and 0.14sec/60˚ (at 6V)
Weight	55g
Limit Angle	180˚
Motor Type	DC Servo Motor

While having better performing speed and less weight, the MG996R would not be able to properly rotate the PV panel and maintain the PV at a set position due to its lower torque compared to the DS3218MG. With a wider angle of rotation, higher torque, and more compact design, the DS3218MG would have a better performance and better fits our needs.

3.2.4.6 Motor Selection

According to Gastreich, "Selecting between a stepper motor and servo motor can be quite a challenge with the balancing of several design factors in cost considerations, torque, speed, acceleration, and drive circuitry all play an important role in selecting the best motor for your application." [59] Based on what solar tracking projects use to change the angle of the panel, we can see that there are two motors that standout the most: Stepper and Servo. Table 21 covers the options used today to perform solar tracking by comparing them side-by-side to understand which motor would be best fit for our work.

Table 21: Stepper motor vs Servo motor Decision Matrix

Motor	Advantages	Disadvantages
Servo	- High output power relative to motor size and weight - High efficiency - Encoder utilization provides higher accuracy and resolution with closed-loop control - High torque to inertia ratio	- requires tuning to stabilize the feedback loop - unpredictable when something breaks - Gear boxes are often required to deliver power at higher speeds - can be damaged by sustained overload
Stepper	- Excellent Low Speed Torque - Repeatability - Overload Safe - Good Choice for Applications Requiring Low Speed with High Precision	- Torque Declines Rapidly with Speed - No Feedback is Used to Indicate Potential Missed Steps

Based on Table 21 we have decided that the best option moving forward for our work was to utilize Stepper motors in the movement of our PV Panel as they provide the efficiency and torque, we need to complete the solar tracking functions. Therefore, the motor to be used for our work would be the Nema 23.

3.2.5 Inverters

The users have the option to send the current solar panel power output to the distribution system that is modeled in OPAL-RT. The network modeled is a balanced three-phase 60 Hz distribution system. It was decided to model it this way since this is how current distribution systems are. Solar panels output DC quantities. Because of this, an inverter to convert the power output from the solar panel from DC to AC was considered. Four types of inverters were looked into: single-phase, three-phase, off-grid, and grid-tied inverters. Since our distribution system is balanced, a single-phase inverter is acceptable. A simple algorithm can be used to make it three-phase for simulation purposes. This can be achieved by using the same voltage magnitude read from the inverter on the other two phases, and just shifting the angle by -120 and 120, respectively.

Grid-tied inverters offer the capability of connecting the solar panel to the power grid. They are very popular for homeowners that install solar panels in their houses. These inverters offer many benefits. When the solar panels are not producing enough power, the system takes power from the grid to supply the difference. When the solar panel are producing more than needed, it sells the power back to the grid. This is done through net metering systems. Net metering allows homeowners to earn money for the excess solar energy that was produced. This benefits the homeowner because it reduces their electricity bill. Figure 27 shows the layout of a grid-tied solar system. [17]

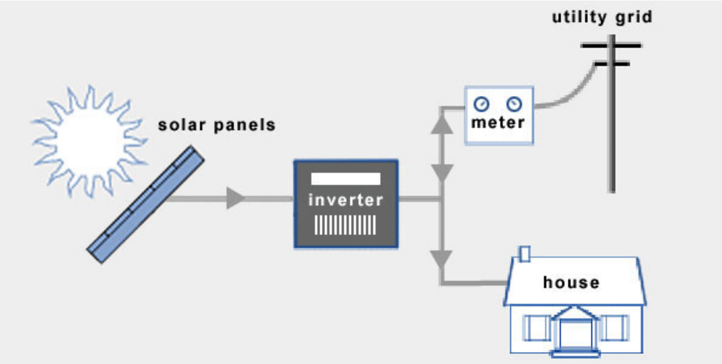

Figure 27: Grid-Tied Solar Systems

Although grid-inverters offer so many benefits, it also requires many permits to connect your solar system to the power grid. Utility companies need to ensure that the solar energy system meets electrical safety standards. Utility companies need to be aware that there is an additional distributed generator in their system. This way they are better able to monitor the power grid. After installation of solar panels, professional engineers inspect your solar system.

3.2.5.1 Off-grid Inverters

There are two main roles that the solar panel plays in our project. First, it allows users to see how the angle change of the panel affects its power output. Second, it sends the power output to the distribution grid modeled in OPAL-RT so that users can see how the variability of power output from the solar panel affects the grid. For the purpose of this project, the solar system does not need to be interconnected to the power grid. Therefore, it was decided to go against grid-tied inverters and investigate off-grid inverters.

Off-grid inverters are used when no connection to the grid is intended. Figure 28 shows an off-grid 700W 12V pure sine wave inverter. [13] The specifications of this inverter are summarized in Table 22. [13] This inverter was considered because it is the same brand as the 100 Watt Solar Panel.

Figure 28: Renogy 700W 12V pure sine wave inverter

Table 22: Renogy Specifications

Renogy 700 W 12V pure sine wave inverter	
Price	$134.99
Continuous Output Power	700 W
Surge Output Power	1400 W
AC Output Voltage Range	115VAC
Output Frequency (Nominal)	60 Hz
Output Waveform	Pure Sine Wave
Efficiency	> 90%
Operating Temp	-4°F - 158°F
THD	< 3%
No Load Current Draw	< 1A
Dimensions	11.75 x 7.38 x 3.32 in
Weight	5.3 lbs
AWG	6 (3 FT)

A cheaper off-grid inverter model was considered, and it is as shown in Figure 29. [18] This inverter converts 12V DC to 120 V AV and outputs 1000 W. Its specifications are as shown in Table 23. [19]

Figure 29: Schumacher 1000 Watt Power Inverter

Table 23: Schumacher Specifications

Schumacher 1000 Watt Power Inverter	
Price	$109.99
Continuous Output Power	Up to1000 W
Surge Output Power	2000 W
Operating input voltage	10.5-15.5 VDC
Nominal Output Voltage	110-125 VAC
Output Frequency (Nominal)	60 Hz
Output Waveform	Modified Sine Wave
Maximum Efficiency	90%
Input low voltage shutdown	.10±0.5 VDC
USB port	One, 2A
Internal fuse	40A x 3

3.2.5.2 Simulink Inverters

The option to model an inverter in Simulink was considered as a cheaper option. As mentioned before, Simulink is where the distribution system was modeled. A simple system was designed in Simulink to test an inverter and it is as shown in Figure 30.

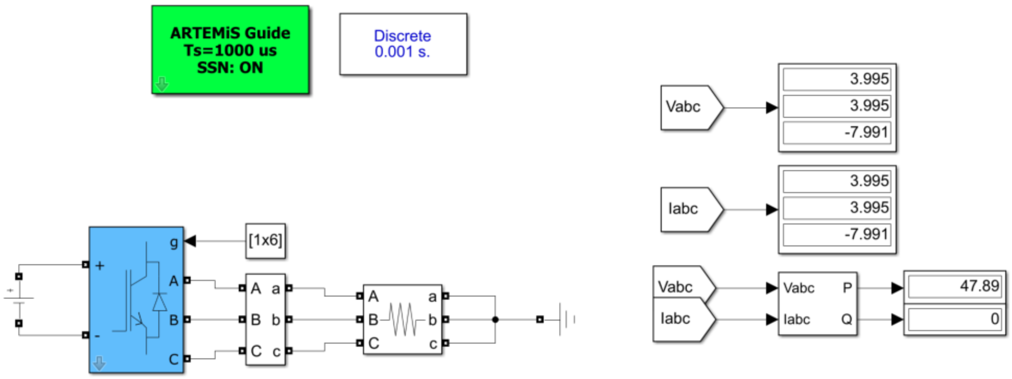

Figure 30: Simulink Inverter Design

The system is composed of a DC voltage source outputting 12 V. The inverter block implements a three-phase power converter that consists of up to six power switches connected in an IGBT-Diode bridge configuration. The outputs from this inverter goes through a bus, which measures its output. The outputs from the bus then goes through a 1 ohm resistor which can be modified as desired. The measurement readings from the bus are as shown in the top right of Figure 30 as Vabc and Iabc. These are the three-phase voltage and current measurements read from the bus. These measurements were sent to a three-phase measurement block to calculate its power output. As expected, there is zero reactive power because the load is purely resistive.

The voltage values from the voltage source in the Simulink design can be updated with the voltage values reading from the solar panels. The inverter converts these values to three-phase, and they will then be sent to the distribution system. The change in voltage at the bus were the solar panel is connected to will cause some disturbances which the users will be able to see in the interactive touch table.

3.2.5.3 Inverter Selection

Table 24 compares the key components that were looked at when selecting an inverter. It was decided against the Simulink inverters because we want to reduce the amount of simulated parts therefore, it was not added to the selection table. When comparing inverters, the key component that was looked at was the operating input voltage. The Renogy inverter specifications paper specified that its operating input voltage is 12 VDC. [13] They did not give a range. Therefore, if the inverter was to be connected directly to the solar panel and the solar panel was not producing 12 VDC, then the inverter would not operate. On the other hand, the Schumacher inverter has an operating input voltage range from 10.5 to 15.5 VDC. [1]

Table 24: Inverter Selection

Component	Renogy	Schumacher
Price	$134.99	$109.99
Continuous Output Power	700 W	Up to1000 W
Operating input voltage	12 VDC	10.5-15.5 VDC
AC Output Voltage Range	115 VAC	110-125 VAC
Frequency	60 Hz	60 Hz
Efficiency	> 90%	90%
Output Wave Form	Pure Sine Wave	Modified Sine Wave

Since a goal is to demonstrate how the fluctuations in solar panels power output can cause disturbances in the grid, the Schumacher's inverter was the better option for our project. The second thing taken in consideration was the price, Schumacher's inverter was the more cost-efficient choice. The third aspect was the output power. Schumacher's inverter offers a larger power output than Renogy's inverter. Efficiency was important as well, but they both offered an efficiency of around 90%. With all these considerations in mind, The

Schumacher 1000-Watt Power Inverter, shown in Figure 29, was selected. Its specifications match our needs while being a cost-efficient option.

This inverter is a one-phase inverter, and it will be connected to a load. The load is a fan, which allows users to see the immediate effect that the angle change of the solar panel has on its power output. This will be accomplished by attaching strings to the fan which shows the speed of the fan. The faster the strings move; the more power is receiving from the solar panel.

After some testing, it was decided to not use the inverter in the project. This is because although the inverter had a range, the voltage output of the solar panel was fluctuating too fast for the inverter. Therefore, the inverter was constantly turning off and on. For this reason, tt was decided to use a 12 V DC fan.

3.2.6 Fan for Solar Panel Load

The fan is used as a load to create current. It was selected based on cost, that it was DC, that the voltage input was 12 V, and that it draws less than the 100 W that the solar panel can output. Based on these factors the Auto Drive 12 Volt Fan show in Figure 31 was selected [136]. Table 25 contains its specifications and compares it to other fans [91, 92, 93].

Table 25: Fan Comparison

	Lasko S16500	Pelonis FS40-19MB	Lasko B20200	Auto Drive 12 Volt
Cost	$29.67 ($21.74 + $7.93 tax/shipping)	$37.45 ($35.00 + $2.45 tax)	$27.26 ($19.88 + $7.38 tax/shipping)	$12.97
Power Usage	43.2 to 64 W	42 W	54 to 82 W	10 W
AC-DC	AC	AC	AC	DC

Figure 31: Auto Drive 12 Volt Fan

3.2.7 Reading AC measurements from Inverter

In order to display the power output of the solar panels in the interactive touch table and send them to the distribution model in OPAL-RT, the AC current and voltage outputs from the inverter needs to be measured and recorded. Therefore, relays were considered for this part of the project. Relays play a very important role in the protection of power systems. They are designed to detect and respond to specified input conditions. Within a few thousandths of a second, it can detect a fault and open the breaker assigned to it. Tripping a circuit breaker, opens the circuit and prevents the fault to spread within the power system. This reduces the number of customers that are affected by faults and increases reliability in the power grid.

3.2.7.1 Relay

Schweitzer Engineering Laboratories (SEL) has donated relays to UCF to be used for research or project purposes. Since it is available to use and it will offer great experience to work with them, they will be used as a part of a project. The role that the relay will play is to measure the phasor Voltage and Current quantities coming out of the inverter, as well as the frequency. Figure 32 illustrates the layout of the system. The measured values will then be sent to the PCB through RS-232 serial communication.

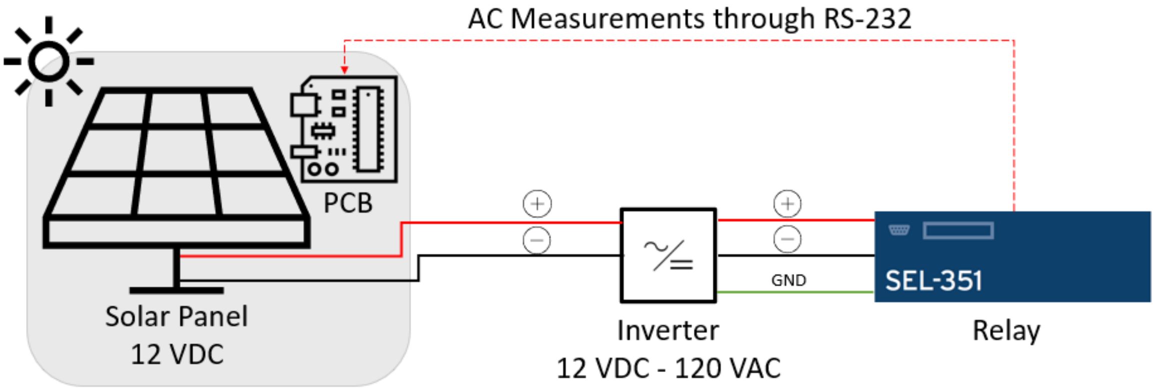

Figure 32: Relay Integration to the system

3.2.7.1.1 SEL-351 Relay

Relay SEL-351 is available to use at UCF. Its rear-panel drawing is shown in Figure 33. [20] Boxed in red are the ports that we will be making a connection to. The serial port shown in box number 1 will be used to transmit the measurements to the PCB through RS-232 serial communication. These values will be accessed by reading the registers were the relay stores these values. This information is provided in the relay manual. In box number 2 the current input is shown.

Please note that only one phase of the inputs will be used. This is because the inverter that we will get is a single-phase inverter. Similar thing is noticed in box 3 where only one phase of the voltage inputs will be used. Box 4 shows where the power supply of the relay will be connected to. Box number 5 shows the ground from the inverter and voltage source will be connected to. It is important to note that the use of ring terminals is recommended when making the connections to the rear panel of the relay.

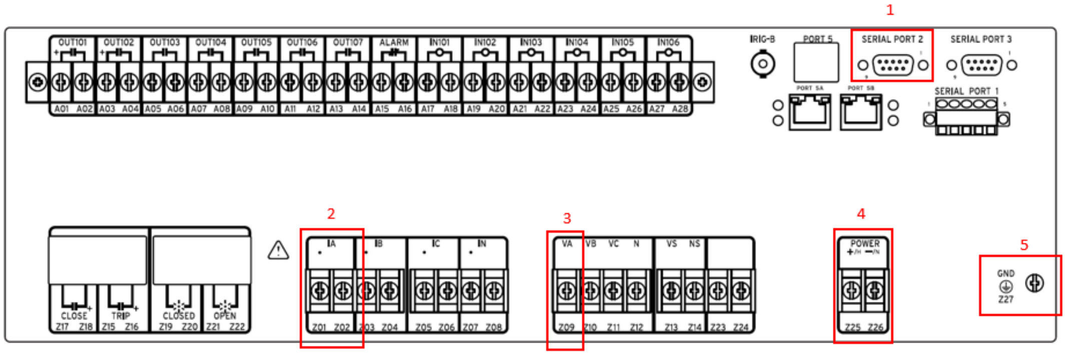

Figure 33: SEL-351 Rear-Panel Drawing

The relay specifications are summarized in Table 26. [21] There are three types of SEL-351: -5, -6, -7. These different versions offer different inputs and outputs, and some have more functions than the other. But they are all capable of measuring current, voltage, and frequency, which is our main use of the relay. The type of SEL that we will use will be based on which one is available and given to us. By looking at the specifications, we were able to make sure that the outputs from the solar panel and the inverter that will be bought are within the specified requirements of the relay.

Table 26: SEL-351 Relay Specifications

SEL – 351 Relay Specifications		
AC Voltage Inputs Nominal Range	Line-to-Neutral	67-120 Vrms
	Line-to-Line (open delta)	115-260 Vrms
	Continuous	300 Vac
	Short-Term Overvoltage	600 Vac for 10 seconds
AC Current Inputs IA, IB, IC, and Neutral Channel IN	5 A Nominal	15 A continuous, 500 A for 1 second, linear to 100 A symmetrical, 1250 A for 1 cycle
Power Supply	Rated (nominal)	125/250 Vdc or 120/230 Vac
	Range	85-350 Vdc or 85-264 Vac
	Burden	<25 W (dc)
Frequency	System Frequency	40-65 Hz
	Frequency Tracking	Zero-crossing detection method, preferred source: VA-N terminals.

3.2.7.1.2 SEL-787 Relay

SEL-787 Relay is also available at UCF. This relay was originally meant for Transformer Protection, but for the purpose of the project it will be used to read AC measurements from the inverter. This relay is shown in Figure 34. It is equipped with as many as four independently operated ports: one EIA-232 port on the front, one EIA-232 or EIA-485 port on the rear, one fiber-optic port, and one EIA-232 or EIA-485 port option card. [120] This is important because RS-232 will be used to send AC measurements from the relay to the PCB. It is also important to mention that EIA-232 is an old name for RS-232.

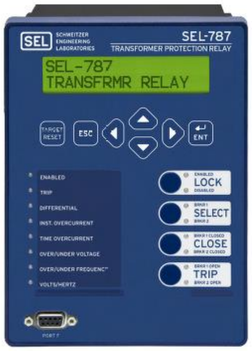

Figure 34: SEL-787 [120]

Figure 35 shows the rear panel of SEL-787 Relay. [121] Boxed in red are the ports that we will be making a connection to. The power supply of the relay is shown in box 1. Box number 2 shows where the ground from the inverter and power supply will be connected to. The serial port shown in box number 3 will be to transmit the measurements to the PCB through RS-232 serial communication. As mentioned for the SEL-351, these values will be accessed by reading the registers were the relay stores these values. This information is provided in the relay manual. In box number 4 the current input is shown. It is important to note that the use of ring terminals is recommended when making the connections to the rear panel of the relay. Table 27 list the specifications of the relay.

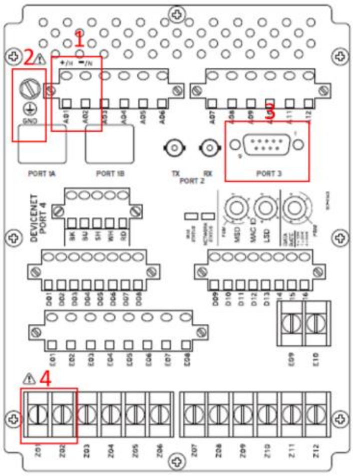

Figure 35: SEL-787 Rear-Panel Drawing [121]

Table 27: SEL-787 Relay Specifications [121]

SEL - 787 Relay Specifications		
AC Voltage Inputs Nominal Range	Line-to-Line (DELTA_Y = DELTA)	100-440 V
	Line-to-Line (DELTA_Y = WYE)	100–250 V
	Continuous	300 Vac
	Short-Term Overvoltage	600 Vac for 10 seconds
AC Current Inputs IA, IB, IC, and Neutral Channel IN	5 A Nominal	15 A continuous, 500 A for 1 second
Power Supply	Rated	110–240 Vac or 110–250 Vdc
	Range	85–264 Vac, 85–300 Vdc
	Burden	<25 W (dc)
Frequency	System Frequency	50, 60 Hz
	Frequency Tracking	20–70 Hz (requires ac voltage inputs option).

3.2.7.1.3 Relay Selection

Table 28 summarizes the key points that were compared when choosing which one to use for our project. It is important to note that SEL has donated this to UCF, and UCF has granted us permission to use this in our project. It is important to note that both relays have two current nominals that depend on which model is given to us by UCF. The first nominal is 1 A and the second is 5 A. The data shown in table 2 is with current nominal at 5 A. As shown in Table 28, SEL-787 was chosen. This is because this relay had smaller dimensions, while being capable of reading the measurements that we need.

Table 28: Relay Comparison

Component	SEL-351	SEL-787
Dimensions	465.1 mm (18.31 in) x 88.1 mm (3.47 in) x 197.0 mm (7.75 in)	144.0 mm (5.67 in) x 192.0 mm (7.56 in) x 147.4 mm (5.80 in)
AC Voltage Metering	67-250 V	50–250 V
AC Current Input Metering	1 – 100 A or (0.2–20.0) • INOM A	1 – 100 A or (0.2–20.0) • INOM A

Due to the fact that an inverter was not used for the project, the relays were not used since they were no longer needed. This is a good solution to read AC voltage and current output. Since the outputs of the solar panel were not converted to AC, a circuit within the

PCB that measures the DC voltage output of the solar panel was developed. The resistance of the was then calculated in order to measure the current.

3.2.7.1.4 Faults Modeled in ePHASORSIM

A stretch goal is for the touch table to demonstrate how algorithms like WAMS can detect the location and the type of the source of disturbances. Because of this, disturbances should be created in the OPAL-RT model. Faults are a type of disturbance. Faults are any irregular electric current. Faults are caused by many things. For example, a branch falling across wires forms an electrical bridge that causes the current to flow from one conductor to the other. This type of fault is classified as phase-to-phase fault. Where current from one phase flows into another phase. Faults can be modeled in OPAL-RT by using ePHASORSIM solver block in Simulink.

3.2.7.2 Multiphase-Faults in ePHASORSIM

The multiphase fault feature can represent phase-to-ground, and phase to phase fault. A phase-to-ground fault can be modeled as a single-phase fault, double-phase fault, or three-phase fault. A phase-to-phase fault can be modeled as a double-phase fault or three-phase fault. The fault is modeled by connecting two impedances to a virtual node. In order words, the impedance from the chosen phase of a bus is connected to the fault point via an impedance $Z_f = R_f + jX_f$. The fault node can be connected to ground, if required, via an impedance $Z_g = R_g + jX_g$. [22] Figure 36 demonstrates how a double-phase-to-ground fault is modeled in ePHASORSIM. Listed below is a summary of the types of faults that can be modeled:

- Single-phase-to-ground fault
- Double-phase-to-ground fault
- Three-phase-to-ground fault
- Phase-to-phase fault
- Three-phase fault

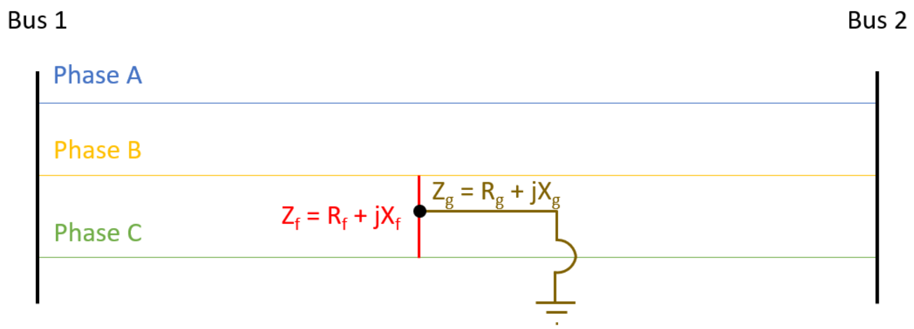

Figure 36: Example of Double Phase to Ground Fault

Once the type of fault is selected and modeled in ePHASORSIM, a value of 1 activates it and a value of 0 deactivates it. This is important because when the user from the interactive touch table decides to activate a fault, a 1 will be sent from the microcontroller-unit, used to power the touch screen, to OPAL-RT. This will be done through Wi-Fi, and the value will be sent to the respective variable to update its status. After the fault is activated, the can see its effect to the grid and how WAMS helps detect these events. Since the stretch goal was not achieved, faults were not implemented in the project since it was no longer required by the project.

3.2.8 Stand-Alone Micro-Controller Unit (MCU)

A stand-alone micro-controller unit is used to process the data coming from the solar panel and send it to OPAL-RT. It processes the data coming from OPAL-RT and implements the user interface on the touchscreen. It also sends the instructions to the PCB to change the angle of the solar panel based on touch table input from the user. For this functionality, the unit has to be able to process large amounts of data. These requirements dictated the need for an MCU with advanced capabilities which could not be satisfied with any of the TI MSP430 MCUs which are frequently used in the UCF ECE department. These advanced requirements could be satisfied by an Arduino Portenta H7 or a Raspberry Pi 4 Model B [37]. The Portenta [28, 33] is more compact than the Raspberry Pi, but for this application that was not an issue. After reviewing the technical specifications for both MCUs, it was determined that the Raspberry Pi would better suit our needs for this project due to its advanced Raspberry Pi Operating System and ease of use. The Raspberry Pi also features a quad core processor while the Portenta’s processor is only a dual core. In addition, the Raspberry Pi was a more cost-effective solution than the Portenta. Figure 37 shows the compact Portenta H7 board.

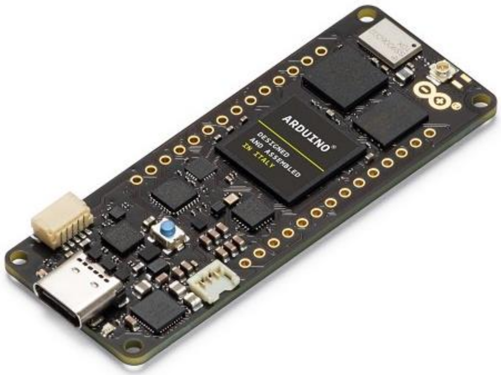

Figure 37: Arduino Portenta H7

Table 29 shows the comparison of the MCUs considered for this project and was used to determine that Raspberry Pi was the best choice because of the advanced processor, large RAM, built-in Wi-Fi, and reasonable cost. This component functions as a small computer instead of as an embedded microcontroller.

Table 29: Stand-alone MCU Comparison

	Raspberry Pi 8GB (specs on board only)	Arduino Portenta H7	MSP430G2ET LaunchPad
Price	$88.50	$103.40	$23.40
Processor	Broadcom BCM2711 Quad core Cortex-A72 (ARM v8) 64-bit SoC @ 1.5 GHz	STM32H747XI dual Cortex®-M7+M4 32bit low power ARM MCU @480 MHz	MSP430G2x32 (single core)
Memory	8GB LPDDR4	8MB SDRAM	256B
Storage	MicroSD card slot available	Interface for SD Card connector (through expansion port only)	8KB flash
Wi-Fi Module	2.4 GHz and 5.0 GHz IEEE 802.11ac wireless	2.4 GHz Murata 1DX dual WiFi 802.11b/g/n	Not included
Power Consumption	500mA maximum	2.95 µA in Standby mode	250µA/MIPS when active (ultralow)
Operating System	Raspberry Pi OS (based on Debian Linux)	None except the SYS/BIOS	None except the SYS/BIOS

3.2.8.1 Raspberry Pi

The Raspberry Pi 4 Model B is the most advanced Raspberry Pi available on the market. It can run on the Raspberry Pi Operating System (previously called Raspian) which is a Linux Debian based OS. It has a minimum of 2GB of RAM with the option to upgrade up to 8GB, a high-performance 64-bit quad-core processor, dual-display output via two Micro HDMI ports with up to 4K resolution, Gigabit Ethernet, MicroSD card slot, 2 each USB 2 and 3 ports, and a 40 pin general-purpose I/O header [37]. Figure 38 shows a technical view and placement of the features of the Raspberry Pi 4 Model B.

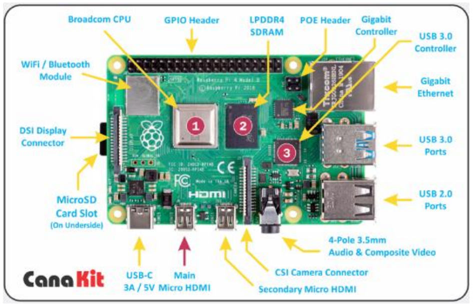

Figure 38: Raspberry Pi Model 4 B

The complete list of the technical specifications can be found below in Table 30. The RP4 Model B (2GB of RAM) can be purchased alone for approximately $40, but the power supply and memory card needed would need to be purchased separately. In addition, a case to keep out dust and debris are helpful as well as heat sinks and a fan to ensure that it remains cool while in operation. CanaKit offers a starter kit that includes the Pi, the 3.5A USB-C power supply with noise filter and a 5-foot cable, a case, 3 aluminum heat sinks, a low noise cooling fan, USB card reader, and a microHDMI cable [34]. Also included is a 32GB MicroSD card preloaded with NOOBS. NOOBS is an acronym which stands for New Out of Box Software, and it is a system that allows easy installation of other operating systems such as the Raspberry Pi OS, formerly called Raspian, which was used for this project. The basic 2GB Raspberry Pi 4 starter kit is $79.95 ($99.95 if upgrading RAM to 4GB or $119.95 if upgrading to 8GB of RAM). A cost analysis on buying all the needed items separately came to approximately $86 (for the 2GB RAM version) and also involved separate shipping charges for each item, so the Raspberry Pi 4 Model B CanaKit was the best solution. To ensure it would be able to process the data coming from the solar panel and OPAL-RT and run the user interface, the upgrade to 8GB of RAM was selected. Even with the upgraded RAM, the CanaKit was still the most cost-effective solution.

Table 30: Raspberry Pi Tech Specs

	Raspberry Pi 4 Model B Technical Specifications
1.	Broadcom BCM2711, Quad core Cortex-A72 (ARM v8) 64-bit SoC @ 1.5GHz
2.	2GB, 4GB or 8GB LPDDR4-3200 SDRAM (depending on model)
3.	2.4 GHz and 5.0 GHz IEEE 802.11ac wireless
4.	Bluetooth 5.0, BLE
5.	Gigabit Ethernet
6.	USB 3.0 ports; 2 USB 2.0 ports.
7.	Raspberry Pi standard 40 pin GPIO header
8.	2 × micro-HDMI ports (up to 4kp60 supported)
9.	2-lane MIPI DSI display port
10.	2-lane MIPI CSI camera port
11.	4-pole stereo audio and composite video port
12.	H.265 (4kp60 decode), H264 (1080p60 decode, 1080p30 encode)
13.	OpenGL ES 3.0 graphics
14.	Micro-SD card slot for loading operating system and data storage
15.	5V DC via USB-C connector (minimum 3A*)
16.	5V DC via GPIO header (minimum 3A*)
17.	Power over Ethernet (PoE) enabled (requires separate PoE HAT)
18.	Operating temperature: 0 – 50 degrees C ambient

3.2.8.2 Communication between OPAL-RT and Raspberry Pi

To create the GUI functionality and implement the WAMS algorithm functionality, communication with OPAL-RT, the real-time power system simulator previously mentioned, was necessary. A link to a guide to setting up the connection between OPAL-

RT and a Raspberry Pi (RBP) was provided by a member of the OPAL-RT administration [35]. The process for setting up a connection between OPAL-RT and the RBP had several steps. The RBP had to be connected via ethernet to the UCF local network. Our team will be able to connect to the computer running OPAL-RT remotely to set up the connection configuration on that end. The connection relies on a TCP socket to maintain communication.

Once the Raspberry Pi Operating System was successfully installed, the RBP was connected to the UCF network via ethernet, the OPAL-RT computer was accessed, and using the command prompt the OPAL-RT computer was able to ping the RBP. SSH was enable on the RBP, and it was confirmed that it had Python 3.7 installed on it.

While remotely connected to the OPAL-RT computer, MobaXterm was opened, and a connection was made to the RBP using an SSH session. Two Python scripts, main.py and ServerRP.py, were downloaded from the OPAL-RT website. These were written by the team who administers OPAL-RT to run in MobaXterm in order to connect with an RBP. The model for the project was then be uploaded to the location where was opened, and a block labeled 'OplPSocketCtrl1' was updated to match the Python script. After the model was compiled, the IP address of the Raspberry Pi appeared in the console as the model loaded. The model then started to execute. Meanwhile, the main.py script was executed on the RBP. After these steps, two-way communication was established between OPAL-RT and the RBP [35]. Later during development, the Python scripts were modified and in the final stage the RBP only needs to run the Python server_opal.py file to connect with OPAL-RT.

3.2.9 Communication Protocols

An electronic or digital device often needs to communicate with other devices. The Federal Communications Commission (FCC) and Department of Communication (DOC) define digital device as:

> *An unintentional radiator (device or system) that generates and uses timing signal pulses at a rate in excess of 9,000 pulses (cycles) per second and uses digital techniques; inclusive of telephone equipment that uses digital techniques or any device or system that generates and utilizes radio frequency energy for the purpose of performing data processing functions, such as electronic computations, operations, transformation, recording, filing, sorting, storage, retrieval or transfer.*

There are several communication protocols that define how information flows between connected and non-connected devices. Given that a major part of this project includes the design of a PCB, selecting an efficient communication protocol is critical. Several technologies will be reviewed and compared before selecting one that is suited for the project application.

Transferring information between devices connected to a bus is possible through parallel or serial configuration. Communication between components is based on voltage signal. Typically, a bus voltage level of 5 V and 0 V are translated as binary 1 and 0. There is usually a set voltage threshold. For example, voltage greater than 4.5 V and less than 5.5

V will indicate a binary 1. This is a fundamental analog to digital conversion principle governing digital devices.

Parallel configuration is designed to send or receive all of the data simultaneously. Unlike serial communication, where it sends or receives one data bit after another. Figure 39 and Figure 40 illustrate parallel and serial data flows. It is important to note that the data flow between a CPU or a microcontroller and a serial or parallel device. Parallel implementation requires one designated channel for each bit. Therefore, for a 8 bit data frame, eight channels will be needed for data flow. Serial on the other hand, only requires a single channel for data flow [40]. These devices also have additional wire for ground but does not always have additional wire for generating clock signal.

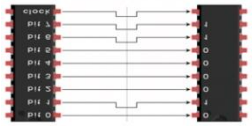

Figure 39: Parallel Communication

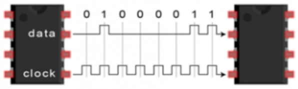

Figure 40: Serial Communication

Wireless communication is very popular and is expected to expand its use for Internet of Things (IoT) application. Wireless communication enables data transfer between remote devices without a wired medium. Instead, Radiated Emission is used to propagate electromagnetic signals that are converted from analog-to-digital by electronic devices to produce information or data. This is a component of Radio Frequency (RF) that is transmitted through air.

There are several types of RF communications in use today. For example, most phones are powered by cellular communication. On the other hand, phones also make use of wireless fidelity (Wi-Fi) communication. While it is common for wireless communication to involve devices separated by long distances, it is also popular for devices that are close to each other. The sections that follow will discuss several wired and wireless communication protocols that are relevant to the project.

3.2.9.1 Wi-Fi

Wi-Fi is a proven technology and is a growing application in embedded systems. The growing demand for IoT is attracting enthusiasm from both commercial and hobbyists. Wi-Fi is backed by the IEEE 802.11 standard. This standard describes the characteristics that Wi-Fi devices should entail to work well with other Wi-Fi devices. Speed and frequency of operation are some of the critical benchmarks. As shown in Table 31, letters are frequently added after the 802.11 to denote the features that were added to newer version of the standard. These are also backward compatible. Wi-Fi continues to improve since it was patented in early 1990s. Wi-Fi enabled devices can act as an Access Point (AP) in a local arena network (LAN) that allows access to the internet. For example, a wireless router. It can also act as a peer-to-peer (P2P) or Wi-Fi direct station (STA). This configuration allows two Wi-Fi devices to communication with each other without utilizing the internet. There are several Wi-Fi system-on-chip (SoC) modules in circulation. They help to avoid the need to build a Wi-Fi circuitry. Instead, the module can be easily wired to an embedded system to enable Wi-Fi communication.

Table 31: Wi-Fi Parameters from the IEEE 802.11 standard

Name	Speed	Frequency	Range	Comments
802.11a	54 Mbps maximum	5 GHz		Not compatible with b or g networks.
802.11b	11 Mbps	2.4 GHz	150 ft	Compatible with g networks
802.11g	54 Mbps	2.4 GHz	150 ft	The most common. Has great speed and backward compatibility.
802.11n	100 Mbps	2.4 and 5 GHz		The fast network. Can reach up to 600 Mbps by using multiple frequencies at the same time and combining them

3.2.9.2 Bluetooth

This wireless connectivity solution has been around for more than two decades. It is also very popular in smart devices. It offers easy and reliable medium for P2P communication. Some of the favorite applications are wireless audio, location services, wearable devices, and automation solution.

This technology has evolved to provide lower energy consumption and wider range. It is also marketed as costing less than all the major competitors. It is argued that Bluetooth Low Energy (LE) will have a 30% market share in IoT industry [40]. The latest version is Bluetooth 5. It adds two more physical layers called PHY to what the Bluetooth 4 had. The PHYs are LE 1M, LE 2M and LE Coded. LE 1M was packaged into Bluetooth 4. Data rate is based on Gaussian Frequency Shift Keying. Its symbol rate is 1 mega symbol per second (Ms/s). The newer version LE 2M PHY increases the speed by 100% to 2 Ms/s. This allows for much more data rates than the previous standard.

The anticipated increase in demand for higher data transfer at low power prompted the move to enhancing speed and even. Cases such as, sports and fitness, medical devices, and Lifestyle Analysis are growing trends generating an abundant of data. These all need speed and less airtime to wirelessly transmit to have spectral efficiency [40]. This new feature enhances wireless firmware updates in a much shorter time. The LE 2M increased the frequency deviation used in Bluetooth 4 from 185 kHz to 370 kHz. Much of the technical aspects are like the LE 1M such as 2-level Gaussian Frequency Shift Keying. Doing the minimum frequency deviation guard against interference.

Bluetooth modules have been reported to record over 350 meters in informal testing Manufacturers have recorded range of over 500 meters in their data sheets. However, Bluetooth 5 is expected to drastically increase the range by about 4 times. This is driven by the third PHY; the LE Coded PHY. This block is tasks with performing error detection and correction. Since broader distance introduce more noise into the transmitted signal – the probability for error in the received data increases. However, the ability to detect and correct errors (as shown in Figure 41) mean that further distance between transmitter and receiver is allowed even at a much lower Signal to Noise Ratio (SNR). The Bluetooth 5 is designed to achieve 0.1% Bit Error Rate. So, while the strength of the signal fades at increasing distances, the LE Coded PHY will ensure that reliable data is delivered to receiver thus enhancing the reach. The error detection is implemented by Cyclic Redundancy Checking. And The error correction is done by Forward Error Correction scheme.

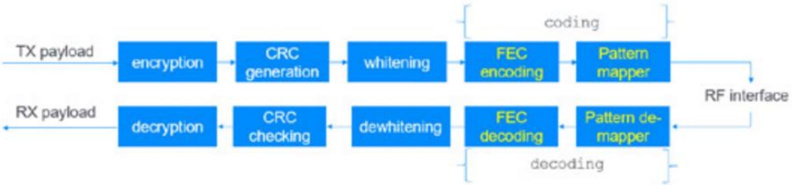

Figure 41: FEC in Bluetooth 5-bit stream processing

3.2.9.3 Inter-Integrated Circuit (I2C)

I2C communication protocol are used in many applications such as sensors and gyroscope modules. Key characteristics, advantages and disadvantages are tabulated in Table 32. This protocol offers multiple master to one slave or vice versa. It does this through an address scheme. The I2C interface includes a Serial Data (SDA) and a Serial Clock (SCL) pin. This protocol uses serial synchronous technology. Bits are transferred and sampled in bit sequence based on the clock signal generated by the master [43].

Table 32: I2C Key attributes

Attributes	Quantity	Advantages	Disadvantages
Wires	2	Uses just 2 wires	Less data transfer rate than SPI
Speed modes	Standard 100 kbps Fast 400 kbps High 3.4 Mbps Ultra fast 5 Mbps	Well supported	Only 8 bits for data
Synchronization	Synchronous	Allows multiple master/slave application	Harder to implement than SPI
Interface	Serial	Data transfer acknowledgement	Does not know slave address ahead of time
Masters	Unlimited	Easier to implement than UART	-
Slave	1008	-	-

Figure 42 illustrates the structure of the I2C data frame. At the start of transmission, the SDA signal goes from high to low followed by the SCL signal that also goes to low. This process is repeated when data flow stops, however both the SDA and SCL goes to high in the order listed. The address frame has the address for the destination for data transfer. Typically, the address is broadcast to all the connected slaves, the slave that has a match replied with a low ACK signal back to the master, but the other slaves keep a high signal, hence taking no action. The Read/Write protocol denotes whether data will be read (low level) or write (high level) to the slave. On the other hand, the ACK/NACK validate whether data was successfully received by the slave or not. After each data frame is sent, an AC/NACK is generated by the interface that is receiving the data. I2C mainly restrict data frame to 8 bits and sends most significant bit (MSB) first.

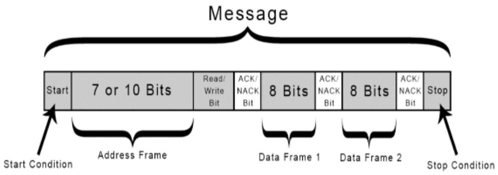

Figure 42: I2C Data Stream

3.2.9.4 Universal Asynchronous Receiver Transmitter (UART)

UART is widely used to connect devices to microcontroller such as Bluetooth modules and RFID modules. UART is unique in that it not technically a communication protocol as I2C and SPI, instead it is a physical circuit in the microcontroller [44]. It can also be a designated IC.

UART only requires two wires to send and receive data. The UART interface must be on the sending device and the receiving device. Data is sent from the pin called TX and received on the RX pin. It transmits data asynchronously. When it needs to transmit, it adds start bit to the data bits to be sent and terminate transmission with a stop bit. The two UART interfaces operate at the same baud rate so sampling of the correct data occurs. Baud rate is the rate at which data is transferred and may only differ by 10% and still receive accurate transmission. Some important features are listed in Table 33.

Table 33: UART Key Attributes

Attribute	Quantity	Advantage	Disadvantage
Wires	2	2 wires	Single master/slave
Speed	Up to 115200 baud	No clock required	10% baud rate between each other
Synchronization	Asynchronous	Error checking	Data frame limit to 9 bits
Interface	Serial	Adjustable data rate	-
Masters	1	Well supported	-
Slave	1	-	-

The UART organize data into packets. Figure 43 below illustrates the start bit, stop bit (one or two bits) and parity bit (0 or 1) to the actual data frame. These additions will be striped by the receiving UART before it is sent as parallel stream to a microcontroller or some other type of device such as memory or sensor. When there is no transmission ready, the UART it is positioned in a high voltage mode. When data is ready to be transferred it toggles from high to low voltage. This configuration uses a pull-down resistor and is interpreted by the receiving UART that data will be transmitted. Hence it starts to sample the line per the chosen baud rate. Data frame can be a maximum of nine bits. This depends on the type of UART and whether parity bit is added to the packet. Parity is used to detect error in data. A 0 or 1 parity bit means even or odd parity. Depending on the selection – all the received 1 bits in the transmission must add to either an even or odd number. If the sum does not agree with the parity, then error is said to be in the data stream. Many factors can cause errors. These include electromagnetic interference, radiation or just plain noise. At the end of the data frame, the UART goes from low to high voltage in one or two cycles.

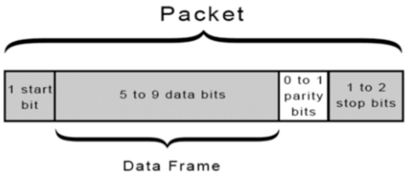

Figure 43: UART bit Stream Representation

3.2.9.5 Serial Peripheral Interface (SPI)

SPI communication module is used as an interface between many devices. 2.4 GHz wireless transmitter/receiver and RFID card reader modules are some examples of devices that use this protocol to communicate with microcontrollers. A key feature (see Table 32) of SPI protocol is that data flows in a continuous stream. This means that there is not break between transmission or data does not have to be packetized.

The fundamental principle behind SPI is the master-slave communication technique [45]. A simplified diagram depicting this relationship is shown in Figure 44. A controlling device, usually in the form of a microcontroller acts as the master. It acts to generate clock signal for its host and for the slave device. Slave devices can be any peripheral devices such as a sensor, motor or another microcontroller.

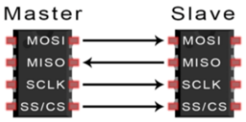

Figure 44: SPI Master-Slave Operation

First, the Master Output Slave Input (MOSI) line is designated for the master to sends data to the slave. Second, the Master Input Slave Output (MISO) accepts data from the slave. The other lines are the Clock (SCLK) for generating clock pulses and the Slave Select/Chip Select (SS/CS) for choosing the slave to transmit data to. Table 34 demonstrates SPI's key attributes.

Table 34: SPI Key Attributes

Attributes	Quantity	Advantages	Disadvantages
Number of wires	4	Continuous data flow	Requires more wires, 4
Maximum speed	Up to 10 Mbps	Addressing not need	No Ack
Synchronization	Synchronous	Send/Receive at once	No error check
Interface	Serial	Greater data rate than I2C	Single master
Number of masters	1		
Number of slaves	Unlimited		

The slave sample bits in sync at the same clock sequence at which the master is outputting data bits. The clock can be configured to transfer one bit at rising or falling edge of the clock. This is available through the clock polarity and phase functions. Since data is transmitted at each clock signal, the data transfer rate is determined by the clock frequency. The master can be used to select and communicate with multiple slaves. There could be multiple SS/CS line to decide which slave to talk to. Another way is to invoke the daisy chain wiring technique that use on SS/CS line.

3.2.10 PCB Modules

This section compares all the modules that will be considered in our PCB design.

3.2.10.1 PCB Vendor and Assembly

Understanding the PCB vendor selection process can save time and money. Factors that were considered were [130]: verified whether the supplier has high quality, found out if they specialize in the type of electronic equipment to be manufactured, distance between you and supplier, minimum quantity, turnaround time, contact potential supplier to find out if they can make PCB, supply files for quote.

3.2.10.2 Wireless Modules

Developing an embedded system to perform custom tasks can be the ideal choice for a project. Deciding on which parts to choose can be difficult. To make an informed decision it was recommended to gather information about each technology. This information helped by showing what areas these parts are strong or weak in.

Another element of development was to strategically select parts that are packaged as modules and can perform the tasks effectively and efficiently. This improved reliability and accuracy in the product. This section will cover some well-known communication module.

There were two main wireless communication modules that were discussed. They were Wi-Fi and Bluetooth standards. The Wi-Fi standard can be customed built, but its stability requires well established tools and knowledge on its working principle. Hence it may be more feasible to buy an available module and embed it in our design. The same is true for Bluetooth and other types of wireless standards. Today, many manufacturers are producing these types of modules. There are also available videos and written tutorials to help designers implement these modules into their design

3.2.10.2.1 ESP8266-12E Wi-Fi Module

This Wi-Fi module was first launched in 2014 and quickly grew very popular. It currently has a large online supporting community. This is now classified as an old model after it was succeeded by ESP8266EX 2018 versions. These versions will be covered later. The ESP8266 model was supported by more than 15 versions [54]. The ESP-01 was the first model and is not widely available. Some other version that are still marketed and readily available are the ESP-12E or ESP-12F. Vast number of product line create many confusions with the different names referenced in various data sheet. Older models seem to be referred to as ESP8266EX and ESP8266 interchangeably. Figure 45 shows the module of an ESP8266MOD from AI Thinker.

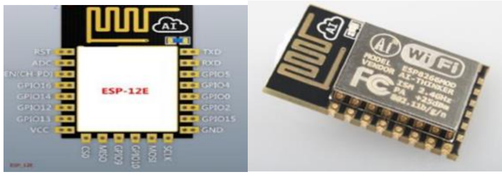

Figure 45: ESP8266-12E Wi-Fi Module (Front and back view)

The ESP8266-12E versions is more than just a Wi-Fi module. There are many Wi-Fi module versions that differ mainly in areas like number of pins and antenna. Table 35 shows comparison among two of the most popular ESP8266 Wi-Fi module versions.

Table 35: ESP8266 series Wi-Fi modules

Name	Active pins	Pitch	Antenna	Shielded	Dimensions (mm)	Notes
ESP-12E	20	2 mm	PCB trace	Yes	24.0 x 16.0 x 3.0	4 MiB flash.
ESP-12F	20	2 mm	PCB trace	Yes	24.0 x 16.0	FCC and CE approved.

The main reason for researching this line of product was to make use of its features. Some key features of the ESP-12E include:

- 802.11 b/g/n
- Integrated low power 32-bit MCU
- Support STA/AP/STA+AP operation modes
- Support Antenna diversity

- SPI, UART, I2C, PWM, GPIO, SDIO
- Integrated TCP/IP/UDP/HTTP/FTP/IPv4 protocol stack
- +20dBm output power in 802.11b mode
- Operating temperature range ~40C ~125C
- Operating voltage 3.0 ~ 3.6 V
- Operating current: Average 80 mA
- SDKs: Arduino, ESP8266 BASIC, ESP Easy, ESP-Open-RTOS NodeMCU, MicroPython

This Wi-Fi SoC was available in package of two on Amazon for $7.66. It offered full internal Wi-Fi networking solution. This allows for it to behave as the host of the application or to hand all the Wi-Fi networking functions to another application processor. Its processing and memory capability made it for integrating with sensors and other devices via its GPIO pins.

3.2.10.2.2 ESP8266EX

This platform has two recommended versions to provide wireless connectivity as a Wi-Fi System on Chip (SoC) or as a development kit. The major difference with the two versions known as ESP-WROOM-02D and ESP-WROOM-02U is than one carries an onboard antenna and the other works with an U.FL IPEX antenna that is external to the module. According to data sheet, it can perform as a standalone application or as a slave to a host MCU. Interfaces like SPI and UART can be used to allow Wi-Fi adaptor interaction between the ESP8266EX and microcontroller. Aside from its Wi-Fi module, the L106 Diamond series 32-bit processor and on-chip SRAM can interface sensors via GPIOs and Software Development Kit (SDK) for custom coding applications. This platform is marketed with robust features such as:

- Quick transition time between sleep and wakeup mode or energy efficient cases
- Adaptive radio biasing for low power operation
- Advance signal processing
- Interference mitigation technology

This platform is Wi-Fi certified through Wi-Fi Alliance and other major organizations. Per the manual, the development kit on-board processor has 80% (< 50 kB) of the processing power free for user application programming and development during operation. One of the three CPU interfaces is the programmable RAM/ROM interface (iBUS) that can be connected with memory controller and used to access flash. Note there is no programmable ROM in the SoC. Hence, user application programming must be stored in an external SPI flash which is supported 512 kB up to 16 MB memory capacity.

The module can operate in Station Mode where it can connect to a Wi-Fi network. It can also operate in SoftAP mode where it can behave as an Access Point so other devices can connect to it over Wi-Fi. Both modes can also be supported at the same time. The module is currently selling for about $3.00 at Mouser where symbol and footprint is also available. Figure 46 shows ESP-WROOM pin layout.

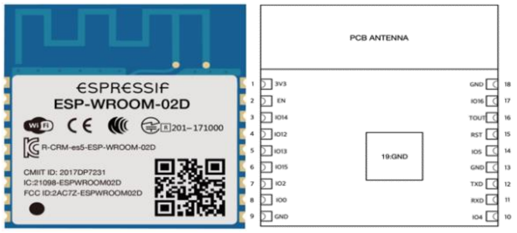

Figure 46: ESP-WROOM-02D version of ESP8266EX with pin layout view on right

3.2.10.2.3 ESP32

This ESP32 series offers more wireless connectivity choices as well as wired connectivity. This option would offer some redundancy in communication options in the event one network is not available. Given that the project will be confined to the main UCF campus where network connection can be unreliable due to the large traffic on the network – having more than one communication options could be a real plus.

This is much more than just a Wi-Fi, Bluetooth or Ethernet module, it is a complete microcontroller that has a Xtensa® single-/dual-core 32-bit LX6 microprocessor(s), with up to 600 MIPS chip design for mobile, wearable electronics, and Internet-of-Things (IoT) applications. It offers ultra-low-power solution. For example, in low-power IoT sensor hub application scenario, ESP32 is woken up periodically when specified condition is detected. The power amplifier output is also adjustable allowing flexibility between communication range, data rate and power consumption. This series of microcontroller can be programmed with the Espressif IoT Development Framework (IDF) whose memory profile includes:

- 448 KB ROM
- 520 KB SRAM
- 16 KB SRAM in RTC
- QSPI supports multiple flash/SRAM chips

In addition to the below Wi-Fi and Bluetooth Key Features, this microcontroller has clocks and timers, basic and advanced peripheral interfaces including SPI, UART, I2C, Ethernet MAC, 12-bit SAR ADC up to 18 channels, 2 x 8-bit DAC, 34 x programmable GPIOs, Motor PWM IR (TX/RX).

Wi-Fi Key Features:

- 802.11 b/g/n
- 802.11 n (2.4 GHz), up to 150 Mbps
- WMM
- TX/RX A-MPDU, RX A-MSDU
- 4 x virtual Wi-Fi interfaces
- Simultaneous support for Infrastructure Station, SoftAP, and Promiscuous modes

Bluetooth Key Features:

- Compliant with Bluetooth v4.2 BR/EDR and BLE specifications
- +12 dBm transmitting power
- Standard HCI based on SDIO/SPI/UART
- High-speed UART HCI, up to 4 Mbps

The ESP-WROVER-32IB ESP32 series by Grid Connect has a PCB trace antenna as well as an U.FL IBEX connector. It is an open-source module allowing users to customize to their suit. GitHub provides example code resources to help with device customizations. It is currently available on Grid Connect for $4.50 for 4 MB Flash and $5.20 for 16 MB Flash. The ESP32-WROVER's footprint is a suitable substitute for the ESP-WROVER-32IB.

3.2.10.2.4 UFL Antenna

The module may require an RF U.FL antenna that is available on Digi-Key for about $7.07. Below are specification for the 66089 U.FL antenna series:

- Frequency range: See table
- Impedance: 50 ohms
- Gain: 3 dBI
- VSWR: 1.7 max
- Radiation: Omni Directional

3.2.10.2.5 CC3100 Wi-Fi Module and Bluetooth

This TI Wi-Fi MCU offers more than wireless connectivity, it is also a complete microcontroller that can be used as a regular microcontroller with the added benefit of a SoC Wi-Fi module. The focus of this section is to highlight the Wi-Fi capabilities. This Wi-Fi MCU is powered by an ARM Cortex-M4 core with a speed of 80 MHz. It provides all the basic interfaces relevant for this project including:

- UART
- SPI
- I2C
- ADC
- SD
- I2S

This module supports station (STA), AP, and Wi-Fi Direct (P2P) connection modes. According to the user manual the processor subsystems features a Wi-Fi Internet-on-a-chip, and a dedicated ARM MCU that can offload the application MCU completely. This feature could be beneficial for the project given that non networking applications can work independent of the Wi-Fi networking workloads.

This product is not as popular as the ESP series covered in the above sections, but TI known to provide documentations and sample code. TI could also provide technical in-person assistant if it is needed. The product is currently selling for $18.88 and $17.71 on vendor sites. Figure 47 is an illustration of the CC3100MID Wi-Fi MCU.

Figure 47: CC3100MOD Wi-Fi module

3.2.10.2.6 Wi-Fi Module Selection

Four Wi-Fi modules were considered for this project. Evaluating these models for a clear winner is rather difficult. To aid in this process, the below criteria were developed:

- Support documentations and community resources
- Ease of use
- Cost

Other senior design projects had used at least one of the modules that were considered. That was also factored in which one was chosen. All the modules that were looked at satisfied the Wi-Fi standard and are certified. See Table 36 for a summary of some of the key features from the four models that were considered. This was important in ensuring reliable data transfer. One of the most important criteria was the ability to get programming and design support and the ESP8266EX scored very high in this category. It also scored high in the perceived ease of use and the 1.5 pin pitch which could make it easier to solder. It also had the lowest price.

The ESP32 models has several on chip communication protocols that made it a very exciting candidate for our project. This was because having multiple wireless communication options offers more redundancy. It even had Ethernet protocol that could offer wired internet connect. It also had competitive price range. It is not clear if this model had all the support that would be required to implement it into our design as it was a newer model.

The CC3100 also offers flexibility but while TI provides reasonably enough support there has not been a lot of project execution among the online community. This was an important selection feature. Given these factors, ESP8266-12E was the selected as our Wi-Fi module. It seemed the easiest to use and more resource materials were available online. It could also work seamlessly with many third-party IDE such as Arduino.

Table 36: Wi-Fi Modules Comparison

Model	ESP8266-12E	ESP8266	ESP8266EX	ESP32	CC3100
Bluetooth v4.2 protocols	No	No	No	Yes	Yes
Bluetooth Low Energy (BLE)	No	No	No	Yes	-
Ethernet protocol	No	No	No	IEEE-802.3-2008	-
Wi-Fi transmit power	+20dBm	< +20dBm	< +20.5 dBm	< +20.5 dBm	17dBm
Bluetooth transmit power	-	-	-	< +9 dBm	-
Interface	SDIO 2.0, (H) SPI, UART, I2C, I2S, IRDA, PWM	SPI, UART, I2C, PWM, GPIO, SDIO	UART/HSPI/I2C/I2S/IR Remote Control	SD card, UART, SPI, SDIO, I^{2}S, PWM, I^{2}C, ADC, DAC	I2C, SD/MMC, SPI, UART
Wi-Fi data rate & range		54 Mbps < 150 ft	54 Mbps < 150 ft	< 150 Mbps* < 150 ft	13, 16, 54Mbps < 150 ft
Bluetooth data rate & range	-	-	-	< 330 ft	-
Ethernet data rate and range	-	-	-	10 - 100 Mbps	-
Operating temperature	-40C ~ 125C	- 40C ~125C	- 40 °C ~ 85 °C	- 40ºC ~ 125ºC	- 20 C ~ 70 C
Costs	~$7.66	~$6.99	$3.00 ~ $3.20	$4.50 ~ $5.20	~ $17.71
Antenna	PCB trace	PCB trace	PCB trace	PCB trace/External	External
Supply current (min)	500 mA	-	500 mA	500 mA	-
Operating current (average)	80 mA	80 mA	80 mA	-	-
No. of power modes	5	5	5	6	5
Power modes ranges	10 µA ~ 170 mA	10 µA ~ 170 mA	20 µA ~ 170 mA	5 µA (min)	-
Dimensions (mm)	16 x 24	16 x 24	18 x 20	18 x 25.5	20.5 x 17.5
Pitch (mm)	2.0	2.0	1.5	1.27	1.27
Support/age	High/old	High/old	High/moderate	Moderate/new	Low/moderate

3.2.10.3 PCB Angle Control Module

In robotics, angle measurement is a key component in the functionality of a robot, from autonomous movement to error correction a rotating component on a mechanical device requires a module that can monitor its rotation and keep track of the current placement of the component. Many mechanical and electronic components that we normally use daily like smart phones, cars, and others all utilize an angle measurement module or an angle control module. The most common angle control modules are usually gyroscopes and encoders. For our PV panel movement, we wanted to utilize some form of angle control module to help us determine where the PV panel is facing to further adjust the position to ensure optimal light detection.

3.2.10.3.1 Gyroscope

A gyroscope, also known as a gyro, is a small integrated sensor dedicated to measuring the angular velocity of a rotating object. The gyro measures angular rotation in degrees per second or revolutions per second. By measuring angular velocity, gyros can determine the orientation of the object to which they are attached to, constantly reading the angular velocity to determine the change in angle leading to the calculation of the orientation based on any of the 3 axis (x, y, and z).

For our PV panel, a gyro would have been needed to ensure that we do not position the PV in an angle that is facing the wrong direction of the sun or to make sure the position of the PV is not creating strain or stress to the motor to which point it could damage it. [60]

Based on the different gyroscopes on the market that can help us collect the necessary data, we have determined that there is a model that can best fit our work: the ITG 3200 3 axis gyroscope. The ITG 3200 is shown in Figures 48 and 49, and Table 37 details the specifications for this gyroscope.

Figure 48: ITG 3200

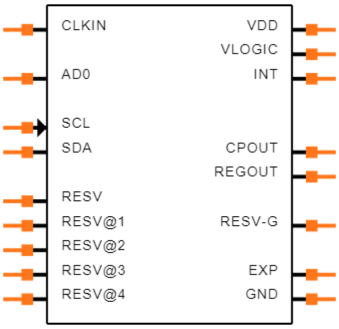

Figure 49: ITG 3200 Footprint

Table 37: ITG 3200 Specifications

Item	Specification
Typical VDD	2.5V
Typical Operating Temperature	25°C
Cross-Axis Sensitivity	2%
Rate Noise Spectral Density	0.03 °/s/√Hz
Gyroscope Mechanical Frequencies	30-36 KHz (x-axis), 27-33 KHz (y-axis), 24-30 KHz (z-axis)
Gyroscope Startup Time	50 ms
Output Data Rate	-

3.2.10.3.2 Inertial Measurement Unit (IMU)

According to Caroline Rees, “An Inertial Measurement Unit (IMU) is an electronic device that uses accelerometers and gyroscopes to measure acceleration and rotation, which can be used to provide position data.” [61] While a standalone gyroscope can determine orientation of an object based on the angular velocity from a turn on an axis, the IMU uses both the gyroscope and the accelerometer to determine position and orientation. These sensors are more commonly used and essential in any system that can be controlled remotely such as drones to enhance their control, stability, and provides the factor of mobile mapping into play as well.

Based on the different gyroscopes on the market that can help us collect the necessary data, we have determined that there is a model that can best fit our work: the MPU 9250 IMU. The MPU 9250 IMU is shown in Figures 50 and 51, and Table 38 details the specification for this sensor.

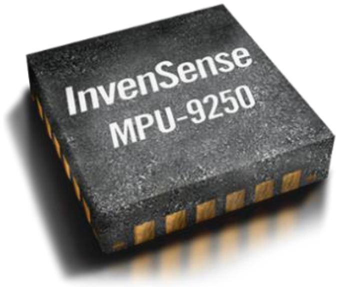

Figure 50: MPU 9250 IMU

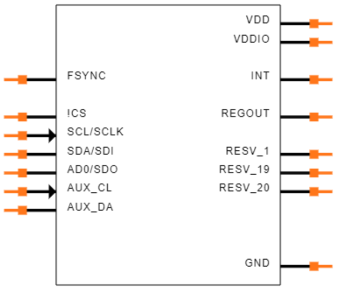

Figure 51: MPU 9250 Footprint

Table 38: MPU 9250 Specifications (Only Gyro Active)

Item	Specification
Typical VDD	2.5V
Typical Operating Temperature	25°C
Cross-Axis Sensitivity	±2%
Rate Noise Spectral Density	0.01 º/s/√Hz
Gyroscope Mechanical Frequencies	25-29 kHz
Gyroscope Startup Time	35 ms
Output Data Rate	4-8000 Hz

3.2.10.3.3 IMU vs Standalone Gyro Module Selection

Based on the two model we have seen that would be beneficial to use in our work, we analyze which would provide the best outcomes. Looking at the similarities both the MPU 9250 and the ITG 3200 share the same VDD and typical operating temperature only. The real differences come in the performance that each system brings. The only factor depicted in Tables 35 and 36 where the ITG 3200 seems to have a better outcome is in the cross-axis sensitivity set at 2% whereas the MPU 9250 has a more variable sensitivity at a ±2%. However, this set cross-axis sensitivity falls back as each of the axis on the ITG 3200 have more broad and different mechanical frequencies whereas the MPU 9250 axis' mechanical frequency all are the same and lower than any of the axis in the ITG 3200. This variable frequency can become a real issue since it could output different results based on the axis you are turning on. Therefore, with a lesser response time, a better set and smaller mechanical frequency range, and a smaller Noise Spectral Density, the better option for our work would have been using the MPU 9250 IMU.

After further testing, we decided that the IMU was not a necessary element to have in our project. After building our first few prototypes, we noticed that each time we moved the PV Panel the angle change was constant at 5˚, therefore we could determine where the PV was facing all the time using a value on our program that would increase or decrease depending on the direction of the movement.

3.2.10.4 RS-232 to TTL Module

As previously mentioned, one possible method to measure current output from the solar panel is by using a relay. The measurement is typically stored inside the relay registers. The relay can communicate its register’s values through Modbus communication protocol. One type of Modbus protocol is the RS232 protocol. This communication protocol could be used to transfer the current measurement stored in the relay’s registers using RS232 protocol to the MCU.

Since the RS232 protocol standard has significant voltage differences compared to most MCUs, an interface is required for communication. The MCUs being considered uses the TTL level UART, where a 0 V is interpreted as low, and 5 V level represents high. With the RS232, a 3 to 15 V level is low, and -3 to -15 V is high. Hence the interface between the MCU TTL level UART and the RS232 should be able to regulate the voltage difference [53]. Figure 52 shows a RS232-to-TTL converter schematic that could satisfy this need.

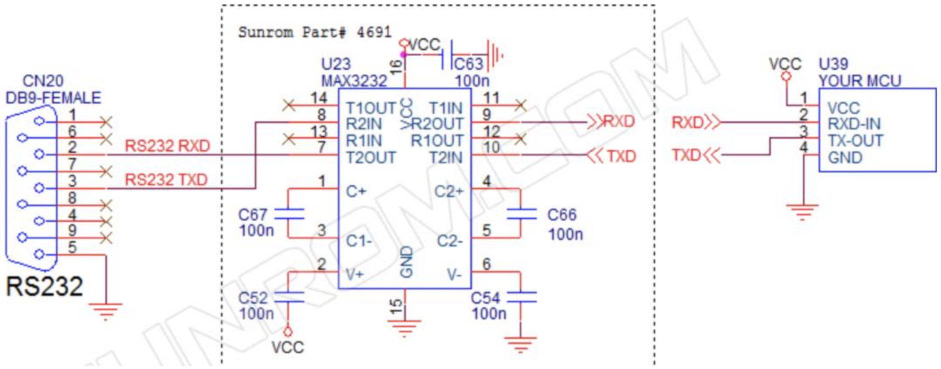

Figure 52: MAX3232 RS232 to TTL Converter schematic (Permission to use granted)

As shown, the MAX3232 family microcontroller integrates the RS232 and the TTL UART interfaces. This is available as module, also known as breakout boards. Average price is currently around $8.08. The MA3232 family of chips are available from various vendors ranging from $0.84 to $1.13. The MA3232 family of chips are manufactured by TI. Hence, the code composer studio IDE could be used to program this module. Instead of going with a module, the MAX3232XXX microcontroller could be integrated into our PCB.

After further research and careful consideration our team decided not to implement a relay in the final design. The relay was to allow the retrieval of voltage and current reading of the PV. As a result, the RS232-to-TTL interface was no longer required in our design.

3.2.10.5 Microcontroller Modules

A major part of our project was to design a PCB. This section reviewed a few microcontrollers that could handle the project needs. Needs include programmable, sensing, ADC, power monitoring, flashing, and low cost. It was important to use a microcontroller that was moderately easy to program, well supported and documented, and has moderately low power consumption. Hence these were the primary features in the decision factor.

3.2.10.5.1 Atmega328p

This microcontroller is arguably the most popular, it is favored by a vast community of designers. This chip has great benefits such as ease of programming and support. Information to work with this microcontroller would be hassle free given the vast number of projects that it has been used in. This chip is also compatible with the Arduino IDE that is an open-source platform and is also very well known. Features of this microcontroller include:

- 32KB flash memory
- 20 MIPS @ 20 MHz
- 2K SRAM
- 1K EEPROM
- 3 Timer/Counter
- 28 pins including 23 programmable I/O lines
- 6-channel 10-bit ADC

The Atmega328p is an 8-bit AVR microcontroller with advanced RISC architecture capable of providing all basic features such as flash memory, peripheral interface and GPIO.

3.2.10.5.2 ESP32

This microcontroller was released in 2016 and quickly captured the attention of designers. Partly because it was an upgrade to the previous dominant model, ESP8266EX and that it packaged a complete Wi-Fi and Bluetooth/BLE modules as SoC. This instantly cut design complexity, reduce development time and cost while offering communication and microcontroller needs all in one package. ESP8266 was the leader in inserting Wi-Fi modules in microcontroller and this ESP32 has taken it to a more advanced level. Its CPU runs the Xtensa dual or single core 32-bit LX6 microprocessor and an Ultra-low power (ULP) co-processor.

Aside from the powerful features, this model has huge community support and documentation. The development platform provided by Espressif is called IoT Development Framework (IDF) and is fully compatible with Arduino IDE. Below are some of the standout features of the ESP32:

- 600 DMIPS @ 160 or 240 MHz
- 520 KiB SRAM
- Wireless connectivity
- Wi-Fi:
  - IEEE 802.11 b/g/n
  - Bluetooth: v4.2 BR/EDR and BLE
- 16 Peripheral interfaces including:
  - 4 x SPI
  - 2 x I2C
  - 3 x UART
  - Ethernet
  - 12-bit SAR ADC
  - 2 x 8-bit ADCs
  - Motor PWM
- Power management
  - LDO regulator
  - Wake up from GPIO interrupt, timer
- Security
  - IEEE 802.11 standard security features including WFA, WPA/WPA2 & WAPI
- Cost
  - $4.50 ~ $5.20

3.2.10.5.3 MSP430FR6989

The MSP430FR6989 is a powerful and popular microcontroller. It can be used in a huge number of applications. It is very well supported and documented by Texas Instrument. Another key plus for this microcontroller is that it was the microcontroller that was used by UCF’s faculty to teach undergraduate students embedded systems. Hence, many students have some basic knowledge about this product. This microcontroller has all the capabilities to implement our project design. Aside from great pricing, this may also offer other integrative features such as energy monitoring that would streamline other project needs. Figure 53 shows the MSP430 LaunchPad Development Kit. Figure 54 is the MSP430FR6989 module without the development kit.

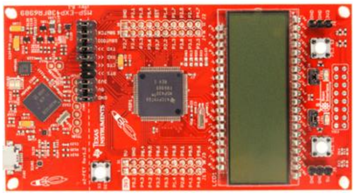

Figure 53: MSP430FR6989 LaunchPad Development Kit

TI is a reputable organization that is essential to the embedded industry. The MSP430 is one of their flagship product series. The MSP430FR6989 support basic functions such as Ultra-low power modes, Interrupts, Multiplexed port pins. Other key features include:

- Embedded Microcontroller
  - 16-bit RISC Architecture 16MHz
  - Wide supply voltage range 1.8 V to 3.6 V
- Optimized Ultra-low power modes
  - Active Mode: Approximately 100 µA/MHz
- Ultra-Low-Power Ferroelectric RAM (FRAM)
  - Up to 128KB of Nonvolatile Memory
- High-Performance Analog
  - 12-Bit Analog-to-Digital Converter (ADC) With Internal Reference and Sample-and-Hold and up to 16 External Input Channels
- Multifunction Input/Output Ports
- Enhanced Serial Communication
  - eUSCI_A0 and eUSCI_A1 Support:
  - UART With Automatic Baud-Rate Detection
  - IrDA Encode and Decode
  - SPI – eUSCI_B0 and eUSCI_B1 Support:
  - I2C With Multiple-Slave Addressing
  - Hardware UART and I2C Bootloader (BSL)
- Cost
  - $7.86 to $8.04 each on Mouser Electronics

Figure 54: MSP430FR6989IPNR by Texas Instrument

3.2.10.5.4 MSP430FR6989 Bootloader (BSL)

Bootloader is one way to program the MSP430FR6989. This will allow us to write the binary files to the microcontroller or read binary files from it [128]. BSL does not offer debugging as JTAG or SBW. However, for our purpose BSL is enough as debugging can be done on a LaunchPad via CCS and JTAG and then write the code via BSL to the MCU. The CCS IDE is equipped with the tools to generate the TI TXT file protocol used by BSL. The files and software needed to perform this process can be found on TI's website. The target device which is the MSP430FR6989 will need an external oscillator to generator clock signal [132].

The team selected the JTAG interface programming instead of the BSL method shortly before we were getting ready to start programming the MSP430FR6989 MCU because this avoids the need for any additional parts. To accomplish this, we used the eZ-FET that is part of the MSP430FR6989 LaunchPad. The jumpers on the launchpad were removed.

Once removed, this separated the eZ-FET from the host MCU. We then use jumper wires to connect the eZ-FET header pins to our custom MCU header pins and use CCS to flash it. This made flashing and debugging very effective, save time and safe.

3.2.10.6 PCB Network Considerations

While talking to UCF's networking staff and faculty, it was discovered that there could be some hinderance to rely solely on Wi-Fi communication including separate networks at the same time. Partly because the project will be at UCF and will need access to the Local Area Network. The problem arises per the original idea to have a field microcontroller communicate over Wi-Fi with second microcontroller. The second would also need to connect over Wi-Fi to the UCF's LAN. This dual Wi-Fi connection is the primary issue. Essentially the second microcontroller can only connect to a single Wi-Fi network per session. Therefore, it may be very difficult to establish Wi-Fi connection with the field microcontroller and UCF's LAN at the same time. As such, other methods of wireless communication were considered.

This section discusses possible solution to the networking complexities being faced. Again, this is because of the difficulty to connect multiple Wi-Fi networks simultaneously. First, a switch implementation will be reviewed and then a server option.

3.2.10.6.1 Network Switch

A switch is a device that connects multiple devices creating a local area network (LAN). All the devices on this LAN can communicate using their MAC addresses. The switch keeps a record of all the connected devices MAC addresses. Switches are plug-and-play devices.

The idea would be to connect the field microcontroller and a second microcontroller to a network switch. The switch would also be connected to the UCF's router. Currently, the switch that is known must be connected to using cable such as an Ethernet. Since one of the requirements for the project is to use a Wi-Fi module this may not be a solution. On the other hand, one of the Wi-F modules that was considered does have Ethernet functionality. However, that was not the module that is preferred. Specific information can be found under Wi-Fi modules comparison section.

3.2.10.6.2 Web Server

Using a web server seems to be a practical solution to the connectivity issues. A web server is a computer system that hosts websites and runs web server software [54]. This would enable the field microcontroller to connect to the UCF's WAN and send and receive request from the webserver. The second microcontroller could perform this same task. The web server could also run on the second microcontroller, in this case a Raspberry Pi 4. This may turn out to be the cheaper option however, it may increase the programming workload. Also, it would demand more memory on the host microcontroller. These potential issues will be discussed in another section of this report.

After further deliberation the team decided not to implement a switch or web server communication model in our project. Instead, we decided on using the TCP Protocol communication technique. More information about this technique can be found under the Communication Systems section of this document.

4. Related Standards

This section goes over standards that were used or considered to be used in this project. The application or use of the standard in our project will be justified. Each standard will be introduced and described.

4.1 IEEE Standard for Synchrophasers for Power Systems

Standards facilitate technology exchange and enable innovation. Standardization improves efficiency in design and development. Standards provide uniformity, allowing for accurate exchange of data between different businesses. There are many benefits in using standards. Therefore, in this project, the IEEE standard that defines synchronized phasor measurements used in power system applications, more specifically IEEE C37.118-2011, was considered for use if the WAMS algorithm was to be implemented. It is important to note that FPL uses this standard.

The use of the standard is important because a long-term goal, after the completion of Senior Design, is to connect the touch screen table to receive synchronized phasor measurements from the actual distribution grid. This standard is vital for a seamless transition between OPAL-RT and the actual power system. Due to time constraints, WAMS algorithm was not implemented, therefore this standard was not used since it was no longer needed.

4.1.1 IEEE Std C37.118-2011

There is an increase in the development of measurement units that are placed in the power system for data acquisition. This provides users the ability to acquire and analyze power system phasor quantities in real time. Different companies develop different hardware and/or software methods to record, transmit, and analyze these measurements. This standard enables uniformity by specifying data output formats, and therefore allowing interchange of data between multiple systems for users of both real-time and post event phasor measurements. This standard is composed of two parts: IEEE Std C37.118-2011.1 and IEEE Std C37.118.2-2011.

IEEE Std C37.118-2011.1 2011 purpose is to define synchronized phasor, frequency, and rate of change of frequency (ROCOF) measurements. [14] In addition, it describes time tag and synchronization methods for the measurements of the quantities listed. IEEE Std C37.118.2-2011 purpose is to facilitate the transmission and collection of data within a phasor measurement system. [15] It is important to note that three communication protocols are supported: TCP only, UDP only, or TCP/UDP. Due to time constraints, WAMS algorithm was not implemented, therefore this standard was not used since it was no longer needed.

4.2 RS232 Communication Standard

In the original project design, a relay was going to be used to capture the solar panel voltage and current. Although it was not utilized in the final design, research was done on the RS232 protocol since the relay would have sent the data to the PCB using this standard.

RS-232 (Recommended Standard 232) is a standard that arose in telecommunications in 1962 and still widely in use today, frequently as in modem applications [79]. It is also known as the EIA/TIA–232–E specification as it was developed by the Electronic Industry Association and the Telecommunications Industry Association (EIA/TIA). The official name of the standard is “Interface Between Data Terminal Equipment and Data Circuit–Termination Equipment Employing Serial Binary Data Interchange” although it is more frequently referred to as RS232. The current revision of this standard came out in 2012 as TIA TIA-232-F [80].

RS232 was created to address serial communication between Data Terminal Equipment (DTE), which is a host system, and Data Circuit-Terminating Equipment (DCE), which is a peripheral system. It is considered a “complete” standard in that is aims to ensure complete compatibility between the systems by addressing three main areas of concern: electrical characteristics, functional characteristics, and mechanical characteristics [79].

The electrical characteristics define the voltage levels, line impedance, and rate of change of signal levels. The standard was written before TTL logic existed, so it doesn’t use 5V logic levels. The logic reads negative voltage as a 1 and positive voltage as a 0. The high level is +5V to +15V and the low level is -5V to -15V. The receiver logic includes a 2V noise margin so can read ±5V to ±15V. Since most systems don’t operate at these voltage levels nowadays, components normally have a RS-232 IC to perform voltage level conversion. These normally invert the signal to change the logic to high level instead of low level.

The impedance of the load seen by the driver is defined as 3kΩ to 7kΩ. The standard originally specified that the cable between the host and peripheral system should be ≤ 15 feet in length but has been revised to specify a maximum capacitive load of 2500pF instead of a specific cable length. The rate of change of signal levels is specified to have a maximum slew rate of 30V/µs and a maximum data rate of 20kbs to reduce the chance of cross talk between adjacent signals [79].

The mechanical characteristics of the standard specify an interface consisting of a 25-pin connector as the minimum that can carry all the signals defined by the standard. However, other connectors are frequently used for RS232 communication with the most common being a 9-pin connector which will be used for this project. This 9-pin connector carries the most commonly used signals while eliminating the ones that are unnecessary and is sufficient to send the solar panel data to the PCB for this project.

The functional characteristics of the RS232 standard define the various signals that are transferred through the pin connectors. These signals are divided into four categories:

common, data, control, and timing. The most common signals that are carried through the 9-pin connector are shown in Table 39 [79].

Table 39: RS232 Common Signals

Signal Name	Direction	Type
Data Carrier Detect (DCD)	From DCE	Control
Receive Data Line (RD)	From DCE	Data
Transmit Data Line (TD)	To DCE	Data
Data Terminal Ready (DTR)	To DCE	Control
Ground	N/A	N/A
Data Set Ready (DSR)	From DCE	Control
Request to Send (RTS)	To DCE	Control
Clear to Send (CTS)	From DCE	Control
Ring Indicate (RI)	From DCE	Control

Since the inverter was not used for the project, the output of the solar panel was no longer AC, it is now DC. Since RS232 was no longer needed to read the values from the relay, this standard was not used.

4.3 High-Definition Multimedia Interface Standard

The RBP outputs to the touch screen display via High-Definition Multimedia Interface (HDMI). This interface is defined by the Consumer Technology Association standard “CTA-861-G: A DTV Profile for Uncompressed High Speed Digital Interfaces” which was originally published in November 2016 [81] and slightly revised in November 2017. The standard is available for free download on the ANSI website. The majority of the extensive CTA-861-G standard deals with the Extended Display Identification Data (EDID) which sinks use to declare their “display capabilities and characteristics” [81]. Annex D of CTA-861-G defines the data block used by HDMI including the bit organization. It notes that HDMI carries each frame in an HDMI packet called an InfoFrame which must be ≤ 30 bytes. It notes that HDMI can support many audio formats including uncompressed and compressed formats.

There have been several versions of HDMI that have been released. Version 1.0 was released in December 2009, and the most recent version is 2.1 which was released in November 2017 [83]. New releases added support for higher resolutions and refresh rates, and the latest version supports a resolution of 10k at 120Hz. The Phillips display that will be used in this project does not specify which version of HDMI it uses, but as they are backwards compatible it will not be problematic.

CTA-861-G covers the data format for HDMI but does not define the type of connectors used. HDMI is a proprietary technology and has used the same general type of 19-pin connector since it began which has allowed backward compatibility [82]. This original

HDMI connector is referred to as a Type A and has outer dimensions of 13.9 mm x 4.45mm for the male connector and 14 mm x 4.55 mm for the female connector. A mini-HDMI connector was later introduced, and then a micro-HDMI connector was released after that. This project will use a standard HDMI Type A connector at the touch screen display and a micro-HDMI at the Raspberry Pi. The micro-HDMI connector is also 19-pin with the same functionality as the Type A, but its outer dimensions are only 6.4 mm x 2.8 mm.

4.4 Universal Serial Bus Standard

Communication between the RBP and the touch screen also requires an additional connection aside from the HDMI as the touch screen needs to output the user touch data to the RBP. This communication is implemented with a Universal Serial Bus (USB) Standard B connector. USB Implementers Forum, Inc. (USB-IF) is a non-profit group founded by companies in the industry, and they developed the USB specifications and maintain the standards for USB devices [84]. The RBP has ports for both USB 2.0 and USB 3.0, but the Phillips USB-B connection supports only the USB 2.0 connection.

USB 2.0 supports a data transfer speed of 480 Mbps while USB 3.0 supports up to 4.8 Gbps meaning that it is 10 times faster. The ports are not backwards compatible. A USB 2.0 can be plugged into a USB 3.0 port, but the 3.0 cannot usually be plugged into a 2.0 port [85]. This is because version 3.0 increased the connection wires from 4 to 8 by adding an additional bus which created a change to the physical shape of the some of the connectors. However, if the connectors do fit, then a 3.0 device can be connected to a 2.0 device, but the data transfer speeds will be limited to the 2.0 maximum of 480 Mbps. To support the higher speed between devices that both have USB 3.0 ports, a USB 3.0 cable is also required.

In addition to the difference in data transfer rates, the USB 2.0 and USB 3.0 versions also differ in their power transfer limits [84, 85]. Version 2.0 can provide up to 500mA of power while version 3.0 can provide up to 900mA of power. However, for this project the power transfer specification is not relevant since it will not be needed.

4.5 I^{2}C Standard

According to previous Senior Design project P.H.A.T.C.A.T., “Inter-integrated Circuit Bus is a widely-used protocol for communication in embedded systems. It was invented by Phillips Semiconductor, which is known as NXP Semiconductors today. As such, NXP maintains the specifications for the protocol.”[111]

4.6 PCB Standards

The seamless integration of Printed Circuit Boards (PCB) in product development may not demonstrate the many years it has been supported by its own standard association. However, the Institute for Printed Circuits (IPC) was formulated in 1957 by six PCB manufactures.

The standard promotes two categories under the terms: “Should” and “Shall.” Should refers to recommendations and is used to reflect general industry practices and procedures for guidance only. Shall covers requirement or attribute that is mandatory for all Product Classes [94].

It is important that throughout our PCB development cycle the standards are adhered to. Hence companies that will be manufacturing the PCB must be in compliant with the IPC PCB standards. For example, as shown in figure 55, whether mounting of Dual-in-Line Pack (DIP) and Single—in-Line (SIP) Pack Pins and Sockets.

This is not only good economically but boost safety and promotes healthy environmental practices. Some of the benefits can be linked to the Product Classes that includes:

- Class 1 – General Electronic Products: These are products suitable for applications where the major requirement is the function of the completed assembly
- Class 2 – Dedicated Service electronic Products: Includes products where continued performance and extended life is required, and for which uninterrupted service is desired but not critical. Typically, the end-use environment would not cause failures
- Class 3 – High Performance Electronic Products: includes products where continued performance or performance-on-demand is critical, equipment downtime cannot be tolerated, and end-use environment may be uncommonly harsh, and the equipment must function when required, such as life support systems and other critical systems.

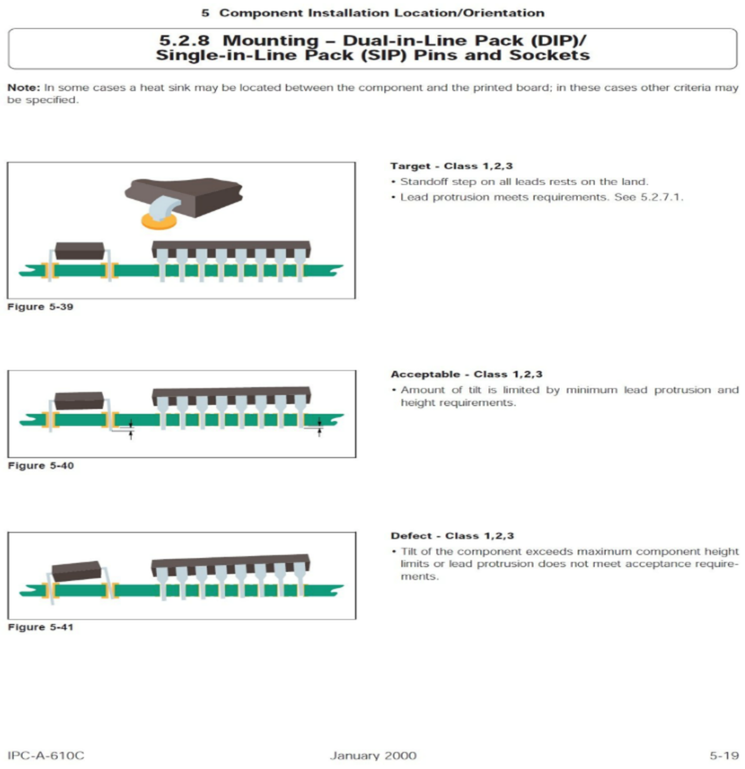

5 Component Installation Location/Orientation

5.2.8 Mounting – Dual-in-Line Pack (DIP)/ Single-in-Line Pack (SIP) Pins and Sockets

Note: In some cases a heat sink may be located between the component and the printed board; in these cases other criteria may be specified.

Figure 5-39

Target - Class 1,2,3

- Standoff step on all leads rests on the land.
- Lead protrusion meets requirements. See 5.2.7.1.

Figure 5-40

Acceptable - Class 1,2,3

- Amount of tilt is limited by minimum lead protrusion and height requirements.

Figure 5-41

Defect - Class 1,2,3

- Tilt of the component exceeds maximum component height limits or lead protrusion does not meet acceptance requirements.

IPC-A-610C January 2000 5-19

Figure 55: Proper Mounting for DIP/SIP pins and sockets.

It should be clear why it is relevant to know which class our product belongs. According to the end-use objective of our product, class 2 is the appropriate designation. Hence it is best practice to have our PCB built by manufacturers well-versed in the industry standards [95]. Example standards detailed information about how a PCB should be manufactured, and how the manufacturing of the board should be documented [95]. For example, covered in the IPC-A-610 standard are how electronic assemblies are to be handled, what the acceptable methods are for hardware installation on the assemblies, what constitutes acceptable soldering results, and many other aspects of manufacturing surface mount and through-hole technology circuit boards. Conversely, IPC J-STD-001G covers requirements for soldered electrical and electronic assemblies. As in figure 56, soldered splices – mesh are illustrating what are acceptable and those that are defective. These are just a few examples; IPC has generated several more standards that all PCB manufacturers and by extension to any entity that works with PCB.

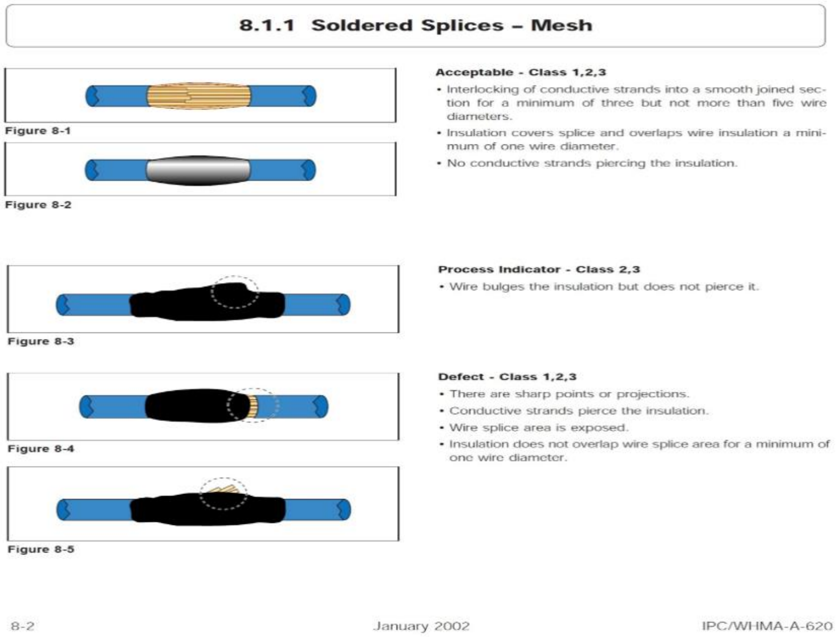

8.1.1 Soldered Splices – Mesh

Figure 8-1

Figure 8-2

Acceptable - Class 1,2,3

- Interlocking of conductive strands into a smooth joined section for a minimum of three but not more than five wire diameters.
- Insulation covers splice and overlaps wire insulation a minimum of one wire diameter.
- No conductive strands piercing the insulation.

Figure 8-3

Process Indicator - Class 2,3

- Wire bulges the insulation but does not pierce it.

Figure 8-4

Figure 8-5

Defect - Class 1,2,3

- There are sharp points or projections.
- Conductive strands pierce the insulation.
- Wire splice area is exposed.
- Insulation does not overlap wire splice area for a minimum of one wire diameter.

8-2 January 2002 IPC/WHMA-A-620

Figure 56: Solder Splices – Mesh method

Other Important terminology to be aware of are [98]:

- Acceptance tests: The tests required to determine whether a product is acceptable, as agreed upon by the purchaser and vendor
- Assembly: Several parts, subassemblies or combinations thereof joined together
- Resist: A coating material used to make or protect certain areas of a pattern during manufacturing or testing from action of an etchant, plating, soldering, etc.
- Integrated circuit: A combination of inseparably associated circuit elements formed in place and interconnected on or within a single base material to perform a microcircuit function
- Flexural strength: The tensile strength of the outermost fiber of a material that must bend

- Critical Operation: One procedure of a total process that has a significant impact on the characteristics of the completed product

4.7 Wi-Fi Standard

The IEEE 802.11 standards started out in the early 1990s. The 802.11 family of standards have become ubiquitous for codifying improvements that boost wireless throughput, range, frequency bands and address technology concerns that improve power consumption.

The Wi-Fi module being implemented in our project follows the 802.11b/g/n family of standards. 802.11b was released in September 1999. It states that this standard shall operate in the 2.4GHz frequency band and stream data rate up to 11 Mbps. 802.11g approved in June 2003 operates in the same frequency band as 802.11b but with data rates up to 54Mbps. October 2009, 802.11n was approved – it codifies the two frequency bands; 2.4GHs and 5GHz that it shall operates in. It also covers the 600Mbps data rates that it can stream [96].

It is important that our modules follow the Wi-Fi standard as they can foster enhanced user experience through product interoperability [97]. Operation in the specified frequency spectrum needs accurate execution to reduce interference with other spectrum devices. Hence it is a sound decision to employ the use of Si-Fi devices that are certified by Wi-Fi Alliance and other appropriate organizations.

4.8 SPI Standard

According to previous Senior Design project P.H.A.T.C.A.T., “Rather than being enforced by IEC or IEEE, it is a ‘de factor standard’. In other words, it is so widely used and accepted that it is, for all intents and purposes, an enforced standard.”[111]

4.9 Ethernet Standard

According to Lantronix, “Ethernet is the most popular physical layer LAN technology in use today. It defines the number of conductors that are required for a connection, the performance thresholds that can be expected, and provides the framework for data transmission.” [112] Thanks to the ethernets simple setup, low cost, and good speed it has become one of the most popular LAN technology options in the market. Because of its popular demand the Institute for Electrical and Electronic Engineers (IEEE) created an Ethernet standard which came to be known as the IEEE Standard 802.3.

Based on Lantronix, “this standard defines rules for configuring an Ethernet network and also specifies how the elements in an Ethernet network interact with one another. By adhering to the IEEE standard, network equipment and network protocols can communicate efficiently.”[112]

4.10 Software Design Standards

Software development is one of the biggest parts in which our work is centered on. Between wireless communication between components, phasor data interpretation for event detection, and the use of the Touch Table, the software design must be well designed to achieve our final goal. Based on this we must implement the software design process to further assist our team to develop each aspect of our work and be able to execute in the most organized way possible. According to Tutorialspoint, "Software design is a process to transform user requirements into some suitable form, which helps the programmer in software coding and implementation [127]." Having the opportunity for our team to have a much more organized coding implementation would be extremely beneficial for us and utilizing the software design we can potentially achieve this. Figure 57 shows a great example of how the software design process is structured and how each step interacts with another to further develop the code being implemented and facilitates in the documentation of the code useful during the debugging of errors.

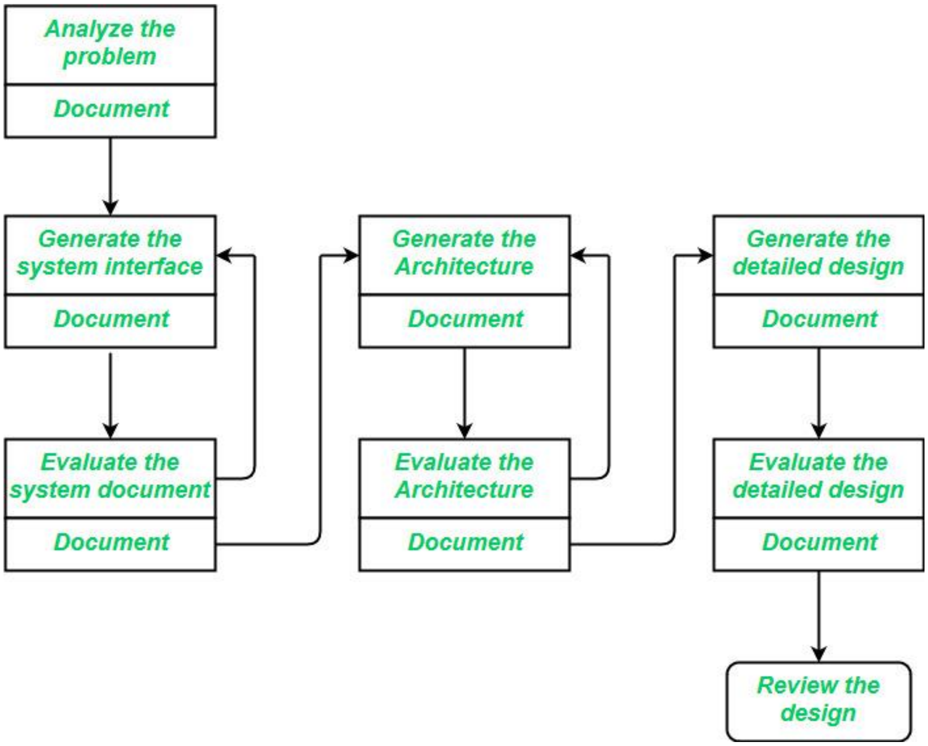
Analyze the problem
Document
Generate the system interface
Document
Evaluate the system document
Document
Generate the Architecture
Document
Evaluate the Architecture
Document
Generate the detailed design
Document
Evaluate the detailed design
Document
Review the design

Figure 57: Software Design Process [124]

Breaking down Figure 57, we first notice how "Document" becomes a part of every step of the software design process. Documentation gives programmers an easier and clearer route to find and fix any problems that may occur in the code while a non-programmer utilizes this documentation to further understand what is taking place in the code. We also see that, similarly to any design process, we begin with defining and analyzing the task at hand. Based on recognizing our areas of focus and generating a preliminary system design, mostly pseudocode and flowcharts, we can begin developing our code. Based on our initial problem there are a variety of systems that serve as results depending on the needs of the work being carried out which can be recognized as software design levels.

4.10.1 Software Design Levels

There are three distinct levels that arise because of the execution of the software design process: Architectural Design, High-Level Design, and Detailed Design. The first, being the Architectural Design, is seen by Tutorialspoint to be “the highest abstract version of the system. It identifies the software as a system with many components interacting with each other. At this level, the designers get the idea of proposed solution domain [127].” Architectural Design refers to the system as a whole being formed by smaller parts or smaller systems communicating with each other and carrying out their tasks in order to reach the desired outcome.

Our work utilizes this concept as our system constantly communicates data from one end to another by its subprograms so we can interpret the data being received and provide this information on our Touch Table. Figure 58 shows how the Architectural Design is seen and implemented into a Software Design by demonstrating the branching and connection of each smaller system working together for a whole.

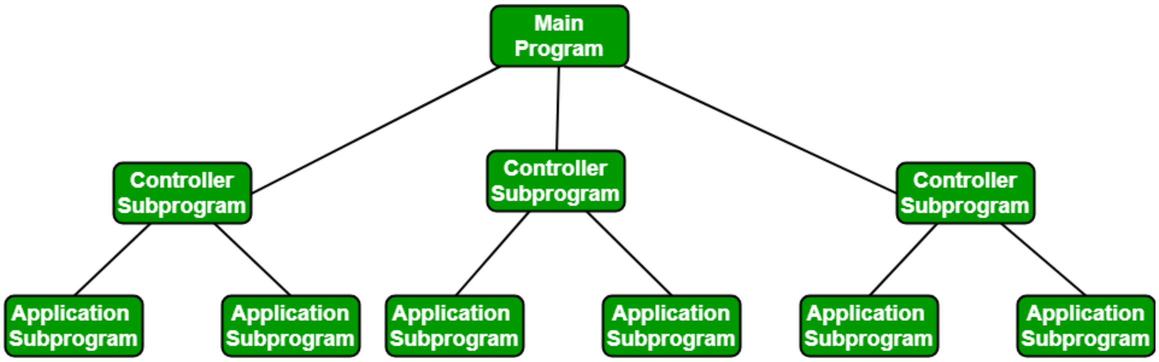

Figure 58: Architectural Design in Software Design Process [123]

Next, we see the High-Level Design, which referencing Tutorialspoint is “breaks the ‘single entity-multiple component’ concept of architectural design into less-abstracted view of sub-systems and modules and depicts their interaction with each other. High-level design focuses on how the system along with all of its components can be implemented in forms of modules. It recognizes modular structure of each sub-system and their relation and interaction among each other [127].” The High-Level Design resonates more in our work as we utilize smaller subsystems which become easier to manage to execute a task. Being able to break down the code in what can be seen as modules.

Modules can break a code into smaller portions and tasks giving the opportunity to run smoother and efficient while giving a better sense of organization and making the code easier to debug. These subsystems create a better communication and dependency with each other that allows our system as a whole to run much more efficiently in the long run. Figure 59 provides a great example on what the High-Level Design may look like. The people represent the various modules that each subsystem executes within the Azure application back-end.

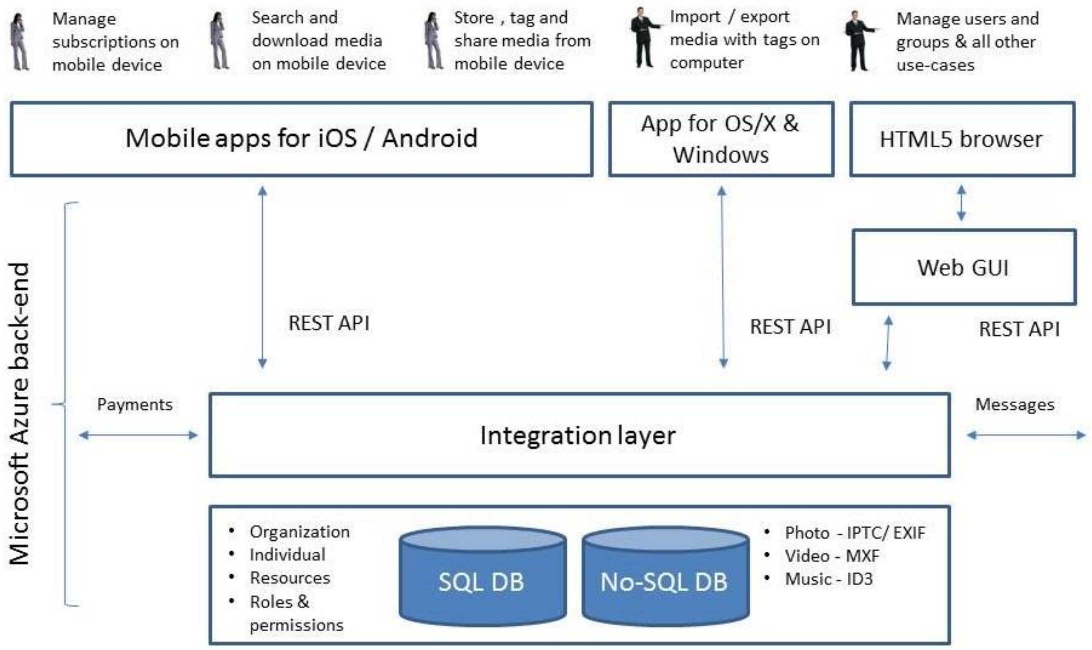
Manage subscriptions on mobile device
Search and download media on mobile device
Store , tag and share media from mobile device
Import / export media with tags on computer
Manage users and groups & all other use-cases
Mobile apps for iOS / Android
App for OS/X & Windows
HTML5 browser
Web GUI
REST API
REST API
REST API
Microsoft Azure back-end
Payments
Integration layer
Messages
• Organization
• Individual
• Resources
• Roles & permissions
SQL DB
No-SQL DB
• Photo - IPTC/ EXIF
• Video - MXF
• Music - ID3

Figure 59: High-Level Design Example of Azure Application [126]

Finally, we see the Detailed Design Level, which is mentioned by Tutorialspoint to "deal with the implementation part of what is seen as a system and its sub-systems in the previous two designs. It is more detailed towards modules and their implementations. It defines logical structure of each module and their interfaces to communicate with other modules [127]." Providing a more direct take onto the implementation of each system and subsystem, the Detailed Design Level focuses on the specifications of the internal elements of each component being used throughout the system. In other words, the Detailed Design Level focuses on implementing the Low-Level Design after the High-Level Design was implemented going into as much detail as possible describing what each module is in charge of executing and the constraints that the system may have or face to implement the design best suited to reach our goal. Figure 60 shows an example of the Detailed Design Level being implemented.

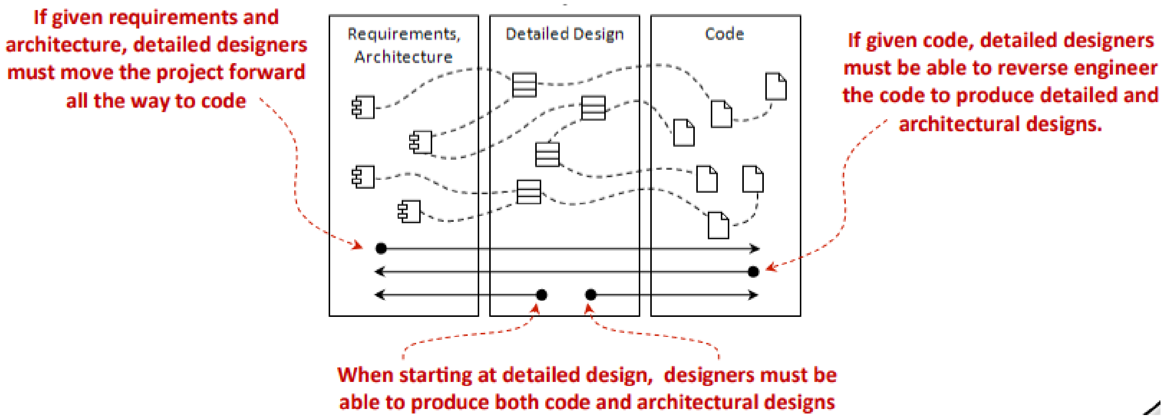
If given requirements and architecture, detailed designers must move the project forward all the way to code
Requirements, Architecture
Detailed Design
Code
If given code, detailed designers must be able to reverse engineer the code to produce detailed and architectural designs.
When starting at detailed design, designers must be able to produce both code and architectural designs

Figure 60: Example of how Detailed Design Level is implemented [125]

4.11 Python Programming Standards

The programming for this project was done using Python 3.7 which is an interpreted high-level language. It was created by Guido van Rossum, and the first version was released in 1991. It is free and open-source, and the Python Software Foundation (PSF) manages and distributes its development packages [116, 117]. The python.org site maintains documentation for Python as well as information and updates on PSF.

Python.org maintains a series of Python Enhancement Proposals (PEPs) which contain all the standards and guidelines for Python. A particularly important PEP to be adhered to in this project is *PEP 8 – Style Guide for Python Code* which was written by van Rossum, Barry Warsaw, and Nick Coghlan in 2001 [118]. In this guide van Rossum notes that "readability counts" and that it is very common for others to read one's code so it should be easy to follow. He developed this guide to improve readability and consistency across Python code [118]. The guide notes that readability is so important that if applying a standard from this guide would make the code less readable, then do not apply it. This could happen when the code being modified is older than the guidelines or the code is for older versions of Python.

The portion of the guide that addresses code lay-out notes that level indentation should always be four spaces. If using the space key, do not mix it with the tab key and vice versa. Lines should be limited to 72 characters, and continuation lines should use a hanging indent or align with wrapped elements. Top-level functions should be surrounded by two blank lines, and method definitions by a single blank line. Extra blank lines should be used sparingly. Extra white space inside expressions should be avoided by placing characters right after a parenthesis or bracket, but a white space after a comma separating two items inside parentheses is proper. Trailing whitespace should also be avoided [118].

The guide notes that comments that contradict the code are unacceptable. Block comments should be indented at the same level as the code to which they refer and should start with a # followed by a single space. Inline comments should be used sparingly and should also start with a # and a space [118].

Naming conventions are also covered in the PEP 8 guide. Class names should always use the CapWords convention which means that the first letter of each word in the name is capitalized. Package and module names should have all lowercase letters. Modules frequently use underscores while packages do not. Function and variable names should be lowercase words separated by underscores for improved readability. Method names and instances should follow this same rule. Constants should be all uppercase with underscores to improve readability [118].

Some of the basic standards that were applied to the Python code have been covered, but the guide is quite lengthy and was consulted for additional standards during the development process. There are other PEPs on the python.org website that were also referenced as needed [116].

4.12 Soldering Standards

The PCB developed in this project required soldering to attach the necessary modules onto its surface. NASA's Technical Standard NASA-STD-8739.2 *Workmanship Standard for Surface Mount Technology* which was published in August 1999 was adhered to for this project [119]. The document notes that the standard covers "hand and machine soldering of surface mount electrical connections" [119]. This standard is lengthy and covers many areas. A short overview of the most important elements relating to this project are discussed here, but the standard can be consulted for more detailed information.

The handling of bare metal surfaces that need to be soldered is not advised. However, if it must be done then "client lint free gloves or antistatic finger cots" should be used [119]. If the surfaces are touched with a bare hand, they should be cleaned with an approved solvent described in the standard.

The solder used should conform to standards ANSI/J-STD-005 or ANSI/J-STD-006 or an equivalent. Hand soldered connections should be made with flux cored wire solder. There are additional requirements for solder paste and flux described in sections 6.12 and 6.13. Furthermore, eye protection and gloves should be worn while soldering, and the area must be well ventilated per OSHA requirements [119].

To prepare for the soldering activity, section 7 advises to check the parts for coplanarity. The portions of the lead or part that will become part of the soldered connection should be tinned with a tin-lead alloy and cleaned ahead of time. The solder paste should also be tested ahead of time for oxidation and cohesion. The PCB should also be inspected for oxidation, discoloration, damage, contamination, and flatness [119].

Section 8 describes methods to deposit the solder onto the substrate and place the parts. The solder should be deposited using a stencil, screen, or syringe. Adhesives should be deposited using a stencil or syringe. The parts must be positioned and aligned with orientation that conforms to the engineering documentation which in this case will be the project PCB board design [119].

Section 9 details specific directions for soldering with several types of reflow soldering systems including heater bar reflow soldering, condensation reflow soldering, convection/radiation reflow soldering, hot gas/air reflow soldering, and automated wave-soldering [119]. It is not clear which type of soldering system will be available for this project. There may be access to one of these reflow systems, or perhaps there may be access to soldering irons.

After the work is finished, any residual solder, flux or oil should be promptly removed, and sections 10 and 11 describe methods and solvents for cleaning up. Section 12 discusses workmanship and examination of the work as it is being performed. It also describes when results should be rejected and redone. This complete standard was consulted and followed during the PCB soldering portion of this project, but there were constraints based on the equipment available in the UCF Senior Design Lab [119].

4.13 Hardware constraint

Given that the PCB will be deployed in an outdoor environment, only hardware that can tolerate outdoor temperatures are deemed suitable for our design. Hence, the parts that were identified were confined to this constraint. For example, the battery supply for the PCB must be capable of operating in temperatures -20 C^o to 54 C^o.

4.13.1 Health Impact of Wi-Fi Devices

The health risk on humans due to Wi-Fi exposure is a complex topic. Some articles, questionable or not, argue in support and against. Wi-Fi is a family of radio frequency (RF) energy on which half a century research has not find conclusive evidence that there is a serious threat to health [129]. But, specific to Wi-Fi, which came about 15-20 years ago, and its ubiquitous growth and exposure to youth, careful studies should be targeted towards those that tend to be more exposed [133]. Sources have stated that radiofrequency electromagnetic radiation is nonionizing radiation, which cannot affect the structures or molecules present in the biological systems as their energies are too low while it can possibly cause, among others, an increase in tissue temperature [133].

5. Project Hardware and Software Design Details

This section contains the details of the project's hardware and software design. Information related to interfacing between components, communication methods used, business logic modules, PCB schematic design, and more was described in this section.

5.1 PCB Design

The project required a PCB that was to be interfaced and read voltage and current data from a relay that would have measured and stored the PV output data. However, this relay interface was not implemented due to design change. See section 3.2.10.4 for more information. The PCB was interfaced with a NEMA 23 stepper motor that enabled the solar panel angle change and sent and received data to the Rasberry Pi through the UCF Wi-Fi network. This section discussed the design elements of the PCB.

5.1.1 Power Supply

The product was designed to be stationed outdoors and this constrained the method of supplying power to the hardware. On the other hand, several of the hardware had various power requirements. Hence, it is not a one size fits all application. This section aimed to design the method to power all the hardware packages. This included battery power, DCDC power for the microcontroller, servo motor power and other hardware.

The diagram in Figure 61 below showed the updated layout of all the hardware that needed to be powered. First, the original plan was to use a 6 V battery but was upgraded to 9V since larger power density was required. This voltage level will serve two roles: 1) It was to drive the DCDC converter and 2) power the Wi-Fi module, LED, voltage measurement operation amplifiers, and MCU. Initially, the Wi-Fi module that was selected needed two voltage levels; 3.3V and 5V, hence two DCDC converters must be designed. However, as the diagrams shows the Wi-Fi module that we selected after the prototyping phase only required one voltage level.

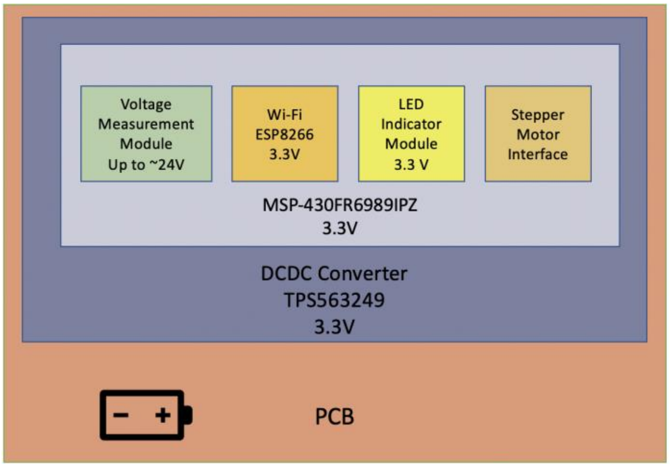
Voltage Measurement Module Up to ~24V
Wi-Fi ESP8266 3.3V
LED Indicator Module 3.3 V
Stepper Motor Interface
MSP-430FR6989IPZ 3.3V
DCDC Converter TPS563249 3.3V
PCB

Figure 61: PCB Power Supply

5.1.2 DCDC Converter

WEBENCH by TI provides a very convenient and efficient platform that was used to design our DCDC converter. The Eagle footprint and supporting files was then downloaded and integrated into our Eagle schematic and board through a service provided by Ultra Librarian. There was some relevant information that was needed before designing a DCDC converter on WEBENCH including: input voltage, output voltage, output current, efficiency, footprint, costs, etc. WEBENCH typically generates several designs per the information that was entered by the user. While on the WEBENCH platform, user can compare or perform online simulation to study the response and output of each design to help select the one that satisfies the application requirement.

Before we decided to change our DCDC model, one 2-6V Buck-Boost DCDC converter was designed to output 3.3V that would drive the PCB hardware including: Gyro, Wi-Fi and RS232-TTL converter. A second Buck DCDC converter to provide the +5V to the Wi-Fi module was designed. It should be noted that the actual input voltage for the Buck-Boost DCDC converter was 2-16V. This would give us flexibility in case there are any issues powering the hardware with the 6V battery. The actual DCDC model that we selected for our project was a 4.5 V to 17 V buck converter. It was design to output 3.3 V and a maximum output current of 1 A.

5.1.3 Battery

Our project was to employ portable swappable power cells. They were to be functioned as low drain but should handle short to medium burst in consumption. They were to be able to operate in outdoor temperatures for long periods – more specifically they should be capable of working at -15 to 50^{o}C. Alkaline AA and 9V batteries are suitable for application where consumption happens slowly.

Both options were reviewed before selection was made. Once again, before we ran into some problems and changed to a stepper motor, the idea was to use a servo motor needed a maximum voltage supply of between 4.8 – 6.8V. It was also our aim to keep footprint to a minimum. Hence, we tried to minimize the number of cells while maintaining specification voltages.

5.1.3.1 9V Alkaline Non-chargeable

This can typically provide more capacity in a single cell with dimension 48.5mm x 26.5mm x 17.5mm. Both Energizer and Duracell’s 9V (IEC-6LR61)) stated operating temperature (-18 – 54^{o}C) and (-20 – 54^{o}C), respectively, can safely manage the operating temperature range stated above. Per Duracell’s data sheet, the delivered capacity is dependent on the applied load, operating temperature, and cut-off voltage. The charts in Figures 62 and 63 below represent some benchmark examples of the energy/service life that the battery will provide for various load conditions [99] [100].

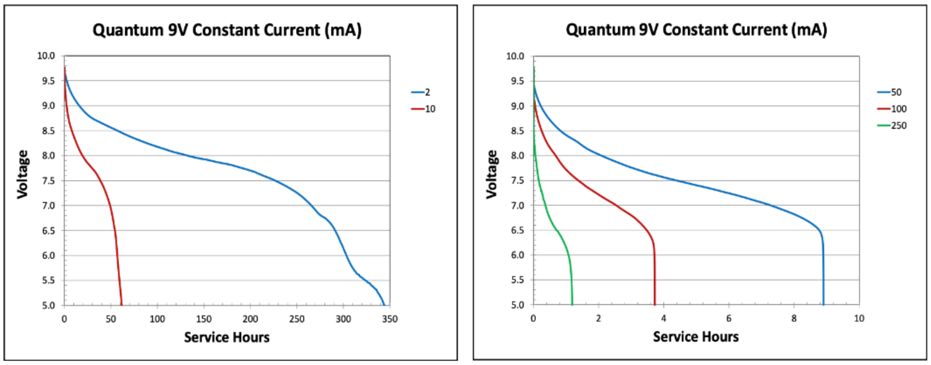

Figure 62: Duracell's 9V (QU1604) performance examples

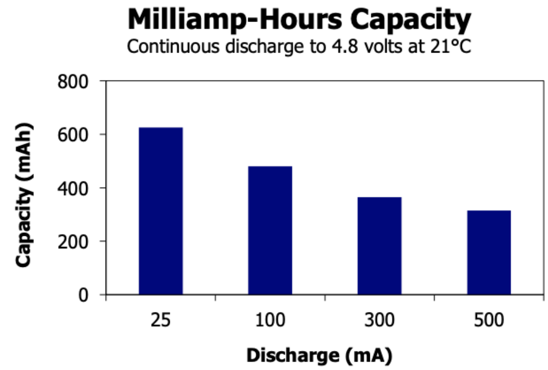

Figure 63: Energizer's 9V (IEC-6LR61) performance example

5.1.3.2 AA Alkaline Non-chargeable

The temperature rating for Duracell's and Energizer's 1.5V AA Alkaline batteries are the same as the 9V. Its dimension is 50.50 mm x 14.5mm. It would take six 1.5V AA to produce 9V output. This means the footprint would increase six-fold. While we are open to use 9V battery supply in our project, the first aim is to use 6V, hence only four 1.5V AA batteries would be required, this is still a significant footprint over the 9V [101] [102]. Figures 64 and 65 illustrate typical example performance for the Duracell's and Energizer's 1.5V AA Alkaline Batteries.

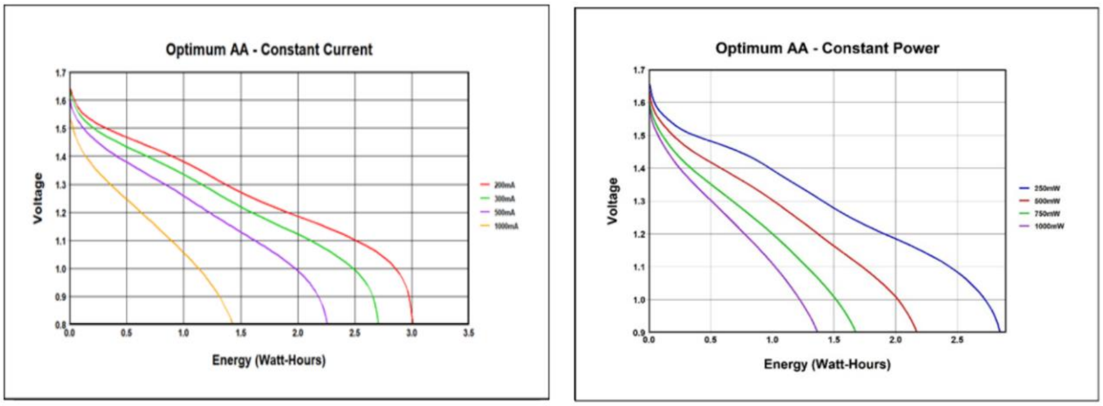

Figure 64: Duracell's 1.5V typical example performance

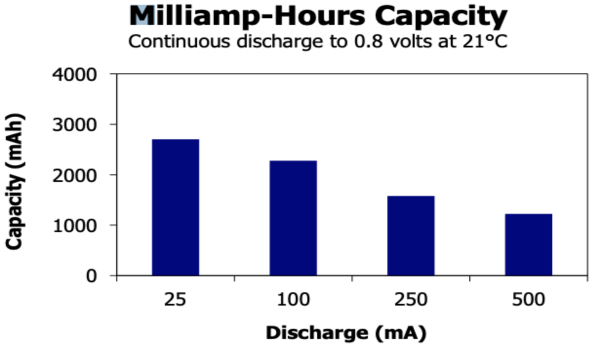

Figure 65: Energizer's 1.5V typical example performance

5.1.4 Wi-Fi Device Provisioning

A wireless embedded device that needs to be connected to a network must be provisioned. This is the process of connecting to a network by providing the network credentials such as SSID and password to the embedded device (station) [106]. In general, there are several ways to perform this task, but this section will be in relation to the CC3100 Wi-Fi module being employed in our design.

The CC3100 SimpleLink Wi-Fi device has a designated network processor and a networking subsystem which has network provisioning built into it [107]. This will allow our host MCU, which is external to the CC3100 and can be connected by multiple interface options, to start the provisioning process (as shown in Figure 66) and the CC3100 built in networking subsystem do all the steps needed to make a connection. As Figure 66 shows, the host MCU start the connection process.

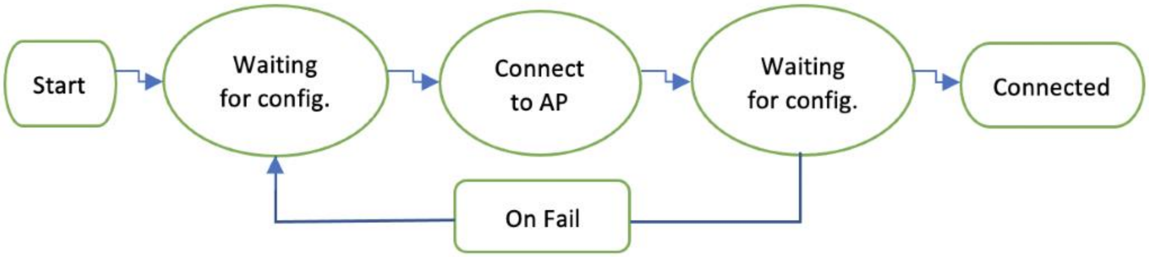

Figure 66: Wireless provisioning process flow

At the *waiting for config.* stage, if supported, can be done through Access Point Mode and SmartConnect a TI proprietary provisioning method to name two. The Station then connects to the AP network and then goes to the second *Waiting for config.* stage where it validates the network credentials. If the information is valid, the connection is successful, if not, it loops until the information entered by the user is correct. The overview for provisioning in Access Point Mode and SmartConfig are laid out in the final paragraph.

Access Point Mode is the most common method for provisioning, according to: [106]

> *[The] un-provisioned device wakes up initially as an AP with an SSID defined by the equipment manufacturer. In this mode, the un-provisioned device also includes a secured embedded web server. After the user connects his smartphone to the un-provisioned device's AP, he opens the smart phone's web browser and browses into the device's web site via a pre-defined local URL or IP address. In the embedded web site, the user chooses (or types in) the home network name and password. The device stores the network credentials in nonvolatile memory and then it switches from AP mode to Station mode in order to connect to the home network using the stored network credentials.*

SmartConfig technology is a is provided as follows: [106]

> *It uses a mobile app to broadcast the network credentials from a smartphone, or a tablet, to an un-provisioned TI Wi-Fi device. The Wi-Fi network name (SSID), that the phone is connected to, shows up automatically on the phone app. The user then adds the network password and presses the "Start" button to begin the process.*

After several efforts without being able to get the CC3100 to connect to any Wi-Fi in station mode, the team decided not to use this module. The ESP-12E was selected to be used in our final project design which also worked during prototyping and testing phases.

5.2 PCB Schematic

PCB schematic phase was the basic starting point for the project design, it served as a blueprint for prototyping and testing all the components and modules that were integrated together. How well a project is implemented relies on the schematic plan that is developed.

PCB layout determined the operation and electrical performance of the design. As such, industry recommended standards such as IPC-2221 was followed. Since it is highly beneficial to have schematic support with a PCB software package, EAGLE software was chosen since it comprised of both schematic and PCB design and it also provided other great features such as Design Link, PCB Quote and Bill of Material (BOM) support from within the application [129].

Figure 67 is an illustration of our project's schematic. It described how different modules were integrated with the MSP430FR6989 microcontroller. During schematic construction, each module's data sheet was referenced to ensure accurate interfacing between components, electrical operating limits are satisfied, and recommended layout followed as close as possible.

The operating environment played a significant role in schematic design. Location and operating temperature limits were two big ones. Battery power supply is due to the system being deployed for outdoor operation and this ties in to ensuring temperature limits of each component was capable of withstanding outside temperatures. Given that we decided not to use CC3100 Wi-Fi module, figure 67 was not included in our final schematic design.

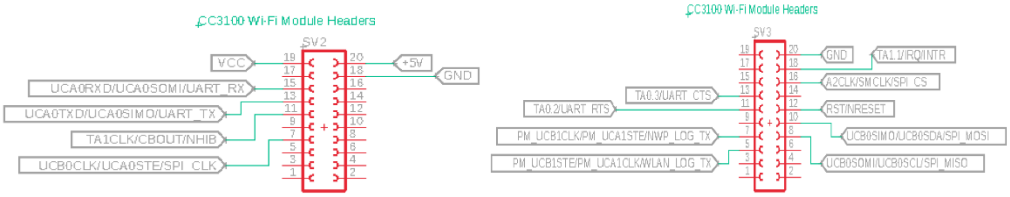

Figure 67: CC3100 Wi-Fi schematic interface

5.2.1 RS232-to-TTL Integration

Another important module that made up the overall schematic is the RS232-to-TTL module, this is shown in Figure 68. It's tasked with reading the external measurement relay's register current and voltage values. As shown in figure 66, this will convert RS232 voltage signals to the MSP430FR6989 voltage levels and vice versa. The data sheet recommends that the coupling capacitors be implemented very close to the chip. Given that we decided not to use any relay in our design, figure 68 was not included in our final schematic design.

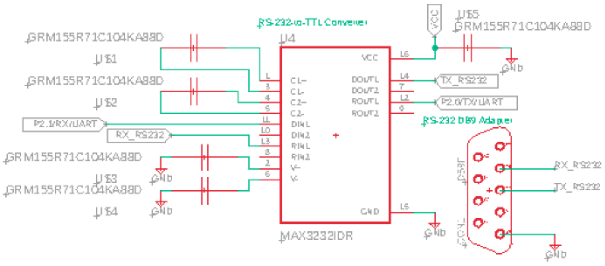

Figure 68: RS232-to-TTL schematic

5.2.2 MSP430FR6989 BSL Programming

Programming the MSP430FR6989 can be done in more than one way, an effective way is through Bootstrap Loader (BSL). Figure 69 illustrates the header programming connection pins that are needed to be interfaced with a terminal or PC to download firmware into its flash memory. A UART BSL converter would have been required to make the connection between header and terminal or PC. TI's Code Composer Studio (CCS) IDE was to be used to perform this process. Note, since we went with the JTAG programming option shown in figure 70, the BSL model shown in Figure 69 was not implemented in final design.

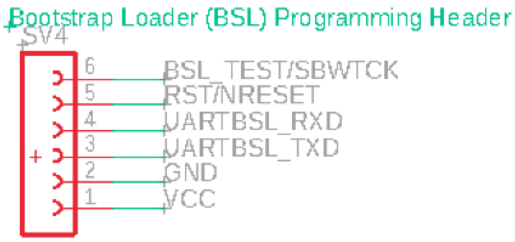

Figure 69: BSL programming schematic interface

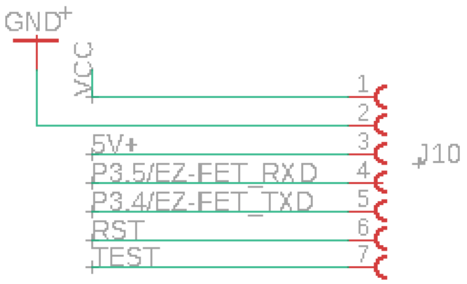

Figure 70 JTAG programming schematic header interface

5.2.3 Gyroscope module

The Gyroscope would have monitored the PV reference angle and communicate the information to the MSP430FR6989 over I2C serial interface. Figure 71 shows the connection between both modules.

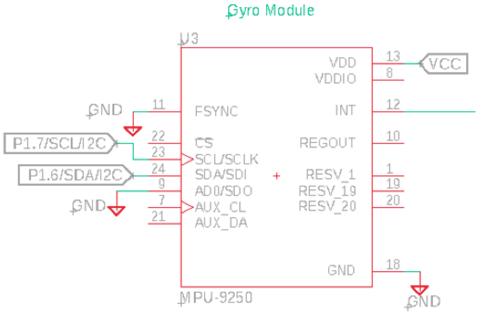

Figure 71: Gyroscope schematic interface

Due to the fact that the Gyroscope Module was not included into our final design, this gyroscope schematic was also discarded.

5.2.4 Wi-Fi Circuit

Connecting to UCF's Wi-Fi network was a fundamental requirement for our project to function and satisfy one of our engineering requirements. Hence, we needed to build a circuit that could integrate our Wi-Fi module within our PCB. The design we used was based on a YouTube tutorial and NodeMCU-devkit-V1.0 document [139][140]. Figure 72 below shows our Eagle circuit diagram designed for our project.

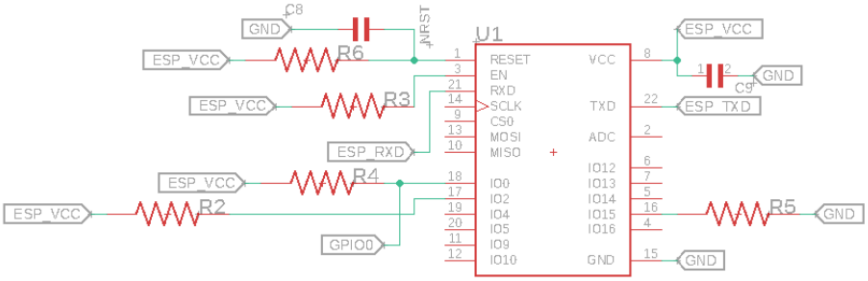

Figure 72: Wi-Fi Circuit

5.2.5 DCDC converter

Providing stable power to the MSP430FR6089 was designed as a switching DCDC converter (shown in figure 73). It was first design as a buck boost converter but was finally changed to a buck converter. This change still facilitated flexibility during development stage. The schematic below displays the battery input and VCC output interface. Figure 74 shows the updated PCB schematic designed in Eagle with all the final components used.

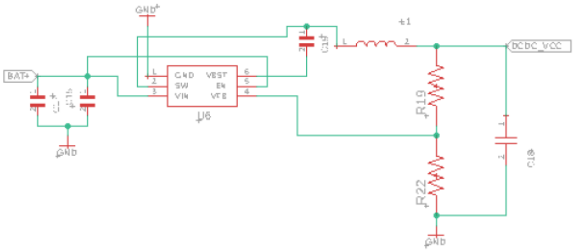

Figure 73: DCDC converter schematic

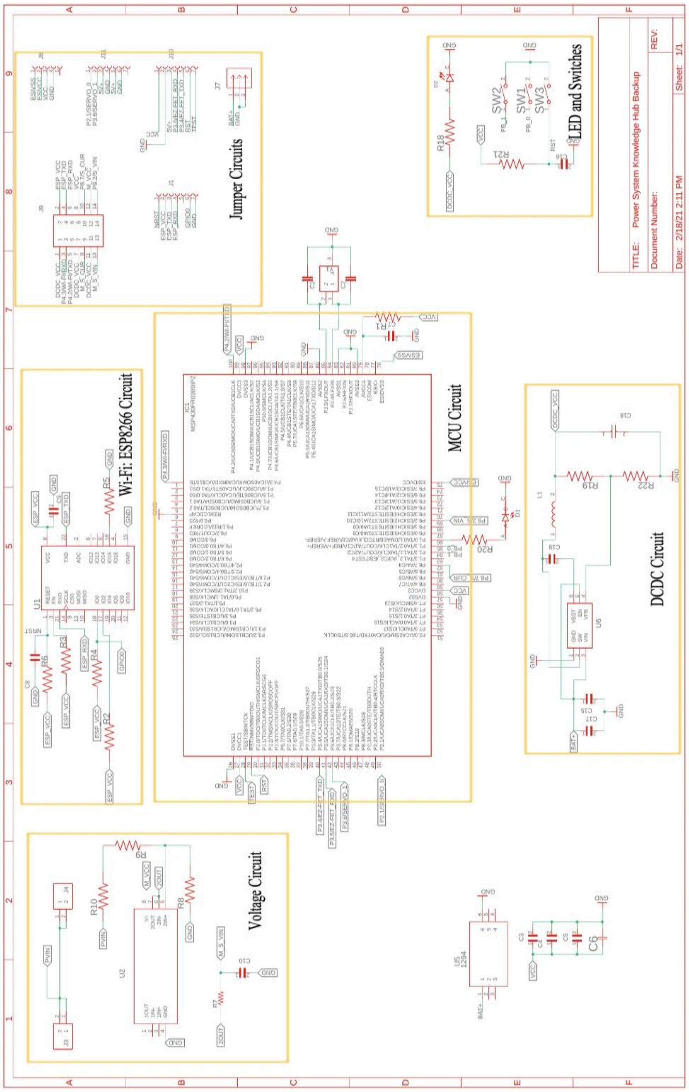

Figure 74: Overall Schematic of PCB Design in EAGLE

5.3 Data Storage

To store to implement the functionality of the software design, a database was thought to be necessary. The solar panel data, educational material, and OPAL-RT data must be stored. The user interface could need access to the database to fetch the educational materials that the user can access through the touch screen. Ultimately, the RBP had enough storage on its memory card to accommodate the data that was collected during normal operation of the project. However, research was done on selecting an appropriate database before that determination was make. That research into MongoDB and MySQL is presented here. Both have free versions that could have been used for this application and they were evaluated and compared for this project.

5.3.1 MySQL vs. MongoDB

MySQL uses the structured query language (SQL) that has been around since 1995 and is widely used commercially. MongoDB is newer with a 2009 release date but is also widely used commercially. MySQL is referred to as relational database while MongoDB is not. In reality, both do use relational properties to access information. The main difference is that MySQL uses structured schemas set up by the administrator to store entries while MongoDB entries are be added without a defining structure. In MongoDB, new fields can be added at any time and contain any type of value. MySQL stores data in tables with strictly defined schema while Mongo stores data in JSON-like documents that can have varied structures. Both use indexing to access data or can read through an entire table (mySQL) or collection (MongoDB) to search for an entry [36].

Both MySQL and MongoDB are compatible with the RBP, and both have methods of replicating databases for security. MongoDB is a better choice if it is anticipated that a table/collection will exceed 10GB or if there is the need to change schema during real-time data processing.

5.3.2 Database Selection and Implementation

Because the data is structured and the team has some experience with MySQL, a MySQL database was selected if one had been needed for this project. To set up the MySQL database, a table would have been defined that contains the educational information with the primary key being the topic. A second table would have been set up that contains the data values to represent the disturbances that can be selected by the user and will likely use an index value as the primary key. Another table would have been set up that records the incoming data from the solar panels along with the time signature which will be the primary key, and another table would have been set up to hold the incoming data from OPAL-RT along with time signature data. The OPAL-RT data from this table would have been used by the WAMS algorithm to determine the details and location of the power disturbance event. The data from these last two tables would have been deleted when it became obsolete based on the time signature to keep the database from becoming overfilled. This could have been done by creating a scheduling event in MySQL.

5.4 Decoding IEEE C37.118 Data with Wireshark

As discussed in other sections of this proposal, IEEE C37.118 is a standard which defines synchronized phasor measurements that are used in power system applications. Had the stretch goal of implementing the WAMS algorithm been completed, it would have been necessary for the RBP to receive data in this protocol from OPAL-RT and decode it so that the WAMS algorithm could use the data.

Wireshark is a widely-used network protocol analyzer tool that analyzes data packets across a network. It is commonly referred to as a “packet sniffer”. It is free to use, and it has tools which are called “dissectors” that can decode the data contained within specific protocols. Wireshark contains a built-in dissector for the IEEE C37.118 protocol. [38]

The main components of the PMU data from the IEEE C37.118 protocol are the synchronized phasor voltages which may be single-phase or three-phase, frequency, and the rate of change of frequency (ROCOF) [29]. Figure 75 shows the organization of the IEEE C37.118 data frame by bytes.

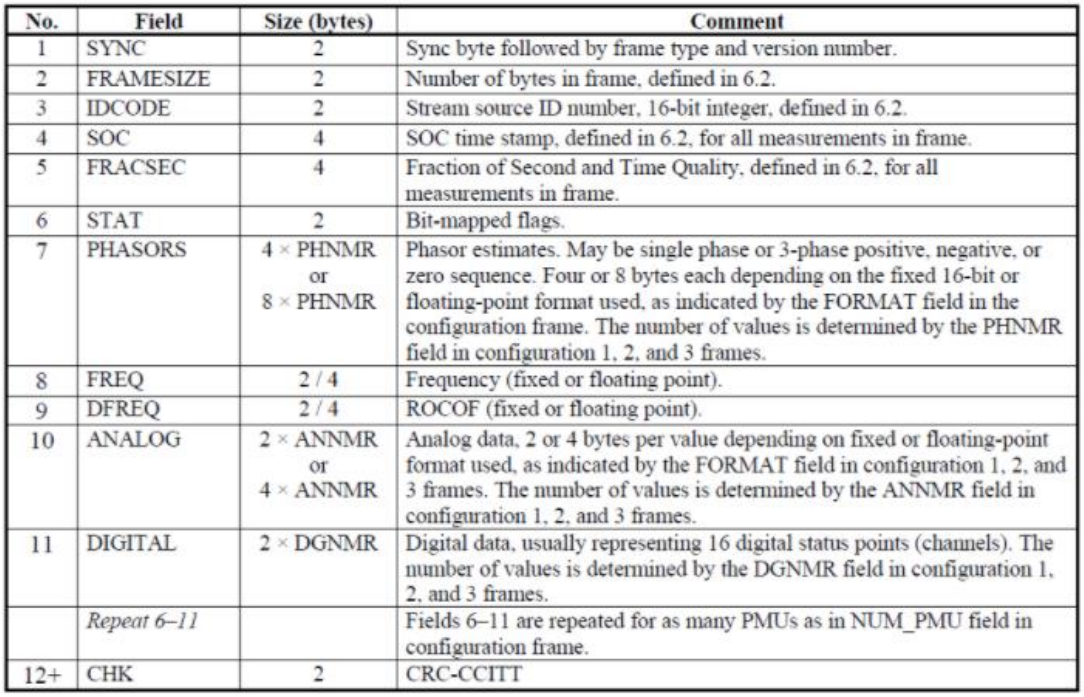

No.	Field	Size (bytes)	Comment
1	SYNC	2	Sync byte followed by frame type and version number.
2	FRAMESIZE	2	Number of bytes in frame, defined in 6.2.
3	IDCODE	2	Stream source ID number, 16-bit integer, defined in 6.2.
4	SOC	4	SOC time stamp, defined in 6.2, for all measurements in frame.
5	FRACSEC	4	Fraction of Second and Time Quality, defined in 6.2, for all measurements in frame.
6	STAT	2	Bit-mapped flags.
7	PHASORS	4 × PHNMR or 8 × PHNMR	Phasor estimates. May be single phase or 3-phase positive, negative, or zero sequence. Four or 8 bytes each depending on the fixed 16-bit or floating-point format used, as indicated by the FORMAT field in the configuration frame. The number of values is determined by the PHNMR field in configuration 1, 2, and 3 frames.
8	FREQ	2 / 4	Frequency (fixed or floating point).
9	DFREQ	2 / 4	ROCOF (fixed or floating point).
10	ANALOG	2 × ANNMR or 4 × ANNMR	Analog data, 2 or 4 bytes per value depending on fixed or floating-point format used, as indicated by the FORMAT field in configuration 1, 2, and 3 frames. The number of values is determined by the ANNMR field in configuration 1, 2, and 3 frames.
11	DIGITAL	2 × DGNMR	Digital data, usually representing 16 digital status points (channels). The number of values is determined by the DGNMR field in configuration 1, 2, and 3 frames.
	Repeat 6–11		Fields 6–11 are repeated for as many PMUs as in NUM_PMU field in configuration frame.
12+	CHK	2	CRC-CCITT

Figure 75: IEEE C37.118 Dataframe Organization

Further investigation confirmed that the RBP is compatible with Wireshark, so running it would not have been problematic although it may have strained the resources of the unit. Wireshark also offers a terminal oriented version called Tshark which could have assisted in conserving resources if the RBP had trouble with the extra demand.

Wireshark could have monitored the port being used for communication with OPAL-RT and captured the data from the incoming packets. It could then decode them and output the decoded data. The dissector can output the data into either a plain text file, CSV format, C arrays, XML format, or JSON [38]. To implement continuous output into a file, a script might have been needed, so Tshark may have been the better option for this project. A decision between full Wireshark or Tshark was never made since the WAMS algorithm was not completed so there was no testing that could be done.

5.5 Communication through a Server

The Raspberry Pi must communicate with the PCB that is attached to the solar panel. Several methods for these components to communicate have been discussed in other sections of this proposal. The original project design proposed setting up a server that they could both access although that was not necessary once the TCP socket communication was successfully implemented. Possible methods were researched to set-up a server and are reviewed in the next sections.

5.5.1 Raspberry Pi Hosted Server

One efficient method would have been to set up a server that both components could access using the UCF Wi-Fi, as discussed in section 3.2.10.5.2. There are many methods to set up a server for both components to access. The easiest way would be to run the server on the Raspberry Pi and allow the PCB to access the server through the UCF Wi-Fi. There are several free options available to host a local server on the Pi which are discussed in section 5.5.1.1. However, setting up the server on the RBP may be problematic since it is difficult for nodes on the UCF to connect with each other since it's not an open network that allows nodes to see each other. One possible solution is to use multicast DNS (mDNS). mDNS is a protocol which resolves hostnames to IP addresses inside local networks which don't have a local name server. It is a zero-configuration service that uses TCP/IP. It operates like the Domain Name System (DNS) by using UDP packets. The protocol is published as RFC 6762 with IETF [24, 31].

5.5.1.1 Python Simple HTTP Server

Python has a built-in library that allows the easy creation of an HTTP server on the RBP [86]. This simple implementation relies on TCP sockets, and is extremely lightweight. The server can be created with only a few lines of code, however, this simple set up only works well to serve static files and fails in dynamic applications are required for this project [89].

5.5.1.2 Web Server Gateway Interfaces (WSGI)

Web Server Gateway Interfaces (WSGI) are stand-alone servers that generally have good performance while using less resources than other types of web servers. The WSGI standardizes communication between servers and Python web frameworks in order to deploy portable Python code [87].

5.5.1.2.1 Gunicorn

Another easy way to build a server on the RBP would have been to use Gunicorn which is a Python WSGI HTTP server for UNIX. Gunicorn is very simply implemented and spares resources which is necessary when using a stand-alone MCU. It is known to be easy to set up and use which is partly due to its great user interface [87]. It's also compatible with many frameworks and has quick response time making it a good choice to implement on the RBP [25, 27].

5.5.1.2.2 Waitress

Waitress is another WSGI server that says it has "very acceptable performance" [88], however, it does not appear to have the same simplicity in configuring and running it that Gunicorn claims to have. It does have some additional functionality that Gunicorn lacks such as HTTP request buffering, but for this project a simple server would have been ideal. Waitress also lacks a good community forum and other project examples to assist in configuring the server.

5.5.1.2.3 uWSGI

uWSGI is a more advanced WSGI server with very good performance for dynamic applications [87]. It can be used as a stand-alone web router (which would be the functionality needed for this project) or can run with a full web server. While it excels in functionality and performance, it can be difficult to configure. The Python documentation only recommends using it if you have a specific need for the advanced functionality [87].

Table 40 compares these various server implementations and shows why Gunicorn would have been the server of choice if it had been necessary for communication.

Table 40: Local Server Frameworks Comparison

	Python Simple HTTP Server	Gunicorn	Waitress	uWSGI
Simplicity of Configuration and Use	Very Good	Very Good	Fair	Poor
Performance	Good	Very Good	Good	Very Good
Advanced Features	Poor	Fair	Good	Very Good
Support and Community Forums	Fair	Very Good	Poor	Good
Ability to Serve Dynamic Content	Poor	Good	Good	Good

5.5.2 Virtual Private Server

Other solutions involve setting up a virtual private network (VPN) server that could have been accessed from anywhere through the internet. The PCB would have been able to access the server through the UCF Wi-Fi without connecting directly with the RBP. There are many ways to implement a VPN server involving different types of full stacks such as MERN, MEAN, WISA, and LAMP stacks. The MERN and MEAN stacks both utilize MongoDB for their databases, so these two stacks were eliminated from consideration. The WISA stack is based on Windows instead of Linux, so it was also eliminated. This leaves the LAMP stack as the best option if a webserver had been necessary.

5.5.2.1 LAMP Stack

LAMP stands for Linux, Apache, MySQL, and PHP. Since our system runs the Raspberry Pi OS which is Linux based, this stack is appropriate for our operating system. MySQL is the database which had already been selected as the preferred database for this project. Apache is an HTTP server that processes requires and serves up web assets. This is the part of the stack that allows access to the server over the internet via a simple URL. Apache is open-source and is widely used across the internet.

PHP is the programming language that is used to create the API in the LAMP stack. It works with Apache to allow access to the database. PHP is not required for the LAMP stack and may be switched out for Perl which is a popular Python language. However, our team has some experience with PHP so it could have remained as the API language for this project.

There are many services available to deploy a LAMP stack VPN. These services generally have fees involved. GoDaddy has a very simple to use LAMP stack server that includes access to a very helpful tool called cPanel, but the fees are approximately $40 per month which are excessive. Both Amazon AWS and Google Cloud Platform offer reasonably priced VPNs that use the LAMP stack, and both are reasonably priced.

5.5.2.1.1 AWS Lightsail

AWS offers their VPN service called Lightsail which is only $3.50 per month with the first month free, and it does support the LAMP stack. This plan includes 512MB of memory, a 1 core processor, 20 GB SSD disk, and 1 TB of transfer data allowance. The managed database must be added on to this plan, but AWS also has a free tier for the MySQL database which can be used for free for 12 months. [41]

5.5.2.1.2 Google Cloud Platform

Google Cloud Platform (GCP) offers a LAMP stack solution; however, their pricing is not as easy to understand as AWS service plan. Their costs are estimated to run around $13.61 per month, but all charges are itemized. This comes with a Google Compute Engine with 1.7GB of memory, a standard persistent 10GB disk. However, GCP also offers a free tier of services that would be sufficient for this project. There they offer their Compute Engine with their version of a SQL database which is called Firestore. [42]

Both AWS and GCP are industry leaders, and their services should both be high quality and reliable. From strictly the cost perspective, the GCP VPN would prevail, but the AWS service appears to be easier based on the documentation. Both services are feasible, and more testing would have been needed in order to make a final decision on which one would have been more appropriate for this project.

5.6 System Communication

As previously mentioned, the RBP was able to connect with OPAL-RT via a TCP socket since both devices are connected to the UCF network via ethernet. The Raspberry Pi acts as the server while OPAL-RT acts as the client.

The connection between the RBP and the PCB was much more difficult. Once testing was done with the RBP connected to the UCF ethernet and a test device connected to the UCF WPA2 Enterprise Wi-Fi network, it was discovered that the device connected to the Wi-Fi was able to ping the RBP. With this knowledge, code development and testing were done to attempt to connect the devices through a TCP socket. The socket session was successful if, and only if, the RBP acted as the server and the Wi-Fi device acted as the client. This allowed the project to continue without the need for a web-server.

Connecting the PCB to the Wi-Fi was much more difficult than a phone or laptop, and that required complete development of new code as well as including the UCF security certificate in the code for the PCB’s ESP8266 Wi-Fi module. This is further discussed in Section 6 of this document.

Figure 76 shows the complete configuration of the system communication for our project. As shown, all components use the UCF network. The RBP and OPAL-RT are hard-wired into the network while the PCB is able to connect to the UCF WPA2 Enterprise Wi-Fi. The diagram shows that they use TCP connections, and the RBP acts as the server for both sockets.

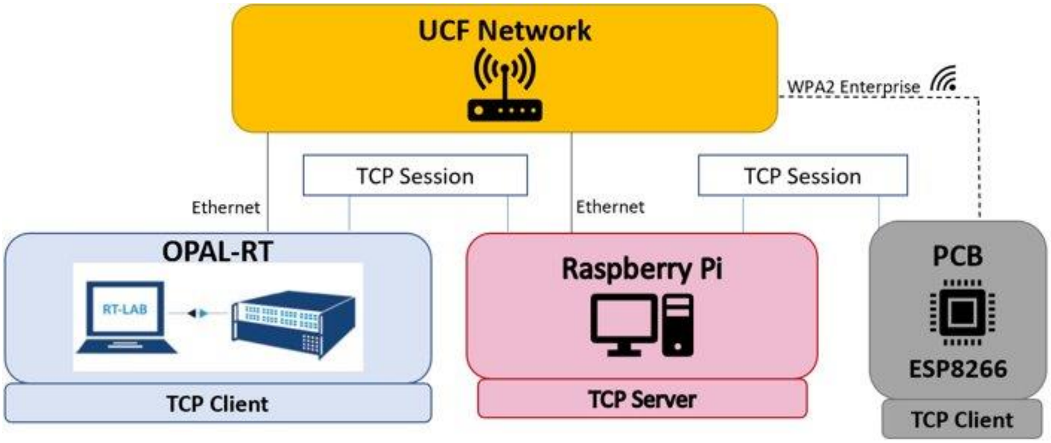

Figure 76: System Communication

5.7 Touch Screen Graphical User Interface

The project's graphical user interface (GUI) is accessed from the touch table and runs on the RBP. This section discusses the programming language selection for the GUI as well as the scope and functionality of it.

5.7.1 Programming Language Selection

Several programming languages were capable of building the necessary GUI, so a decision matrix was done to decide which should be used and is shown in Table 41. Based on this decision matrix, Python was the first choice and was used to build the interface. Java was a second option to keep in case any problems arose with implementing it in Python but was not ultimately needed. [30] Both have excellent libraries to assist in the GUI development and are easy to use to ensure that the project was finished by the end of Senior Design 2.

Table 41: GUI Programming Language Decision Matrix

GUI Programming Language Decision Matrix			
Language	Pros	Cons	GUI Libraries
C/C++	• Good performance since compiled • Team has some experience in C	• Difficult to use • High level of complexity to create a GUI • Memory can be difficult to manage	• Over 35 GUI libraries available
Java	• Team already proficient in Java • Advanced libraries to use for GUIs • Eclipse IDE provides advanced support	• Performance may be slow on lower end computers such as the Raspberry Pi	• Swing • JavaFX • AWT
Python	• Easy to develop GUIs • It is pre-installed in Raspberry Pi OS • Interfacing with OPAL-RT will be done in Python	• Team has limited experience with Python • Performance may be slow during heavy data processing since its interpreted	• Tkinter • PyGUI • Kivy • PyQT • WxPython
JavaScript HTML/CSS	• Team has experience in JS/HTML/CSS • Web-based GUI may be advantageous if an online server is used for communication	• Usually used for web pages and applications • May need additional applications to be able to access resources needed to execute the GUI	Bootstrap

5.7.2 Functions and Scope of the Graphical User Interface

The GUI has three main functions. The first provides a method for users to change the angle of the solar panel and receive real-time readings on how this changes the power output. The second allows the user to interact with a real-time distribution simulation by injecting the energy of a solar panel farm into the system. The final function provides educational material related to power systems to the user.

To implement the first GUI function of interacting with the solar panel, the main GUI screen has a block in the upper right corner dedicated to the solar panel. This block has interactive buttons to tilt the solar panel up or down or rotate it. The three boxes in that block display the real-time voltage, amperage, and wattage being produced by the solar panel as the user moves the panel. The voltage and power output are also displayed in a graph so that the user can see the history of the changes as they interact with the panel. As the user activates the buttons to tilt the solar panel up or down, a pop up message appears to let the user know that the command was successfully sent to the PCB and that the panel will move 5 degrees in the requested direction. The application keeps track of how many requests are sent to the panel. When the panel is flat, meaning parallel to the ground, the tracking variable is at zero. The variable increments or decrements depending on which direction the panel moves, and once the variable reaches positive or negative seven, the application will give the user a message that the panel is at the maximum angle for that direction. This protects the stepper motor from attempting to tilt the angle further than the mechanical limitations of the panel frame.

In the interactive distribution system block of the GUI, a commercial building graphic represents the distribution system and a solar panel graphic to represent the solar panel farm. There is a message panel which shows the three-phase per unit voltage of the simulated distribution system as received in real-time from OPAL-RT. The base OPAL-RT model voltages fall outside of the optimal range, so the user can activate a button to inject the energy of a solar panel farm into the distribution system simulation. This injection is based on the real-time readings of the demo solar panel connected to the PCB. This value is sent to the OPAL-RT model, and the model uses a multiplier to similar a solar panel farm instead of a single panel. The results are sent back from OPAL-RT, and the message panel will tell the user how the injection affected the system. There is another button for the user to reset the system to the original state prior to the injection. This allows the user to try again after changing the angle of the solar panel to see how these changes affect the outcome.

There is another panel on the bottom right of the GUI screen where the user can access educational material related to power systems. There are five main topics with touch buttons to access them. There is also a sixth button to access more topics. This button is not currently functional, but in future development should take the user to a secondary GUI screen dedicated to the educational material where they can choose from a larger range of topics. Selecting the topics from the main GUI screen or the secondary screen opens a panel where the selected topic is shown.

Figure 77 is a screenshot of the main GUI screen. The left side panel is the distribution system simulation. The upper right panel is the solar panel center, and bottom right panel is the education center. Figure 78 shows the message panels displayed to users when interacting with the solar panel controls. All of the buttons were designed to be large to make them easy to use. During testing it was determined that small buttons were difficult to activate on the touch table due to parallax.

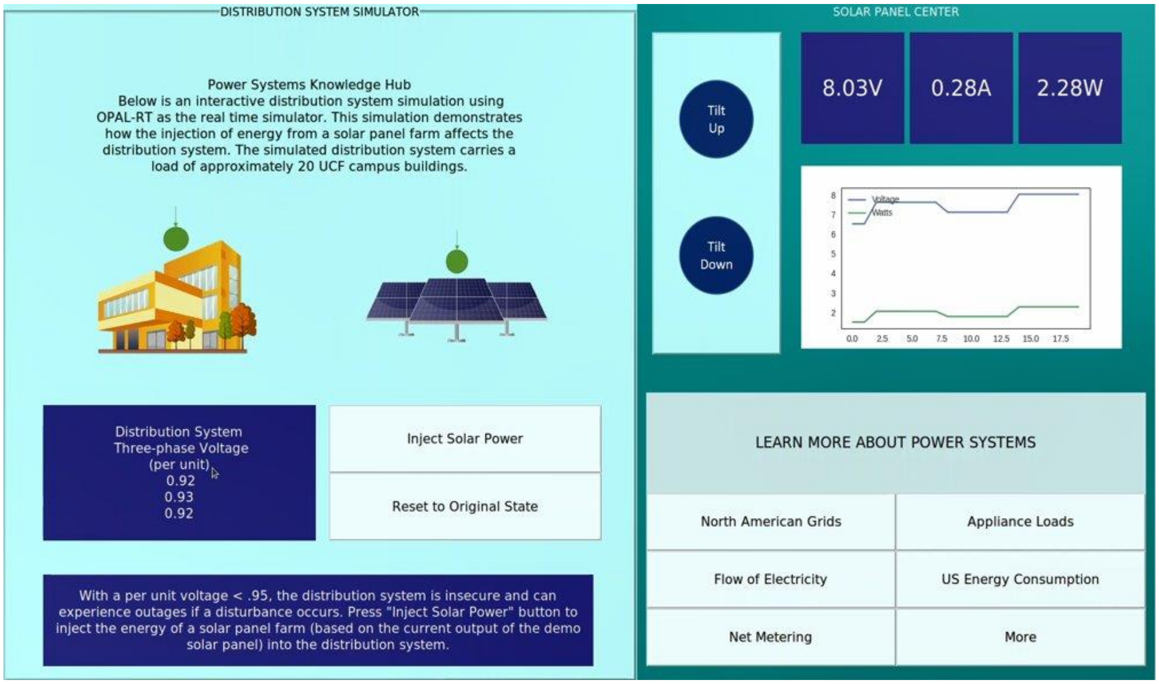

Power Systems Knowledge Hub
Below is an interactive distribution system simulation using OPAL-RT as the real time simulator. This simulation demonstrates how the injection of energy from a solar panel farm affects the distribution system. The simulated distribution system carries a load of approximately 20 UCF campus buildings.

Distribution System
Three-phase Voltage
(per unit)
0.92
0.93
0.92

With a per unit voltage < .95, the distribution system is insecure and can experience outages if a disturbance occurs. Press "Inject Solar Power" button to inject the energy of a solar panel farm (based on the current output of the demo solar panel) into the distribution system.

8.03V 0.28A 2.28W

Figure 77: GUI Screenshot

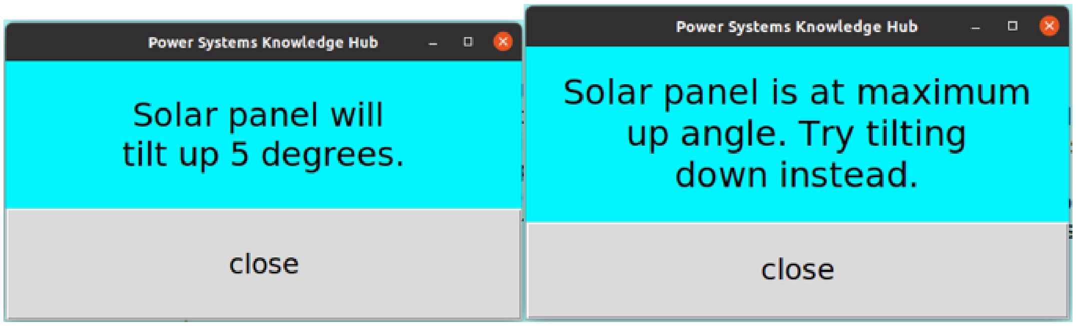

Solar panel will tilt up 5 degrees.

Solar panel is at maximum up angle. Try tilting down instead.

Figure 78: Solar Panel Tilt Messages

5.7.3 Educational Material

As previously discussed, the touch table users can access educational material on power systems from the GUI. Figure 79 shows the pop up window on top of the main GUI page when one of the topics is selected. Table 42 lists some of the different topics that are currently provided and a short description of what they will cover [114, 115].

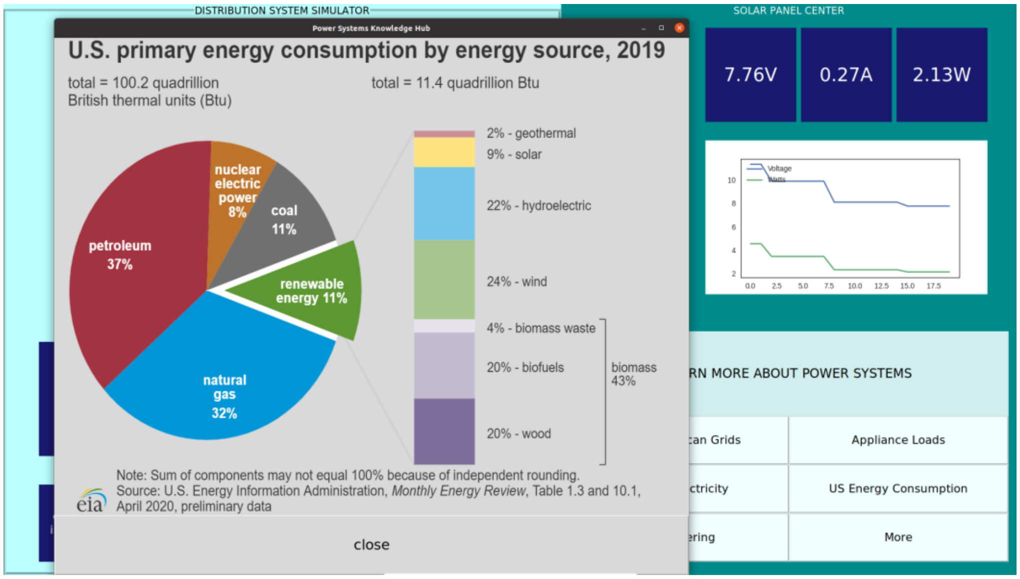

U.S. primary energy consumption by energy source, 2019

Note: Sum of components may not equal 100% because of independent rounding.
Source: U.S. Energy Information Administration, *Monthly Energy Review*, Table 1.3 and 10.1, April 2020, preliminary data

Figure 79: Educational Material Pop Out Panel

Table 42: Educational Topics

Topic	Material Covered
North American Grids	A map of the US and Canada showing the areas covered by the different grids including the Western Interconnection, the Texas Interconnection, the Eastern Interconnection, and the Quebec Interconnection.
Flow of Electricity	A graphic from FPL that shows the flow of power from the substation all to the residential and commercial service including all steps in between.
Net Metering	Graphically shows a high level view of how renewable energy is injected into the grid using inverters and bi directional meters.
Appliance Loads	Graphs displaying the power load of various appliances in relation to each other including ranges, refrigerators, HVAC units, dishwashers, washers, and driers.
US Energy Consumption	Displays a graph from 2019 depicting how US primary energy consumption by energy source. Sources include petroleum, natural gas, renewables, coal, and nuclear. The renewal energy category is further broken down into subcategories.

5.8 Event Source Location

A stretch goal for our project was to determine the location of events on a power distribution system. An event is defined as any big shift in every part through the distribution feeder, which are known to be the power lines distributing energy to their regions. Common actions that could lead to events include load switching, capacitor bank switching, connection, or disconnection of distributed energy resources (DERs), inverter malfunction, a minor fault, etc. [62] Events can be detected in a variety of methods that allow us to understand what problems may arise in power systems. However, even though we can detect an event occurring, the biggest issue we face daily is now finding where this change is occurring.

This brings to light the core purpose of our work, being able to educate the public on how we can locate a change within the power systems utilizing Distribution-level Phasor Measurement Units (PMUs), more commonly known as micro-PMUs (μPMUs). The use of these μPMUs can help us locate the source of any event in the system using the GPS-synchronized phasor measurements that these provide help us have a level of insight into the distribution system that allows us to understand and locate where an event can occur. [62] Due to time constraints the stretch goal was not achieved. Therefore, this section of the project was not implemented. This section would be a great addition to the already developed project.

5.8.1 Compensation Theorem

A small change in an electrical circuit could produce a variety of changes throughout the entire system. To help us understand what changes were caused in a circuit due to an event, we will apply the Compensation Theorem. According to F. F. Judd and P. M. Chirlian, the Compensation Theorem is “the calculation of current change ΔI may be carried out by replacing the added impedance ΔZ by the series combination of a voltage source I(ΔZ) and impedance ΔZ, while at the same time replacing all sources in network N_1 by their equivalent impedances.” [63] This means that to detect an event at a certain location we must use an equivalent circuit to understand what event is occurring and where is the change originating.

Using the Compensation theorem and an equivalent circuit would make the detection of an event location much simpler as seen in Figure 80. From this figure we can better visualize how the Compensation Theorem utilizes an equivalent circuit by switching out the resistor where the event took place for an equivalent current source that reflects the same change in current through the network.

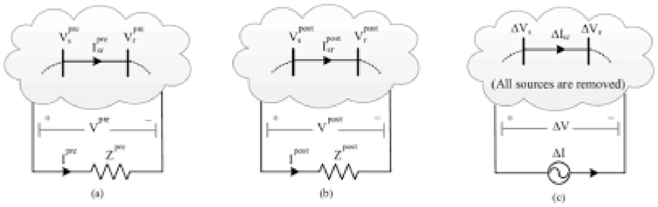

Figure 80: Compensation Theorem Application: a) Pre-Event, b) Post-Event, c) Equivalent Circuit Applied

Based on Figure 73 we see a change in impedance represented with Z. Using the Compensation Theorem, we switch out this impedance that caused the event with a current source that shows the change in current represented with the equation:

$$\Delta \mathrm{I} = \mathrm{I}^{\mathrm{post}} - I^{pre} \tag{4}$$

where $\mathrm{I}^{\mathrm{post}}$ represents the current after the event, $\mathrm{I}^{\mathrm{pre}}$ represents the current before the event, and ΔI represents the change in current, which is the current source.

5.8.2 Minimum Spanning Tree (MSP)

Implementation of this Event Source Location Identification (ESLI) relies on an important prerequisite; Event Detection (covered in a later section). As seen in Figure 81, the prescribed algorithm is capable of finding the source location of in the IEEE 123-bus test case when two or more µPMUs are used. Figures 81a and 81b show two interesting results: 1) Same as Bus 5 and 2) Same as Bus 22. In Figure 81a, bus 22 to bus 44 has the same discrepancy measures as bus 5. This is because there is no PMU placement starting at bus 22 through 44. So, they take on the same weight as that of bus 5 since this is the bus to which bus 22 is connected. Similar explanation goes for figure 81b. This concept is referred to as minimum spanning tree (MST). Hence, to be able to cover all the buses on a feeder at least two µPMUs are needed (placed at both ends of the feeder). Figure 82 shows the IEEE 123-bus test system when four µPMUs are connected thus covering all the buses in the network. Figure 82 depicts the outcome with all four µPMUs included.

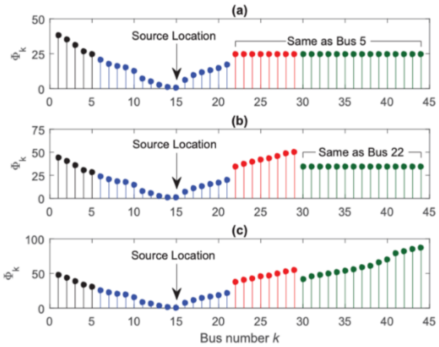

Figure 81: Source Location based on the IEEE 123-bus test system, with data from a) two µPMUs, b) three µPMUs, and c) four µPMUs

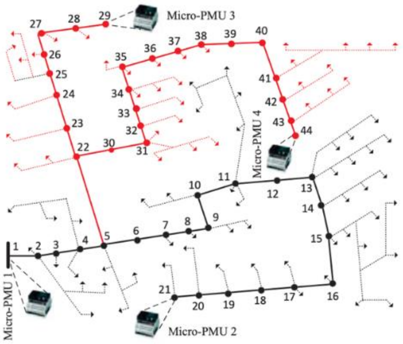

Figure 82: IEEE 123-bus test system with complete network coverage

5.8.3 ESLI Algorithm

After being able to detect an event, we then must begin identifying where exactly this event took place. There exist three possible locations where an event may occur: upstream of a PMU, downstream of a PMU or between the two PMU. The impedance helps us determine where this event could have occurred. A negative impedance in the upstream or downstream indicate a change leading to an event in either one (whichever is negative means the impedance is upstream or downstream), or if both impedances are positive then the event lies between the two PMUs. Knowing this we can begin to calculate the nodal voltages using KVL to measure the current injection from the event occurred. Measuring these voltages and currents would then help us determine more precisely the location of the event by comparing the voltages both upstream and downstream from every node where these voltages must be identical or almost equal.
Before being able to detect where an event is occurring, we must first verify if an event is taking place. Using the algorithm and information provided in the previous section we can determine a change in the system. The question now remains how we can detect the location of the given event. By implementing a series of equations and a new algorithm to the Event Detection Algorithm we can create a larger program that can carry out both functions at once beginning with detecting the root of the event.

Using PMUs and an array of busses in our distribution system we can create a layout of three possible locations where an event could be detected based on the voltage and current running through the system. The three different regions are: upstream of one PMU, downstream of the second PMU, and between both PMUs. To be able to determine in which of the three regions the event is taking place, we must first determine the impedance of the equivalent upstream and downstream seen by both PMUs. To do so we define the impedances as:

$$Z^u \triangleq \frac{\Delta V^u}{\Delta I^u}, \tag{5}$$

$$Z^d \triangleq \frac{\Delta V^d}{\Delta I^d}, \tag{6}$$

where Z^u and Z^d are the upstream and downstream impedances, ΔV^u and ΔV^d are the difference in the upstream and downstream voltages captured by the two PMUs before and after an event was detected, and ΔI^u and ΔI^d are the difference in the upstream and downstream phasor currents captured by the two PMUs before and after an event was detected. Based on these calculations we can see where the event is taking place. A negative upstream impedance, $Z^u < 0$, indicates that the event occurred upstream of the PMU; A negative downstream impedance, $Z^d < 0$, indicates that the event occurred downstream of the PMU; Both positive upstream and downstream impedances indicates that the event occurred between the PMUs. The task at hand now becomes how to determine the event location when it is occurring between the two PMUs.

Locating the source in the bus between the PMUs could seem troublesome, but using the Compensation Theorem explained previously we can place a current source with a current representing the change in the bus to create an equivalent circuit as shown in Figure 83. The voltages at the nodes and the current through the branches of this equivalent circuit are going to be equal to the change in nodal voltages and branch currents. Knowing this we can begin to calculate the nodal voltages using KVL to measure the current injection from the event occurred. Measuring these voltages and currents would then help us determine more precisely the location of the event by comparing the voltages both upstream and downstream from every node where these voltages must be identical or almost equal. Determining what the discrepancy is by calculating the change in voltages going forward and backward through the bus serves as a comparison point to verify at what point or points the voltages do not match. Knowing this we can determine at what points of the bus the event is taking place. [62]

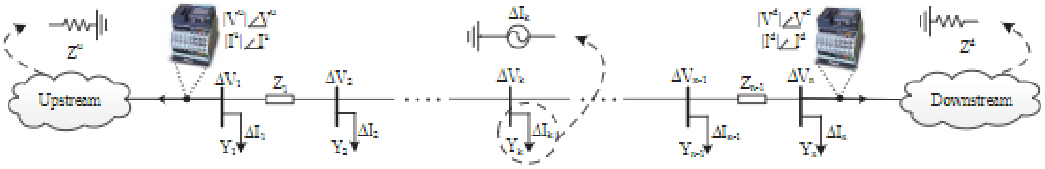

Figure 83: Distribution system utilizing compensation theorem to locate event between PMUs

5.9 Event Detection

Before executing an ESLI function, it is meaningful to detect whether there is an event or not. This section covers the basic concepts of how event detection is implemented. The algorithms proposed by [62] for the *anomaly detection architecture* improved on state of the art with the capability of: 1) near real-time analysis, 2) three-phase distribution grid equations, and 3) quasi steady-state condition considered as the *normal regime* of operation. These will be expanded upon in further discussion.

Going into a deeper understanding of event or anomaly detection, according to Pramit Choudhary, event detection is “a technique used to identify unusual patterns that do not conform to expected behavior, called outliers. It has many applications in business, from intrusion detection (identifying strange patterns in network traffic that could signal a hack) to system health monitoring (spotting a malignant tumor in an MRI scan), and from fraud detection in credit card transactions to fault detection in operating environments.”[108] Using event detection in various industries is nothing new, instead it has served as a functional stepping stone for many projects and devices throughout the years. The ability to monitor the conditions of a system at every point to make sure it is operating at an optimal level is crucial. In our work, event detection plays a significant role as the monitoring of a distribution grid is key for the desired work to be carried out.

5.9.1 PMU Data

Being able to classify and locate events in a system is an incredibly helpful tool needed to monitor systems as previously stated and automated detection is essential for a deeper analysis of any events to be detected moving forward to prevent any damages or problems, and allows a more precise planning for maintenance or even prevention of the event occurring again. Figure 84 allows us to see how the grid is distributed using PMUs to retrieve the data of any given point. The PMU analyzes the data first at a circuit level at various nodes throughout the system where this data is then sent and archived into a database to monitor the system in real time. This information is then processed and verified to make sure the system is running at an optimal level as desired.[109]

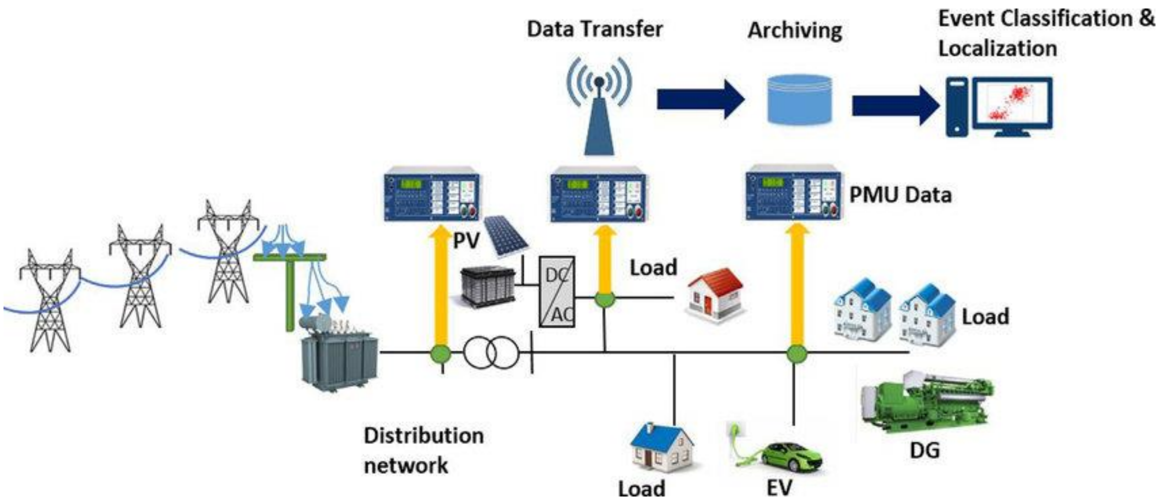

Figure 84: PMU data retrieval from a distribution grid

Various events can be detected based on the data received from the PMU and monitored in the database. Quantities such as voltage magnitude, frequency drift, current magnitude, active power, reactive power, and others serve as the key points into event detection of the grid. [109]

5.9.2 Changes in voltage magnitude

The voltage must operate between a certain range given by power quality standards in order to ensure optimal performance of the system which means that any change in the voltage magnitude that exceeds the normal threshold results in an event being detected. Utilizing the formula

$$\Delta V = V^{post} - V^{pre}\,, \tag{7}$$

where the change in voltage is measured by subtracting the voltage after the event occurred, V^{post}, from the voltage retrieved before the event, V^{pre}, we can determine the event began to occur and can work on a solution to ensure the voltage falls back into the given threshold.

5.9.3 Changes in Active and Reactive Power

The most important quantities to monitor in a distribution grid calculated from the data received from the PMUs is the active or real power and reactive power in the system. According to Jean Jacques Meneu, “real power is the power actually consumed due to the resistive load and apparent power is the power the grid must be able to withstand.”[110] Additionally, Jacques Meneu describes reactive power as “electrical energy stored in the coil that then flows back to the grid”.[110] This information gives us a better understanding on how the system is functioning based on the power being distributed throughout the grid.

(8)

Utilizing the phasor measurements gathered from the PMUs we can calculate the apparent power as

$$S_{mn} = P_{mn} + Q_{mn} = diag(v_m)i_{mn},$$

where S_{mn} is the apparent power, P_{mn} and Q_{mn} are the three-phase active and reactive powers, m and n are busses, diag is a function that returns a square diagonal matrix with the elements of the vector, in this case the phasor voltage v_m, and i_{mn} is the phasor current. Based on this we can track the power flow change in the system which is preferred over monitoring the phase angle differences due to the resistances of the lines are not negligible making the direction of the power flow not known from the phase angles meaning that power does not normally flow from a higher angle to a lower one.

Changes in the active and reactive power can still occur even if the voltage magnitude does not go over or under the given threshold due to the load which can potentially affect the current magnitude and the phase angles. Because these changes can occur the system runs a risk and must be addressed quickly by determining the location of the event, discussed in section.

5.10 Solar Panel Interface

This section shows the outline of how the output from the solar panel was to be measured and processed by our PCB before our design moved from a relay model. The solar panel was stationed where it could absorb light energy. The original task was to convert light energy into electrical energy. Another twist, was to generate Alternating Current (AC) signals since the solar only output Direct Current (DC) and our power system model operates with AC. This challenge was addressed by incorporating an inverter to the output of the solar panel. The inverter takes DC input and output AC. This converted AC electrical energy was to be communicated to our server over Wi-Fi. But, before this could have been done, we needed to measure this converted electrical output value with our PCB. After going through some options, we decided to use a relay that can measure the inverter outputs. The PCB was to then interface with the relay to read the values it measures and stores in its registers. Figure 85 shows a simple design block of interfaces related to the host MCU and the solar panel.

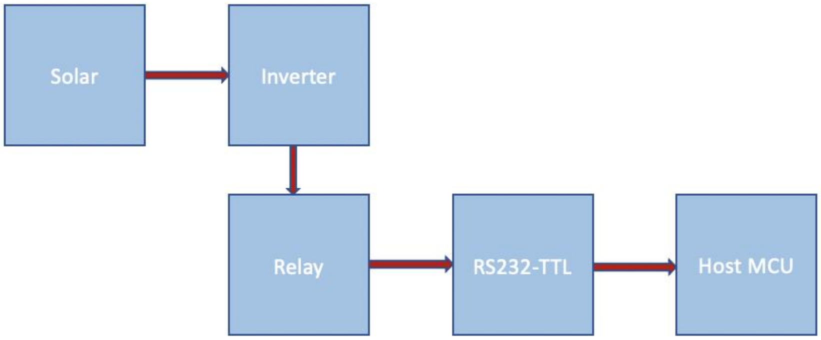

Figure 85: Block diagram for solar and PCB interface

The device we initially selected for interfacing the PCB with the relay was the RS232-TTL converter. This was to be implemented by the MAX3232 MCU device. This device required 3-V to 5.5-V VCC supply as such it would have been powered with the same DCDC converter that was design to power the host MCU. The supply current was typically around 300 uA. This low operating current would be a benefit to our application since we would be using battery to power the PCB. Low current draw minimizes the battery drain rate and lengthen the battery replacement window.

Given that we decided not to use a relay to acquire voltage and current reading, we needed a new approach to measure or calculate these values. The block diagram in figure 86 below shows the representation of the interface.

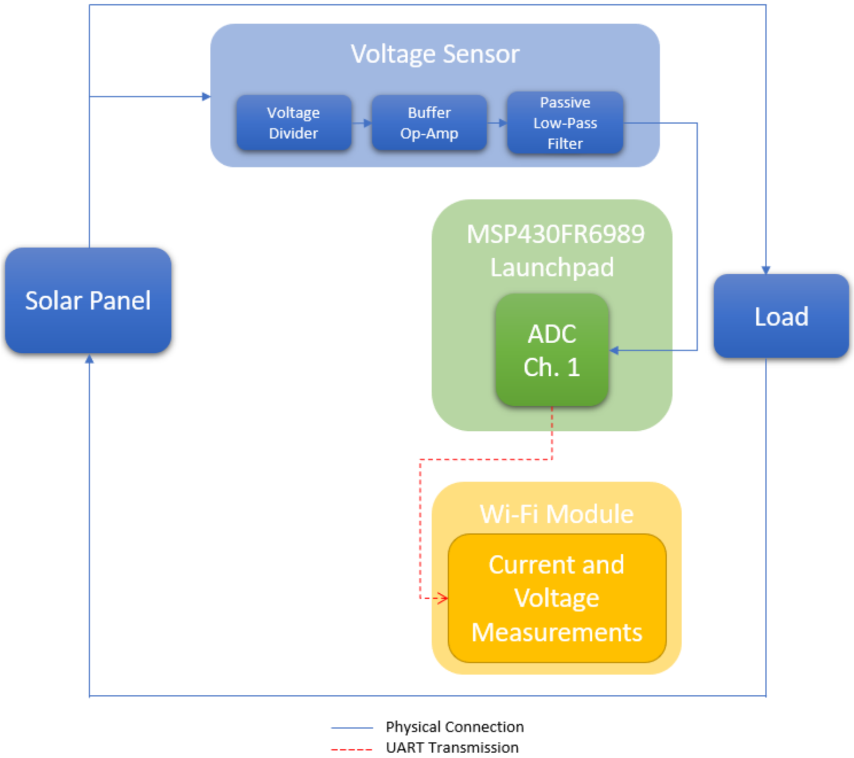

Figure 86: PV voltage measurement interface

The design was based on TI Voltage, Current, and Temperature Monitoring for Solar Module Level Power Electronics [138]. As recommended by the documentation, the voltage module was design to ensure the maximum output from the measurement module is 1.77.

This would correspond to the maximum voltage out from the PV, which is 24 V in our case. Therefore, to determine the actual voltage per what was seen at the ADC input, the ADC signal was multiplied by a ratio of 24/1.77. This low analog signal protected the ADC from a high input value that could damage the PCB. Figure 87 below shows the MATLAB Simulink simulation model of the voltage measure design.

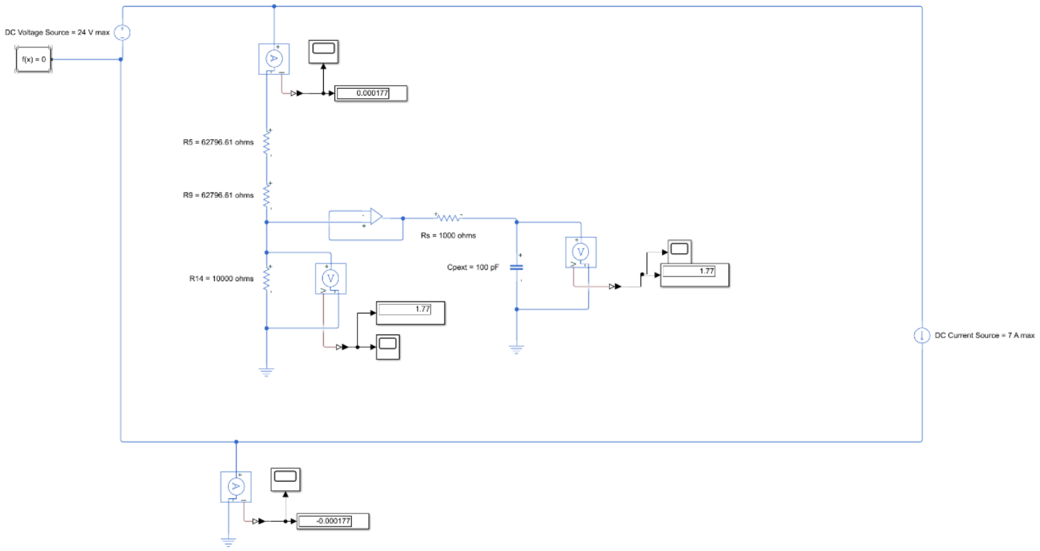

Figure 87: MATLAB Simulink voltage measurement circuit simulation

5.11 PV Angle Change

This section discusses methods and implementation of solar tracking used to change the angle of the solar panel. It covers an algorithm that could track the best theoretical angle for the PV and describes how the user can change this angle to create a reduction in power output thereby creating a disturbance in the system.

5.11.1 Solar Tracking

As previously stated, to receive the optimal amount of energy using our PV Panel we wanted to construct a system that could perform solar tracking. Solar tracking requires the PV Panel to follow the sun's position throughout the day. We can better determine the position of the sun on a certain day based on the time and the season by calculating the azimuth angle. Based on Christiana Honsberg and Stuart Bowden, "the azimuth angle is the compass direction from which the sunlight is coming. At solar noon, the sun is always directly south in the northern hemisphere and directly north in the southern hemisphere."[113] Honsberg and Bowden explain that the azimuth angle of the sun based on the time of year and latitude can vary as seen in Figure 88.

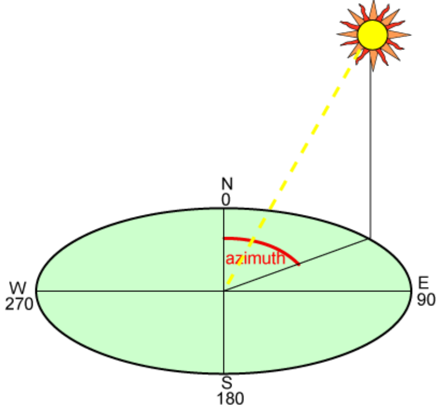

Figure 88: Azimuth angle of the sun

The exact azimuth angle that helps indicate the sun's position throughout the day can be calculated by:

$$Azimuth = \cos^{-1}\left[\frac{\sin\delta\cos\varphi - \cos\delta\sin\varphi\cos(HRA)}{\cos\alpha}\right] \tag{9}$$

where α is the elevation, φ is the latitude, δ is the declination, and the HRA is the hour angle. All these parameters have formulas of their own to fully calculate the azimuth angle. In order to calculate the azimuth angle of the sun we must first define the Local Standard Time Meridian (LSTM) as

$$LSTM = 15° \times \Delta T_{GMT}\ , \tag{10}$$

where ΔT_{GMT} is the difference between the local time and the Greenwich Mean Time (GMT). After defining the LSMT, we can then calculate the Equation of Time (EoT),

$$EoT = 9.87\sin(2B) - 7.53\cos(B) - 1.5\sin(B), \tag{11}$$

where B is defined by the equation

$$B = \frac{360}{365}(d - 81), \tag{12}$$

where d is the number of days since the start of the year. Figure 89 shows an example of a graph of how the EoT is visualized.

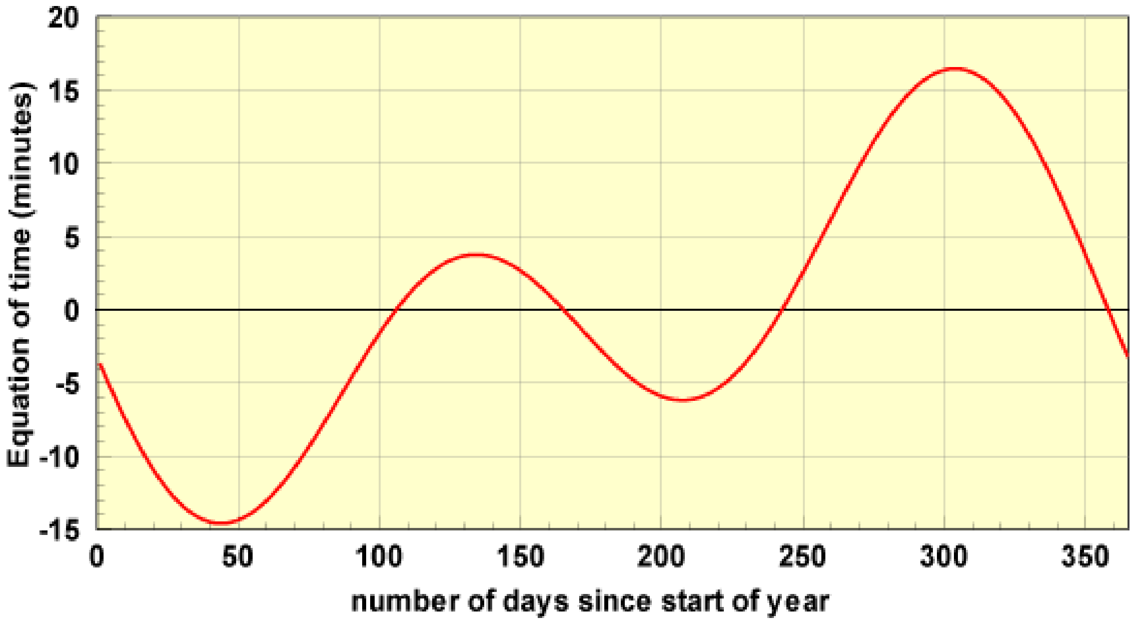

Figure 89: Graph of time correct EoT

The EoT has been used throughout history in order to tell time based on the position of the sun. The earliest known use of the EoT was during the creation of the sundial. Sundials used the position of the sun to make one of the first working clocks and they included the EoT on them to provide the correct time based on the day throughout the year. Figure 90 shows an example of a sundial utilizing the EoT correction to tell time.

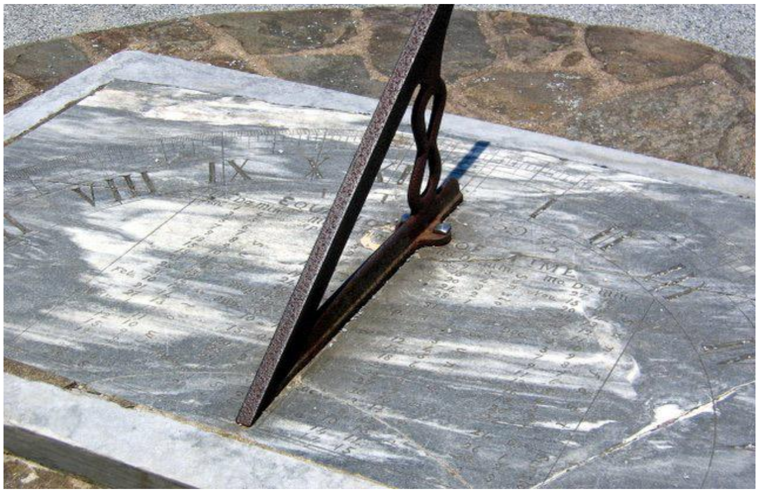

Figure 90: Sundial utilizing EoT to determine time

Utilizing the newly found LSMT and EoT, we can now define the Time Correction Factor (TC). The TC, according to Honsberg and Bowden, "accounts for the variation of the Local Solar Time (LST) within a given time zone due to the longitude variations within the time zone"[113], which is defined as

$$TC = 4(Longitude - LSMT) + EoT. \tag{13}$$

The factor of 4 seen in the definition of TC accounts for the four minutes the Earth needs to rotate 1 degree. Using this TC we can now use these corrections in order to determine the LST, defining it as

$$LST = LT + \frac{TC}{60}, \tag{14}$$

where LT refers to the Local Time. The newly calculated LST allows us to know the Hour Angle (HRA as previously stated). The HRA, according to Honsberg and Bowden, "converts the local solar time (LST) into the number of degrees which the sun moves across the sky."[113] The HRA is expressed as

$$HRA = 15°(LST - 12). \tag{15}$$

Now that we obtained the HRA, we must now define the remaining two parameters that help us obtain the azimuth angle: declination and elevation. The former is defined as

$$\delta = 23.45° \sin\left[\frac{360}{365}(d - 81)\right], \tag{16}$$

where d is again the number of days since the start of the year, and the latter can be defined as

(17)

$$\alpha = \sin^{-1}[\sin\delta \sin\varphi + \cos\delta \cos\varphi \cos(HRA)],$$

where φ is the latitude of your current location. Now with every parameter defined we can properly create an algorithm that updates the PV panel's angle over time to ensure optimal energy generation.

After testing and further consideration, solar tracking was not implemented in the final stages of our project. Angle movement by the user provided enough data where the changes in the system were registered.

5.11.2 User Interaction

In order to demonstrate a non-ideal situation where the PV panel is not following the position of the sun and ultimately not generating enough energy, we can remotely adjust the PV by manually updating the angle from the touch table. Pushing an up or down button, users could remotely change the angle of the PV Panel in order demonstrate the loss or gain of power in a system when there is a change in voltage.

5.11.3 Movement of PV Panel

The PV Panel's initial movement was based on the use of the azimuth algorithm, the motor, and the PCB angle control module. Using the data given by the algorithm, the motor, using a constructed 5:1 gear ratio to ensure the proper amount of torque needed, could have move the PV in order to perform solar tracking. Figure 91 has a rough schematic on how the system would operate.

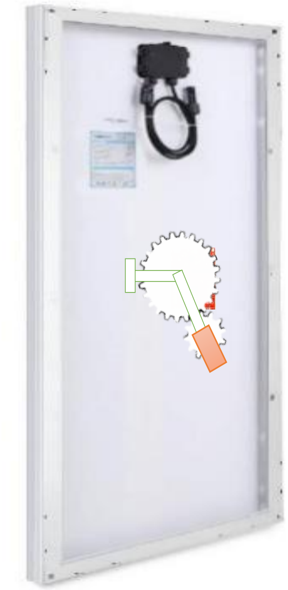

Figure 91: Rough schematic of PV Panel movement design

The panel was going to have a set of braces (shown as the green rectangles) attached to the back connected to a gear. This set would have acted as the pivot point of the PV. The motor (shown as the red rectangle) would be directly connected to a smaller gear in order to create a high torque gear ratio. Utilizing the PCB angle control module, we could monitor the PV’s position and update it based on time to reach the desired angle to perform the solar tracking. For the user to control the PV remotely or the PV to automatically update its position, the motor would begin to run at a slow speed, to ensure correct readings, until the value of the angle retrieved from the PCB matches the angle calculated by the algorithm. After testing, this design was not used and was replaced multiple times until reaching its final version.

5.11.4 Solar Panel Mount Design

For our solar panel mount design, we wanted to go with a simple approach with a structure similar to that of a drafting table. This design utilized 80/20 aluminum extrusions and aluminum C-Channels utilized in VEX Robotics as the primary support pieces of the mount which could easily hold the weight of the solar panel. We placed the motor on the base of a cascade pulley system. The pulley system was constructed using small 80/20 aluminum extrusions. The design works as a linear actuator pushing and pulling the solar panel by a single point. This is made possible by winding and unwinding a string attached to the bottom part of the first extrusion making its way back to the motor. By winding the string the aluminum extrusions slide up pushing the solar panel. The pattern the string goes through each of the extrusions allows it to distribute the weight evenly making it easier for the motor to move the solar panel even if the motor itself is not strong enough to do so. The solar panel was also elevated only a foot from the ground for a low center of mass to provide a sturdier base.

5.11.5 Required Torque Calculation

To have a better understanding on how much torque was required to be able to move the solar panel from its extreme points (-40˚ and 40˚), a practical measurement was used. Utilizing a specific point on the solar panel mount as a handle (the same point from where we push and pull our panel) we can determine the amount of torque necessary by applying a force the opposite direction which we could measure. Setting a bag on this point, bottles of water were used as our counteracting force in order to measure the torque required. Utilizing bottles of water and the properties of water itself, we were able to determine the torque required by multiplying the total number of bottes (in this case 6 bottles provided enough weight) times the milliliters per bottle times the density of water. After executing these calculations all that was left was to multiply the result by gravity to find the force we needed (approximately 4.9 N/m). The selected motor, the Nema 23 Stepper Motor, only provides 1.9 N/m of torque.

5.11.6 Cascade Pulley System

Since the selected motor had almost 3 times smaller torque than the minimum required to move the solar panel from its extreme points, a system was needed to redistribute the force. The system chosen was a cascade pulley system. Behind the physics of pulley systems, weight and force are distributed evenly throughout the system. The cascade pulley system designed consists of four stages compacted into a small space in order to provide the correct amount of rotation needed on the solar panel by pushing and pulling the system the same way a linear actuator operates. The design was also Madeira of a cascade lift in order for the system to never block the sunlight on the solar panel. The Nema 23 motor pulls continuously on a string that raises and lowers the stages of the cascade lift every half rotation providing 5 ̊ of rotation. The pulley system has the same effect as that of a 4:1 gear ratio on a gear box, this means it provides 4 times the amount of torque of the motor by sacrificing 4 times its speed giving us the ideal torque needed to move the solar panel.

5.11.7 Motor Communication

The motor must possess a form of communication in order to know when the PV must be moved and for how long. Utilizing the PCB to read the data from the angle control module and the wireless communication with the touch table we can direct power to the motor, positive for one direction and negative for the other, to carry out the movement of the PV panel.

5.12 Wi-Fi Interface

At this phase of the design, we initially decided on using TI’s CC3100 Wi-Fi module instead of the ESP8266EX module that was initially selected. As we progressed to the prototyping and testing phase, we decided on going with ESP-12E. We were and maintained strong support of using TI microcontroller. No conclusive evidence was found when searches were conducted to determine the compatibility between the ESP8266EX and MSP430FR6989. As such, it seemed to be a better idea to pair two TI products together. As such, the below showed the original discussion about the interface between our host MCU, the msp430fr6989 and the CC3100 Wi-Fi module.

The CC3100 is available as a Wi-Fi module SoC or as a Wi-Fi BoosterPack. Either package requires a host MCU. To successfully interface this module with our main MCU, the CC3100 BoosterPack that is often marketed by TI peering with the MSP430F6629 LaunchPad, will be studied. According to TI all CC3100 customer need an EMUBOOST for flashing the CC3100 BoosterPack.

In Figure 92, the CC3100 BoosterPack and its peripherals are labeled. The 2x20 pin LP Connector is the maintain interface for the host MCU. Knowing the pin layouts of the CC3100 is the gateway to making it talk to the host MCU. Integrating CC3100 with the MSP430F5529 is only a plug-and-play exercise excluding the flashing requirements. However, a major project requirement is to design our own PCB hence this will inform how the interface must be built to ensure it can communicate with the CC3100 Wi-Fi module. The table on either side of the CC3100 includes color codes to indicate which connectors are used or unused.

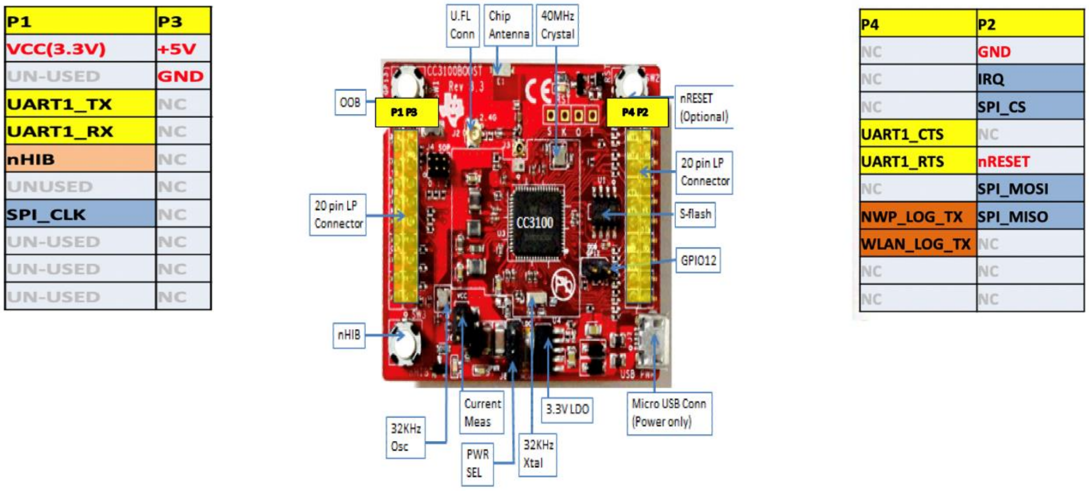

P1	P3
VCC(3.3V)	+5V
UN-USED	GND
UART1_TX	NC
UART1_RX	NC
nHIB	NC
UNUSED	NC
SPI_CLK	NC
UN-USED	NC
UN-USED	NC
UN-USED	NC

P4	P2
NC	GND
NC	IRQ
NC	SPI_CS
UART1_CTS	NC
UART1_RTS	nRESET
NC	SPI_MOSI
NWP_LOG_TX	SPI_MISO
WLAN_LOG_TX	NC
NC	NC
NC	NC

Figure 92: CC3100BOOST Signal Assignments

Per the CC3100 User Guide, it can consume up to 400mA of current peak from the 3.3V VCC. TI states that some LaunchPads, including the MSP430FRAM do not provide enough current to power CC3100 BoosterPack. One way to address this concern is to provide the CC3100 BosterPack with its own power. This will relieve the host MCU of worrying about how to power the Wi-Fi module. There is one other concern to take into consideration when designing the power unit to drive the PCB. This is because the CC3100 requires a +5V on pin P3.1. In the CC3100 BoosterPack, an onboard USB interface was added so to provide this +5V from a PC. Since we will not operate our PCB or Wi-Fi module from a PC, we must design our power supply to satisfy this requirement. More information can be found under the Power Supply section.

Connecting the CC3100 to our host MCU through headers is a secure method to merge the two devices. To do this, the host must be design with the same header spacing dimension. This means that’s we must be able to ascertain the CC3100 2x20 pin LP connector spacing dimension. One way to achieve this is to utilize the CC3100 data sheet. If this information is not available, another way to get it is to physically measure the header spacing dimension after buying the device.

5.13 Motor Interface

To enable the solar module to move, the team initially decided to use a servo motor but later changed to a stepper motor. The servo motor must provide angular rotation for an applied pulse width modulation duty cycle. As the duty cycle of the applied signal is varied, the angular displacement of the motor also varies [105]. The applied signal should have been capable of generating bi-directional mechanical rotation.

As the case for the servo motor, stepper motor usually requires higher supply voltage rating than the host MCU. MSP430™ device GPIO pins allow for a maximum output of 3.3 V, depending on its VCC level. However, most servo and stepper motors typically operate at 5-V rail or greater voltage and therefore require some form of voltage level translation to be driven by the microcontroller. It is possible to use an N-channel MOSFET as a logic switch, as shown in Figure 93 with the CSD18537NKCS, or a unidirectional voltage translation device (such as from the SN74LV1Txx family) to accomplish this task [105].

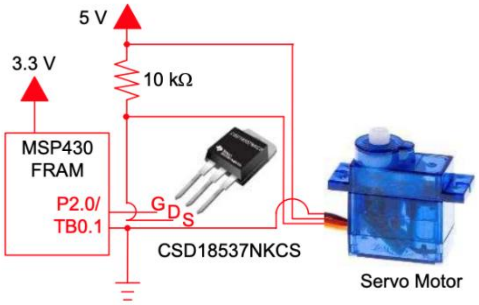

Figure 93: Servo Motor circuit diagram

5.14 LED Interface

It was a good practice to use visual indication to show that a device is on or off or has logic high or low. For this reason, a simple LED interface was included in the PCB to indicate when it is powered on. The two leads of the LED, anode or positive lead and the cathode or negative lead. As shown in Figure 94, LED needs to be biased with approximately 1.7-2.2 voltage difference across both leads [104]. The LED current also known as the forward current should also be limited to a safe level. Detail LED specification are frequently provided by the manufacturer.

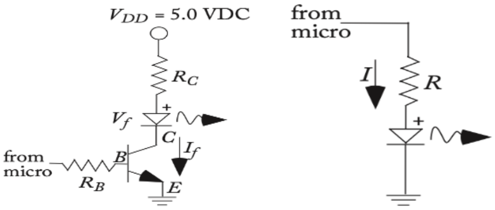

Figure 94: LED biasing circuit

6. Project Prototype Testing Plan

This section is composed of describing unit tests that were performed in order to achieve a successful project. Our project communicates with various equipment, and it is vital to ensure that each component is compatible with each other. The unit tests described will also help isolate issues.

6.1 Phasor Measurement Data Transmission through UCF's HEC Network

The stretch goal requires the touch table to display and analyze the PMU streams that are coming from the distribution system modeled in Simulink. As previously explained, this phasor measurements will be transmitted following the IEEE C37.118 standard. To test that the PMU streams are indeed being transmitted through the network in UCF's HEC building, a PMU Connection Tester was installed to a computer at HEC. [16] This test will ensure that the interactive touch table will indeed be able to receive these PMU streams.

The PMU Connection Tester application was developed by Tennessee Valet Authority (TVA) to support the North American Synchrophasor Initiative (NASPI). This application verifies that the data stream from phasor measurement devices is being received. PMU Connection Tester can decode and verify the following phasor protocols IEEE C37.118, IEEE 1344-1995, BPA PDCstream, and Virginia Tech FNet. To run this test, an example model developed by OPAL-RT was used. This model is called "C37.118 Slave" and it is available and ready to use. A screenshot of this model is shown below in Figure 95.

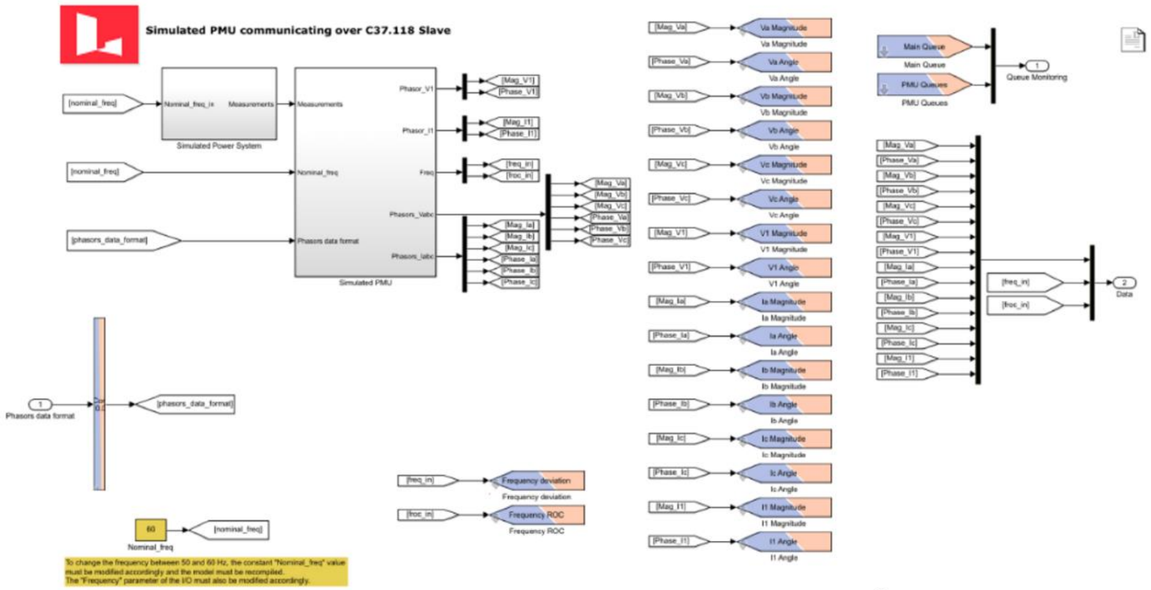

To change the frequency between 50 and 60 Hz, the constant "Nominal_freq" value must be modified accordingly and the model must be recompiled.
The "Frequency" parameter of the I/O must also be modified accordingly.

Figure 95: Simulink model outputting 8 PMU phasor streams

Some modifications to this model were done to the model to match the purpose of this test. The original model was transmitting analog and digital signals, and these were removed because only the verification of the transmission of phasor measurements was required.

This model outputs 8 phasor streams using the IEEE C37.118 protocol. The outputs are Va, Vb, Vc, V1, Ia, Ib, Ic, and I1. Both the magnitude and angle of each are being transmitted. Three communication protocols are supported: TCP only, UDP only, or TCP/UDP. But for the purpose of this test, the communication protocol being used is TCP. The model shown in Figure 86 was then ran in real-time. The PMU Connection Tester was used to verify that the streams are being sent and following the IEEE C37.118 protocol.

Th PMU Connection Tester was then configured with the IP address and TCP port number of OPAL-RT. As shown in Figure 96, it was able to display the frequency variation in real-time as well as the phasor angles. This confirmed that the PMU streams were indeed being sent and that it was following the IEEE C37.118 protocol. It is important to note that the IP address and the TCP port number were hidden for security purposes.

It is also important to note that the model used for this example generates random values, it does not represent the actual behavior of a real power system. For our project, a distribution system model was designed with the use of ePHASORSIM to represent the behavior of a real distribution power system.

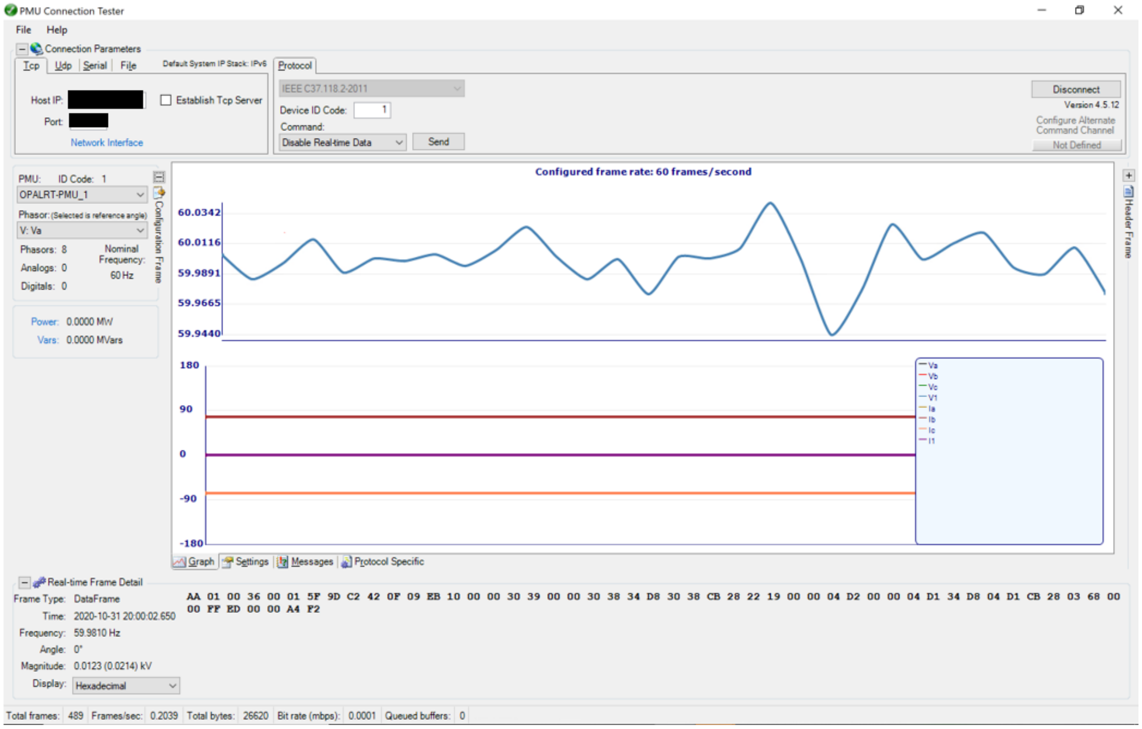

Default System IP Stack: IPv6

Host IP: [redacted]

Port: [redacted]

□ Establish Tcp Server

IEEE C37.118.2-2011

Device ID Code: 1

Command: Disable Real-time Data

Version 4.5.12

Not Defined

PMU: ID Code: 1

OPALRT-PMU_1

Phasor: (Selected is reference angle) V: Va

Phasors: 8

Analogs: 0

Digitals: 0

Nominal Frequency: 60 Hz

Power: 0.0000 MW

Vars: 0.0000 MVars

Frame Type: DataFrame

Time: 2020-10-31 20:00:02.650

Frequency: 59.9810 Hz

Angle: 0°

Magnitude: 0.0123 (0.0214) kV

Display: Hexadecimal

```
AA 01 00 36 00 01 5F 9D C2 42 0F 09 EB 10 00 00 30 39 00 00 30 38 34 D8 30 38 CB 28 22 19 00 00 04 D2 00 00 04 D1 34 D8 04 D1 CB 28 03 68 00
00 FF ED 00 00 A4 F2
```

Total frames: 489 | Frames/sec: 0.2039 | Total bytes: 26620 | Bit rate (mbps): 0.0001 | Queued buffers: 0

Figure 96: Simulink model outputting 8 PMU Phasor Streams

While performing this test, it was noticed that the license for RT-Lab allows for the transmission of sixteen PMU streams. This amount needs to be further verified but sixteen PMU streams is double of the amount of PMU streams sent in the test performed. This allows for the transmission of 3-phase voltage and current phasor values of 2 buses. The four other PMU streams can be used as desired but are not enough for one more bus, since each bus required six PMU streams. Although this test produced good results, since WAMS was not implemented, this section was not implemented in the final product of the project.

6.2 Communication between OPAL-RT and Raspberry Pi

Unit testing for communication between OPAL-RT and the Raspberry Pi has been completed in the Siemens Lab on the third floor of the Harris Engineering Building at UCF. To prepare for the testing, the microSD card containing NOOBS that came with the CanaKit was inserted into the Raspberry Pi. Then the cooling fan was hooked up, and the Pi was snapped into its case. An HDMI monitor, a USB keyboard, and a USB mouse were connected, and the Pi was powered on. NOOBS facilitated an easy installation of the Raspberry Pi Operating System, and then the Pi was verified to have Python 3.7.3 already installed. Next, SSH was enabled in the settings [77]. The Pi was then connected to an active ethernet port in the lab to connect with the UCF ethernet. Once connected, a static IP ethernet address was assigned to the Raspberry Pi [78].

MobaXterm was installed on the lab computer that runs OPAL-RT. A command prompt was opened, and the static IP address of the Raspberry Pi was successfully pinged to be sure it could be seen. MobaXterm was started, and an SSH session was initialized and the lab computer was able to successfully SSH into the Raspberry Pi via ethernet.

Next the webpage titled "RT-LAB + Raspberry PI + Python + UDP" in the OPAL-RT Technologies Knowledge Base [35] was accessed and the two python scripts and sample OPAL-RT model zip files from that webpage downloaded to the lab computer and extracted. The main.py file was opened in a text editor and edited to reflect the static IP address that was just assigned to the Raspberry Pi.

Both the main.py and ServerRP.py scripts were then dragged and dropped into the Raspberry Pi's file system via MobaXterm, and the main.py was executed on the Pi through MobaXterm. This script calls the server script, so there is no need to run that one. The MobaXterm SSH session then displayed "Waiting for connection from simulator" which indicated that the scripts been successfully executed.

The OPAL_RPI file contained a model which is a modified version of an example async_ip used by OPAL-RT Technologies and had been modified using MATLAB by the author of the Knowledge Base entry. It was opened and the block 'OpIPSocketCtrl1' (in sm_ip_test subsystem) was modified to match the Raspberry Pi's static IP address. The model was then compiled, loaded, and executed. As the model ran on OPAL-RT simulator, the values being sent by the model were appearing in the Raspberry Pi SSH session in MobaXterm thereby verifying that communication was taking place. Constant values were then changed in the running model, and the changes were shown in the SSH session [35]. This concluded the successful testing of communication between OPAL-RT and the Raspberry Pi.

Further testing was done with the Raspberry Pi connected to an ethernet port downstairs in the UCF Harris Engineering Building (HEC) to ensure that they could still communicate. However, the two locations do not appear to have the same gateway, so the static IP address did not work. UCF IT department advised that a static address would need to be reserved in order to guarantee that it would be available for us. We reserved an address in the HEC lobby at a port convenient for viewing an outside area in the front of HEC where the solar panel was stationed during testing and demos. The reservation expires in May 2021, so future development teams would need to request a new reservation.

6.2 Receiving and Decoding PMU data from OPAL-RT to the Raspberry Pi

Since the stretch goal of implementing WAMS was not completed, the testing for the receiving and decoding of the PMU data from OPAL-RT was not done. If WAMS is to be developed in future, the following paragraphs describe the testing that would need to be done.

Once the PMU data has been successfully transmitted from OPAL-RT to the Raspberry Pi, the Pi needs to capture those packets and convert the IEEE C37.118 protocol into usable data. As previously mentioned in this paper, Wireshark or TShark, a command line version of Wireshark, will be installed on the Raspberry Pi to accomplish this. Testing will first occur with Wireshark, but if the Raspberry Pi's resources are significantly diminished with it, then TShark will be tested as the alternative. This testing will need to be done on UCF campus.

To test that the packets are being received are able to be decoded and used, OPAL-RT will connect to the Raspberry Pi as described in Section 6.2 using MobaXterm. Wireshark (or TShark) will be started on the Pi, and a filter will be set up to capture packets from the ethernet connection to OPAL-RT only [38]. The model described in Section 6.1 will be executed, and random PMU data in IEEE C37.118 format will be transmitted to the Raspberry Pi. Wireshark will be checked to ensure that the data packets are being received and decoded.

Wireshark is supposed to save incoming real-time data into a temp file, and that file will be located and opened to make sure that it is updating in real time [38]. If the file is not updating in real time, then further investigation will need to be done into accessing the incoming decoded PMUs. A script may need to be written to export the data every few seconds for the WAMS algorithm to access, but that will be addressed if it is necessary.

6.3 Testing Solar Panel

This section goes over how to safely install and test the 100 W 12 V solar panel.

6.3.1 General safety and precaution measures

The solar panel may generate DC voltages greater than 30 V when exposed to the direct sunlight. [122] Coming of contact with 30 Vdc can be hazardous. Therefore, safety precautions were taken when testing the solar panel. It is important not to disconnect the wires connected to the solar panel if it is exposed to sunlight, this can lead to burns, start fires, and/or create other problems. While testing the solar panel, the following safety precautions were be followed:

- No children around during transportation and installation
- Completely cover the module with an opaque material during installation to ensure no electricity will be generated
- Do not wear metallic ring, watchbands, etc. while working with the PV
- Use approved insulated tools when working on electric installations
- Only use equipment that is appropriate for use in solar electric systems

6.3.2 Installation

When starting installation, it is important to ensure that the small drainage holes on the undersize of the module is not blocked. The module should be placed facing true south. The solar panel must be tested in a location that meets the following requirements:

- Operating Temperature within -40°F to 194°F
- Relative humidity within 45% to 95%
- Avoid trees, buildings, or obstructions

In order to maintain the fire class rating, the distance between the PV modules (front glass) and the surface should be at least 5 in. [122] It is important to note that drilling holes in the module frame, modifying the frame, will void the warranty. The frame of the PV module must be grounded to avoid electrical shock. Appropriate grounding consists of using an appropriately sized EGC or racking system that can be used for integrated grounding. [122]

The frame of the PV already has pre-drilled holes marked with the grounding sign. The grounding wire must be properly fastened to the module frame to assure food electrical contact. The solar panel came with two stranded, PV rated, output MC4 cables. Where the positive connector is a male connector and the negative connector is a female connector.

6.3.3 Testing

Below is a list of how the tests that were performed:

- Voc and Isc were performed by exposing it to the sun, without any load connected to it.
- Voc was tested with the use of a digital multimeter
- Isc was measured by directly connecting the digital multimeter in the two terminals of the PV. The rated current of the load should be more than 1.25 times than the rated short-circuit current.

After these values were measured, it was verified that the values were compatible with the inverter. Since the values were compatible, it was then connected to the inverter.

6.4 Testing Inverter

This section will go over how to safely test and implement the inverter.

6.4.1 General safety and precaution measures

It is important to follow safety precautions when using the inverter. The inverter may result in damage and personal injury if safety practices are not followed. Below are listed some safety instructions that were followed when testing the inverter [121]:

- Inverter should not be exposed to rain
- Inverter must be placed in a flat surface
- Should not be placed in direct sunlight
- Do not try extending or changing the 12 V power cord supplied with the inverter
- Do not connect a load that draws a higher wattage than the inverter produces

6.4.2 Testing

The inverter was connected to a 12 V battery to test its performance before connecting it to the solar panel. This ensured that the inverter worked. Before turning on the inverter, both the inverter and the battery were grounded. After the inverter was up and running, a load was connected to it. The load that we used for testing was a fan. After ensuring that the inverter was working, it was shut off and disconnected from the load.

The inverter was then connected to the solar panel by following the instruction manual and the safety precautions. When connected to the solar panel, the inverter kept turning on and off due to the variable output voltage of the solar panel. The fan was connected to the inverter and it was never able to turn on. Therefore, it was decided against using the inverter for our project.

6.5 CC3100BOOST Wi-Fi Module Testing

This Module was not used in our design but the information about how it was tested was still presented. To begin hardware testing, the CC3100BOOST Wi-Fi module was firmly connected to the CC31XXEMUBOOST emulation board by way of the 2x20 header pins. The mini-USB cable that came with the Wi-Fi module was used connect via the J6 USB interface to provide power to the devices. The EMUBOOST main function is to program the Wi-Fi module.

The first test that was carried was in AP mode. The object of this test to was to ensure that other devices could connect to the CC3100BOOST Wi-Fi module wirelessly. With the board powered, SW1 was pressed and hold, while holding SW1, SW3 was pressed and released and SW1 released after one second. This put the Wi-Fi module in AP mode. Note, the default mode for the Wi-Fi module is Station mode. After this, an iPhone 6 was used to connect to the module by selecting its SSID (shown in figure 97) which in this case was

MySimpleLink-43E0D0. No password was used since the default AP configuration is Open. The connection was made successfully.

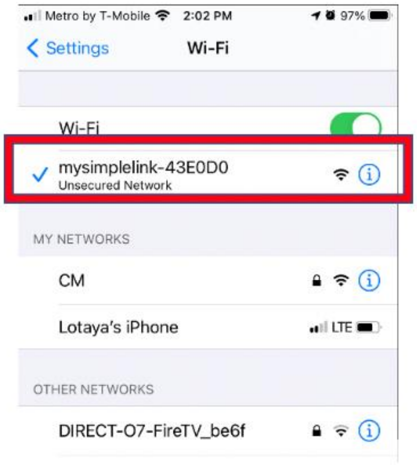

Metro by T-Mobile 2:02 PM 97%

< Settings Wi-Fi

Wi-Fi

✓ mysimplelink-43E0D0
Unsecured Network

MY NETWORKS

CM

Lotaya's iPhone LTE

OTHER NETWORKS

DIRECT-O7-FireTV_be6f

Figure 97: CC3100 Wi-Fi module providing Wi-Fi connection to iPhone6 in AP mode

The second test was to configure the Wi-Fi module to work in Station mode. A successful configuration would result in the Wi-Fi module connect to an AP, in this case my personal Wi-Fi Network. At the time of recording this progress a successful connection was not made, however more testing needs to be done to validate the Station mode as not all the options were attempted.

6.6 RS232-to-TTL testing

This interface was removed from our final design, but the testing information was still given. This device was not physically tested at the time of preparing this document. However, the procedure for testing it will be covered here. One simple way to test a serial to TTL device is to do a loopback test. First the TXD and RXD terminals are shorted together with a single jumper wire. The RS232 interface is then connected to the PC. You can verify that the device was recognize by Device Manager. Once the device has been recognized, you can move on to the next phase. That is to download an RS232 Terminal (for example, Termite by CompuPhase). With this software you can use it to send data text to the RS232 terminal. Since the TXD and RXD are shorted, the sent message should be received back and displayed on the RS232 terminal reader if everything is working properly.

6.7 Connecting Wi-Fi module to UCF's network

ESP8266-12E was used as the Wi-Fi module. Since OPAL-RT is connected to UCF's network, our PCB needed to be connected to UCF's WPA2 Enterprise network as well. Multiple tests were done in order to achieve this connection. The tests were implemented by using ESP8266 NodeMCU. As shown in Figure 98, it contains ESP8266-12E chip. A code was developed in order to connect the NodeMCU to UCF's WPA2 Enterprise by following the "ESP8266 Non-OS SDK API Reference" guide. It was then noted that UCF's CA certificate was needed. UCF's IT department was able to provide the CA certificate to us. The CA certificate was then exported as Base-64 encoded and added to the script. With this, the NodeMCU was able to successfully connect to UCF’s WPA2 Enterprise.

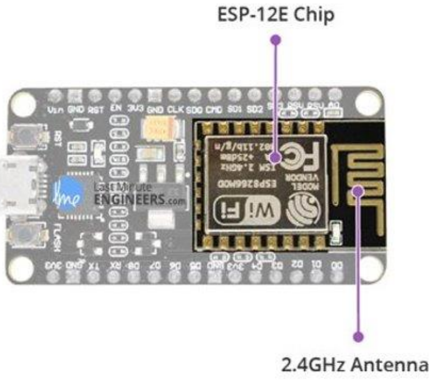

Figure 98: ESP8266 NodeMCU [137]

7. Administrative Content

This section goes over the project milestones as well as the financial aspects of the project. A table was developed to describe the tasks that were completed, the dates by which they were completed, and which team members were responsible for them. In addition, a table listing the price of the parts purchased to complete this project was developed for this section. It is important to note that this project is sponsored by FPL.

7.1 Project Milestones

Table 43 details the project milestones, due dates, and which team members worked on each milestone. This table includes information for both semesters of Senior Design thereby covering the entire project's timeline.

Table 43: Project Milestones

PROJECT MILESTONES SENIOR DESIGN I - FALL 2020 (08/24/2020 - 12/12/2020)		
Task	**Deadline**	**Team Members**
Choose Final Project	09/11	All
Divide & Conquer Document v1.0	09/18	All
Divide & Conquer document v2.0	10/02	All
Research on how to change PV angle	10/02	Hector Chris
Divide & Conquer document v2.0	10/02	All
Start building ePHASORSIM model	10/08	Ivelisse
Research and mock-up user interference	10/30	Christy
Research on how to read PV data with PCB	11/08	Ivelisse Chris
Research how to send data from PCB to Raspberry Pi	11/08	Chris Christy
Research parts selections for all components	11/13	All
Research how to decode the C37.118 inputs at RBP	11/13	Christy
60 page Draft	11/13	All
Research how to connect Raspberry Pi to OPAL-RT	11/20	Ivelisse Christy
Complete remaining research	11/27	All
Complete PCB schematic	11/27	All
Buy and receive parts to begin testing and development	12/8	All
Final Documentation	12/8	All

Senior Design II - SPRING 2021 (01/11/2021 - 05/04/2021)		
Order PCB	1/29	All
Write code for PCB	2/5	Ivelisse Christy
Write code for User Interface/Business Logic	2/26	Christy
Write server code for RBP	2/26	Christy Ivelisse
Test PCB with breadboard	2/26	Ivelisse Chris
Build moving solar panel frame	3/5	Hector
Build Prototype	3/19	All
Test, Redesign, Unit Testing	3/22	All
Final Prototype	4/9	All
Write WAMS algorithm	4/18	Hector
Demo & Showcase Videos	4/18	All
CDR Presentation	4/18	All
Committee Review	4/22	All
Final Report	4/27	All

7.2 Budget and Financing

Table 44 displays the itemized final cost for this project which was fully sponsored by FPL. While the budget did have to be updated as work progressed and was slightly higher than the originally anticipated budget before any parts were purchased, the final amount spent is slightly less than the final proposed budget of $2,447.85.

Table 44: Budget and Financing

Item	Price	Description
OP5600	$0.00	UCF had it available, and allowed us to use it free of charge
Relay	$0.00	UCF had it available, and allowed us to use it free of charge
Solar Panel	$96.73	Renogy 100 Watt Monocrystalline Solar Panel
PV Cables	$23.99	
Inverter	$23.48	Schumacher 1000 Watt Power Inverter
Servo Motor	$41.73	High Torque 20 KG Digital Servo Motor
Stepper Motor	$29.99	
Stepper Motor Driver	$11.52	

Item	Price	Description
Touch Screen	$1678.00	55” multi-touch full HD screen: 4.17 ft width and 2.43 ft height – Power Consumption: 76 W
Raspberry Pi CanaKit	$119.99	Raspberry SC15184 Pi 4 Model B Quad Core 64 Bit 8GB
PCB	$188.82	Wi-Fi Module, Batteries, MCU, ESP8266, etc.
Table Parts	$245.94	Wood, screws, brackets, casters
Fan	$13.81	Will serve as the load of the inverter
Total Cost:	**$2,460.19**	

8. Conclusion

This report has outlined the motivation for implementing the Power Systems Knowledge Hub (PSKH) project. The need for engineers who specialize in power systems is outweighing the number of available engineers, and this project was designed to interest in this area of expertise. It is anticipated that this will lead to an increase in students who major in the power systems track of electrical engineering.

Another motivating factor for this project arises from the need for better reliability in the power grid. As green energy increases the complexity of the grid, the need for betting grid monitoring increases. This project assists students in understanding how injecting solar energy can affect grid distribution systems. Preventing and reducing the duration of power outages is of great importance to society. Healthcare facilities, government facilities, distributors, retailers, manufacturers, and private citizens all count on having electricity readily available as needed, and keeping these demands satisfied is of the utmost importance to power companies.

This document outlines the PSKH project and details how it was implemented. As described in the Project Description in Section 2, PSKH consists of a touch table where users can go to see how changes to the distribution system affect the grid by injecting solar energy into the system. By interacting with the touch table's graphic user interface, users can view, in real time, voltage, current, and power readings coming from a solar panel outside. They can also use the touch table to change the angle of the remote solar panel to see how the power fluctuates due to the changes. Users can also access educational materials about power systems from the touch table's user interface. Section 2 also contains the Requirements and Specifications for the PSKH as well as the House of Quality.

Section 3 contains the research into the technologies and parts needed to build PSKH. Here the reader can find descriptive comparisons into these different technologies and tables comparing potential parts to provide insight into why each part was selected. This section delves into the parts that were used to implement the PCB, the touch table, and automated solar panel frame. It also describes the OPAL-RT Real-Time Simulator that allows simulations of power systems using ePHASORSIM.

Section 4 discusses the standards and constraints that were considered during the design and implementation of the project.

Section 5 contains detailed information on the hardware and software designs of the project. Communication between the different components of the project, GUI design, database selection, and the event source location algorithms needed to implement WAMS are all covered in this section. The section also covers the decoding of the IEEE C37.118 data.

Section 6 discusses the project prototype testing plan. It describes the unit tests that have been done and the testing of the functionality of the PCB components. It also discusses testing of the communication between the all the project components are covered. The ePHASORSIM model, communication of the model parameters and outputs, decoding of the IEEE C37.118, and relaying that data to the WAMS algorithm are also important unit tests covered here.

Section 7 covers the administrative content of the project which includes the timeline that was followed for project milestones and the budget. Florida Power and Light sponsored this project and paid for all items shown in the budget. It should also be noted that this budget reflects the price that was paid for parts including any discounts. It doesn’t include items that were donated or resources that were able to be used for free. The previous sections of the document discuss the full prices of all the components so that readers may evaluate the cost of reproducing this project.

This document contains the detailed plan that was followed to build the PSKH project including technology research, parts selection, software and hardware implementations, and how unit testing was conducted. This project successfully achieved the two primary objectives of promoting interest in power systems related engineering and emphasizing the importance of increasing situational awareness in the distribution grid as it becomes more complex with the increase in green energy. The objectives were also achieved by reaching the advanced goal of including a real-time distribution simulation in the interactive touch table utilizing OPALRT. The project has been described in detail including the background and motivation for selecting it for implementation. A complete guide is contained within, and this concludes the proposal documentation.

Appendices

Appendix A: References

[1] *Jain, Alok & Bhullar, Suman. (2018). Micro-phasor Measurement Units (µPMUs) and Its Applications in Smart Distribution Systems. 10.1007/978-981-10-8249-8_7.* OPAL-RT TECHNOLOGIES Inc https://www.opal-rt.com/company-profile/.

[2] "Real Time Simulation | Real Time Consultants | OPAL-RT." *OPAL*, www.opal-rt.com/company-profile/.

[3] "DOE Energise Project." *DOE Energise Project – Dr. Zhihua Qu*, www.ece.ucf.edu/~qu/doe-energise-project/.

[4] "Real Time Digital Simulator | Real Time System | OP5600." *OPAL*, www.opal-rt.com/simulator-platform-op5600/.

[5] "MATLAB." *MathWorks*, www.mathworks.com/products/matlab.html.

[6] "Simulink." *Simulink Documentation*, www.mathworks.com/help/simulink/index.html?s_tid=srchtitle.

[7] "Application-Oriented Course, OP-204 Electro-Mechanical RT Simulation with ePHASORSIM*," OPAL-RT Technologies*, 2, 10/18/20

[8] *Large-Scale Power System Real-Time Simulation - OPAL-RT*. www.opal-rt.com/wp- content/uploads/2019/04/one-pager-ephasorsim_web.pdf.

[9] "100 Watt 12 Volt Monocrystalline Solar Panel (Compact Design)." *Renogy United States*, www.renogy.com/100-watt-12-volt-monocrystalline-solar-panel-compact-design/.

[10] "NewPowa 100W 12V Polycrystalline Solar Panel." *Newpowa*, www.newpowa.com/products/newpowa-100w-12v-poly-high-efficiency-solar-panel.

[11] "Solar Panel Efficiency - Understanding STC and PTC Ratings." *Intermountain Wind & Solar*, 14 July 2017, www.intermtnwindandsolar.com/solar-panel-efficiency-understanding-stc-and-ptc-ratings/.

[12] -, Solar Mag., et al. "[Comparison] Monocrystalline vs Polycrystalline Solar Panels." *Solar Magazine*, 5 Nov. 2020, solarmagazine.com/solar-panels/monocrystalline-vs-polycrystalline-solar-panels/.

[13] “700W 12V Pure Sine Wave Inverter.” *Renogy United States*, www.renogy.com/700w-12v-pure-sine-wave-inverter/.

[14] "IEEE Standard for Synchrophasor Measurements for Power Systems," in IEEE Std C37.118.1-2011 (Revision of IEEE Std C37.118-2005) , vol., no., pp.1-61, 28 Dec. 2011, doi: 10.1109/IEEESTD.2011.6111219.

[15] "IEEE Standard for Synchrophasor Data Transfer for Power Systems," in IEEE Std C37.118.2-2011 (Revision of IEEE Std C37.118-2005) , vol., no., pp.1-53, 28 Dec. 2011, doi: 10.1109/IEEESTD.2011.6111222.

[16] GridProtectionAlliance. “Release PMU Connection Tester v4.5.12 · GridProtectionAlliance/PMUConnectionTester.” *GitHub*, github.com/GridProtectionAlliance/PMUConnectionTester/releases/tag/v4.5.12.

[17] “Grid-Tied, Off-Grid, and Hybrid Solar Systems.” *Solar Reviews*, 15 July 2019, www.solarreviews.com/blog/grid-tied-off-grid-and-hybrid-solar-systems.

[18] “Schumacher 1000 Watt Power Inverter - Converts 12V Battery Power to 110V House Power PC1000.” Advance Auto Parts, shop.advanceautoparts.com/p/schumacher-1000-watt-power-inverter-converts-12v-battery-power-to-110v-house-power-pc1000/11021653-p?product_channel=local.

[19] Shumacher Electric. "PC-1000, -C-1500 Power Converter." *Owners Manual* (n.d.).

[20] SEL. (n.d.). Optimize Protection, Automation, and Breaker Control. *SEL-351-5, -6, -7 Protection System.*

[21] SEL. (n.d.). Instruction Manual. *SEL-351-5, -6, -7 Protection System.*

[22] “RT-LAB Quick Start Guide.” *Blobtestweb.opal-Rt.com*, blobtestweb.opal-rt.com/medias/L00161_0582.pdf.

[23] “Buy the Philips Signage Solutions Multi-Touch Display 55BDL4051T/00 Multi-Touch Display.” *Philips*, 2020, www.usa.philips.com/p-p/55BDL4051T_00/signage-solutions-multi-touch-display.

[24] Cheshire, S., and M Krochmal. “Multicast DNS.” *IETF Tools*, Internet Engineering Task Force, Feb. 2013, tools.ietf.org/html/rfc6762.

[25] “Deploying Gunicorn.” *Deploying Gunicorn - Gunicorn 20.0.4 Documentation*, 2020, docs.gunicorn.org/en/latest/deploy.html.

[26] Grice, Amy, et al. “Today’s Power Engineering Shortage – An Alarming Problem.” *Cdn.selinc.com*, Tacoma Price, Schwietzer Engineering Laboratories, Inc., Jan. 2008, cdn.selinc.com/assets/Literature/Publications/Technical Papers/6303_TodaysEngineeringShortage_JP_20071026_Web.pdf?v=20151202-215825.

[27] “Gunicorn 'Green Unicorn' Is a Python WSGI HTTP Server for UNIX. It's a Pre-Fork Worker Model. The Gunicorn Server Is Broadly Compatible with Various Web Frameworks, Simply Implemented, Light on Server Resources, and Fairly Speedy.” *Gunicorn*, 2020, gunicorn.org/.

[28] “Home.” *Arduino*, www.arduino.cc/.

[29] “IEEE C37.118 Protocol.” *Typhoon HIL Documentation*, Typhoon HIL, Inc., 2020, www.typhoon-hil.com/documentation/typhoon-hil-software-manual/References/c37_118_protocol.html?hl=c37#c37_118_protocol.dita__table_z51_135_dkb.

[30] Mitchell, Robin. “Which Programming Language Should I Choose? Graphics and GUIs: Custom.” *Maker Pro*, Maker Pro, 11 Nov. 2020, maker.pro/custom/tutorial/which-programming-language-should-i-choose-graphics-and-guis.

[31] *Multicast DNS*, 2020, www.multicastdns.org/.

[32] “Philips Commercial Displays 55BDL4051T 55’ T-Line Android-Powered 10-Point Touch FHD Commercial Display.” *Full Compass Systems*, 2020, www.fullcompass.com/prod/516524-philips-commercial-displays-55bdl4051t-55-t-line-android-powered-10-point-touch-fhd-commercial-display?dfw_tracker=36058-516524&gclid=Cj0KCQjw7ZL6BRCmARIsAH6XFDLaU5SPZSEYOEkyQghCeiSpLJ_VIvqk31ua67MkTEwrF3gp1zdLYqoaAjFPEALw_wcB.

[33] *Portenta H7*, Arduino, 2020, store.arduino.cc/usa/portenta-h7.

[34] “Raspberry Pi 4 2GB.” *CanaKit*, CanaKit Corporation, 2020, www.canakit.com/raspberry-pi-4-2gb.html?cid=usd&src=raspberrypi.

[35] “RT-LAB Raspberry PI Python UDP.” *Real-Time HIL RCP FPGA Knowledge Base │ OPAL-RT*, OPAL-RT Technologies, 16 Mar. 2020, www.opal-rt.com/support-knowledge-base/?article=AA-01661.

[36] Sarig, Matan. *MongoDB vs MySQL: the Differences Explained*, Panoply, 13 Nov. 2019, blog.panoply.io/mongodb-and-mysql.

[37] "Teach, Learn, and Make with Raspberry Pi." *Raspberry Pi*, Raspberry Pi Foundation, 2020, www.raspberrypi.org/.

[38] *Wireshark User's Guide*, Wireshark, 2020, www.wireshark.org/docs/wsug_html/.

[41] Nijim, Sharif. "Learning Amazon Lightsail." *Amazon*, Lynda.com., 2020, aws.amazon.com/lightsail/.

[42] "LAMP Stack." *Google Cloud Platform*, Google, 2020, console.cloud.google.com/marketplace/product/click-to-deploy-images/lamp?utm_source=google&utm_medium=cpc&utm_campaign=na-US-all-en-dr-bkws-all-all-trial-e-dr-1009135&utm_content=text-ad-none-any-DEV_c-CRE_345746074699-ADGP_Hybrid | AW SEM | BKWS | US | en | EXA ~ Marketplace Partners ~ Lamp Stack ~ google cloud lamp stack-KWID_43700043558206419-kwd-315498383215&utm_term=KW_google cloud lamp stack-ST_google cloud lamp stack&gclid=CjwKCAiA17P9BRB2EiwAMvwNyOS4CKJWPSKPNb1JY6Li_MiJ6WshZCC-9YeuB3G6cW4AFmXH2YIN6BoCLrUQAvD_BwE.

[39] Serial VS Parallel Interface, (nd), Retrieved 20 Oct. 2020: https://www.newhavendisplay.com/app_notes/parallel-serial.pdf

[40] Woolley, W., *Bluetooth Core Specification: Version 5.2 Feature Overview*, 6 Jan. 2020

[43] Campbell, S., (nd), *Circuit Basics: Basics I2C Communication Protocol:* Retrieved November 12, 2020: https://www.circuitbasics.com/basics-of-the-i2c-communication-protocol

[44] Campbell, S., (nd), *Circuit Basics: Basics of UART Communication:* Retrieved November 12, 2020: https://www.circuitbasics.com/basics-uart-communication/

[45] Campbell, S., (nd), *Circuit Basics: Basics of the SPI Communication Protocol:* Retrieved November 12, 2020: https://www.circuitbasics.com/basics-of-the-spi-communication-protocol

[46] "IEEE C37.118.1-2011 - IEEE Standard for Synchrophasor Measurements for Power Systems." *IEEE SA - The IEEE Standards Association - Home*, standards.ieee.org/standard/C37_118_1-2011.html.

[47] "Eastern Interconnection Frequency Oscillation Observed." *Min H. Kao Department of Electrical Engineering and Computer Science*, 17 Jan. 2019, www.eecs.utk.edu/eastern-interconnection-frequency-oscillation-observed/.

[48] DISPLAY 4k - Touch International. touchinternational.com/wp-content/uploads/2020/07/Spec-89-OFM-4K-55-001.pdf.

[49] Hall, Reggie, et al. “Whitepapers.” *Solar Power World*, www.solarpowerworldonline.com/category/special-features/white-paper/.

[50] 802.11ac: The Fifth Generation of Wi-Fi. www.cisco.com/c/dam/en/us/products/collateral/wireless/aironet-3600-series/white-paper-c11-713103.pdf.

[51] Transmission Planning Paper. EISPC, pubs.naruc.org/pub.cfm?id=53A151F2-2354-D714-519F-53E0785A966A.

[52] Guide: *which ESP8266 module to choose, power supply, how to program it in C++ with Arduino IDE*, MicroPython, ESP: Retrieved 12 Nov. 2020: https://diyprojects.io/guide-which-esp8266-module-choose-power-supply-how-to-program-it/#.X5hVpy9h2J8

[53] Bindu, B., (nd). Student Companion Electronics: *PIC Microcontroller Communication with RS232 Serial Bus – Mikroc*: Retrieved 12 Nov. 2020: https://www.studentcompanion.co.za/pic-microcontroller-communication-with-rs232-serial-bus-mikroc/

[54] Knowledge Center, (July 8, 2020). *Web Server and Application Server | Explained:* Retrieved November 12, 2020: https://www.youtube.com/watch?v=thJSev60yfg

[55] “History of Solar Energy: Who Invented Solar Panels?” *History of Solar Energy: Who Invented Solar Panels? | Vivint Solar Learning Center*, www.vivintsolar.com/learning-center/history-of-solar-energy.

[56] Hymel, Shawn, (nd). *Alternating Current (AC) vs. Direct Current (DC)*, learn.sparkfun.com/tutorials/alternating-current-ac-vs-direct-current-dc/all.

[57] Earl, Bill. “All About Stepper Motors.” *Adafruit Learning System,* learn.adafruit.com/all-about-stepper-motors.

[58] Gastreich, Wally. “What Is a Servo Motor and How It Works?” *RealPars*, 26 Jan. 2020, realpars.com/servo-motor/.

[59] Gastreich, Wally. “Stepper Motors Advantages and Disadvantages.” *RealPars*, 23 Sept. 2020, realpars.com/stepper-motors-advantages/.

[60] “What Is a Gyroscope.” *Gyroscope*, learn.sparkfun.com/tutorials/gyroscope/all.

[61] Rees, Caroline. “Selecting an Inertial Measurement Unit (IMU) for UAV Applications.” *Unmanned Systems Technology,*

www.unmannedsystemstechnology.com/feature/selecting-an-inertial-measurement-unit-imu-for-uav-applications/.

[62] M. Farajollahi, A. Shahsavari, E. M. Stewart and H. Mohsenian-Rad, "Locating the Source of Events in Power Distribution Systems Using Micro-PMU Data," in IEEE Transactions on Power Systems, vol. 33, no. 6, pp. 6343-6354, Nov. 2018, doi: 10.1109/TPWRS.2018.2832126.

[63] F. F. Judd and P. M. Chirlian, "The Application of the Compensation Theorem in the Proof of Thevenin's and Norton's Theorems," in IEEE Transactions on Education, vol. 13, no. 2, pp. 87-88, Aug. 1970, doi: 10.1109/TE.1970.4320572.

[64] M. Jamei, A. Scaglione, C. Roberts, E. Stewart, S. Peisert, C. McParland,and A. McEachern, "Anomaly detection using optimally-placedμpmusensors in distribution grids,"IEEE Trans. on Power Systems, Oct. 2017.

[65] Mark, I., *Montrose Printed Circuit Board Design Techniques for EMC Compliance* http://citeseerx.ist.psu.edu/viewdoc/download?doi=10.1.1.454.5885&rep=rep1&type=pdf

[66] Bob O'Hara; Al Petrick, "IEEE 802.11g higher data rates in 2.4 GHz frequency band," in *IEEE 802.11 Handbook: A Designer's Companion*, IEEE, 2005, doi: 10.1109/9781118098851.ch14.

[67] K. P. Schneider, B. A. Mather, B. C. Pal, C. W. Ten, G. J. Shirek, H. Zhu, J. C. Fuller, J. L. R. Pereira, L. F. Ochoa, L. R. de Araujo, R. C. Dugan, S. Matthias, S. Paudyal, T. E. McDermott, and W Kersting, "Analytic Considerations and Design Basis for the IEEE Distribution Test Feeders," IEEE Transactions on Power Systems, 2017.

[68] W. H. Kersting, "Radial distribution test feeders," 2001 IEEE Power Engineering Society Winter Meeting. Conference Proceedings (Cat. No.01CH37194), Columbus, OH, USA, 2001, doi: 10.1109/PESW.2001.916993.

[69] IEEE Power Engineering Society - Distribution System Analysis Subcommittee. "IEEE 4 Node Test Feeder." n.d. Document.

[70] IEEE Power Engineering Society - Distribution System Analysis Subcommittee. "IEEE 123 Node Test Feeder." n.d. Document.

[71] "Circuit Analysis of 3 Phase System - Balanced Condition." *Circuit Globe*, 3 July 2020, circuitglobe.com/circuit-analysis-of-3-phase-system-balanced-condition.html.

[72] "OP5700 - Hardware Products Documentation - Wiki OPAL." *RT*, wiki.opal-rt.com/display/HDGD/OP5700.

[73] “Home.” Samsung PM49H 49 Inch Smart Signage Touch Screen Display, 2020, www.touchwindow.com/c/SamsungPM49H.html.

[74] LG 49TA3E: 49” Class TA3E Series - Effective Customer ... 2020, www.lg.com/us/business/digital-signage/lg-49TA3E.

[75] “LG Electronics TA3E Series Digital Signage - 43.” Tigerdirect, 2020, www.tigerdirect.com/applications/SearchTools/item-details.asp?EdpNo=6000423&CatId=1449.

[76] “43’ Touch Screen Digital Table, 10pt PCAP Touch, 450cd/m2 Brightness, Wheels - Black.” Displays2go, 2020, www.displays2go.com/P-40694/Interactive-Touch-Table-Multi-Point-Touchscreen-Group-Collaboration?st=Search&sid=touch table.

[77] “SSH (Secure Shell).” SSH (Secure Shell) - Raspberry Pi Documentation, 2020, www.raspberrypi.org/documentation/remote-access/ssh/.

[78] “How to Give Your Raspberry Pi a Static IP Address - UPDATE.” The Pi Hut, 16 July 2014, thepihut.com/blogs/raspberry-pi-tutorials/how-to-give-your-raspberry-pi-a-static-ip-address-update.

[79] Application Note 83 Fundamentals of RS–232 Serial ... Dallas Semiconductor, 9 Mar. 1998, ecee.colorado.edu/~mcclurel/dan83.pdf.

[80] Analog | Embedded Processing | Semiconductor Company | TI.com. 2020, www.ti.com/lit/an/slla037a/slla037a.pdf.

[81] “CTA 861-G-2016 (ANSI): A DTV Profile For Uncompressed High Speed Digital Interfaces.” ANSI Webstore, 2016, webstore.ansi.org/standards/ansi/cta8612016ansi.

[82] “HDMI Connectors - Type A, B, C, D, E (Mini-HDMI & Micro-HDMI).” Electronics Notes, 2020, www.electronics-notes.com/articles/audio-video/hdmi/hdmi-connectors.php.

[83] “HDMI Versions: 1.1, 1.2, 1.3, 1.4, 2, 2.1 - Differences & Compatibility.” Electronics Notes, 2020, www.electronics-notes.com/articles/audio-video/hdmi/hdmi-versions.php.

[84] “Home.” USB, 2020, www.usb.org/.

[85] EDUCATION: USB 3.0 SUPER SPEEDS. USR- A Division of Unicom Global, 2020, www.usr.com/education/usb3-peripherals.

[86] “Http.server - HTTP Servers.” Http.server - HTTP Servers - Python 3.9.1rc1 Documentation, 2020, docs.python.org/3/library/http.server.html.

[87] Web Applications & Frameworks - The Hitchhiker's Guide to Python, 2020, docs.python-guide.org/scenarios/web/.

[88] “Waitress.” Waitress - Waitress 1.4.4 Documentation, 2020, docs.pylonsproject.org/projects/waitress/en/stable/.

[89] “Python -m SimpleHTTPServer.” Python -m SimpleHTTPServer - Raspberry Pi Forums, Raspberry Pi Foundation, Mar. 2015, www.raspberrypi.org/forums/viewtopic.php?t=104453.

[90] Mohammad Shahraeini and Mohammad Hossein Javidi (March 7th 2012). Wide Area Measurement Systems, Advanced Topics in Measurements, Md. Zahurul Haq, IntechOpen, DOI: 10.5772/35466. Available from: https://www.intechopen.com/books/advanced-topics-in-measurements/wide-area-measurement-systems

[91] “Lasko 16’ Oscillating Pedestal Stand 3-Speed Fan, Model S16500, Black.” Walmart.com, 3 Sept. 2020, www.walmart.com/ip/Lasko-16-Oscillating-Pedestal-Stand-3-Speed-Fan-Model-S16500-Black/42379869.

[92] “Pelonis 16’ Oscillating 3-Speed Pedestal Fan, FS40-19MB, Black.” Walmart.com, 25 Aug. 2020, www.walmart.com/ip/Pelonis-16-Oscillating-3-Speed-Pedestal-Fan-FS40-19MB-Black/284466015.

[93] “Lasko 20’ Box 3-Speed Fan, Model B20200, White.” Walmart.com, 25 Aug. 2020, www.walmart.com/ip/lasko-20-box-3-speed-fan-model-b20200-white/42388499.

[94] N. Davis, The History and Basics of IPC Standards: The Official Standards for PCBs, Retrieved 11/22/2020: https://www.allaboutcircuits.com/news/ipc-standards-the-official-standards-for-pcbs/

[95] VSE, (n.d.). A Guide to IPC Assembly Standards for PCB Manufacturing. Retrieved 11/22/2020: https://www.vse.com/blog/2019/09/24/a-guide-to-ipc-assembly-standards-for-pcb-manufacturing/

[96] Shaw, K., (3/23/2020), 802.11x: Wi-Fi standards and speeds explained, Retrieved 11/22/2020: https://www.networkworld.com/article/3238664/80211x-wi-fi-standards-and-speeds-explained.html

[97] O’Hara, B., (01/10/2005), Why Standards Are important for Wireless Security, Retrieved 11/22/2020: https://www.computerworld.com/article/2556747/why-standards-are-important-for-wireless-security.html

[98] Guide to IPC Standards for PCBS, (4/1/2019), Retrieved 11/23/2020: https://www.mclpcb.com/ipc-standards-for-pcbs/

[99] Energizer Product Datasheet, (n.d.), Retrieved 11/24/2020: https://data.energizer.com/pdfs/ind-6lr61pl_eu.pdf

[100] Duracell datasheet, (n.d.), Retrieved 11/24/2020: https://www.duracell.com/wp-content/uploads/2016/03/QU1604_US_UL1.pdf

[101] Duracell datasheet, (n.d.) https://www.duracell.com/wp-content/uploads/2016/03/OP1500_US_OP1.pdf

[102] Energizer Product Datasheet, (n.d.), Retrieved 11/24/2020: https://data.energizer.com/pdfs/alk-power-aa.pdf

[103] Tenergy, Ternergy Alkaline Batteries, (n.d.), Retrieved 11/24/2020: https://power.tenergy.com/1-box-12pcs-tenergy-9v-size-6lr61-alkaline-batteries/

[104] Barrett, S., Pack, Daniel., *Microcontroller Programming and Interfacing with Texas Instruments MSP430FR2433 and MSP430FR5994 - Part I, 2nd Ed.* Morgan & Claypool Publishers series Synthesis Lectures on Digital Circuits and Systems, 2019

[105] Servo Motor Controllers using MSP430 devices, (n.d.), Retrieved 11/24/2020 https://www.ti.com/lit/an/slaa784/slaa784.pdf?ts=1606318095665&ref_url=https%253A%252F%252Fwww.google.com%252F

[106] Reiter, G., (1/2019), Texas Instruments: A primer to Wi-Fi provisioning for IoT applications. Retrieved 2/27/2020: https://www.ti.com/lit/wp/swry011a/swry011a.pdf?ts=1606061356263&ref_url=https%253A%252F%252Fwww.ti.com%252Fproduct%252FCC3100

[107] Fernandez, A., et al, (2/15/2019), Connect: Wi-Fi Provisioning, https://www.youtube.com/watch?v=0Mj0qsppUEA

[108] Choudhary, Pramit. “Introduction to Anomaly Detection.” *Oracle Data Science*, blogs.oracle.com/datascience/introduction-to-anomaly-detection.

[109] Jamei, M., Scaglione, A., Roberts, C., Stewart, E., Peisert, S., McParland, C., & McEachern, A. (2018). Anomaly detection using optimally placed µPMU sensors in distribution grids. IEEE Transactions on Power Systems, 33(4), 3611-3623. http://dx.doi.org/10.1109/TPWRS.2017.2764882 Retrieved from https://escholarship.org/uc/item/3zf1f06g

[110] Meneu, Jean Jacques, and Arrow Electronics. “Power Triangle: Real Power vs Apparent Power vs Reactive Power.” Arrow.com, 28 May 2019, www.arrow.com/en/research-and-events/articles/real-vs-reactive-power.

[111] Ross, Brett, et al. PHASOR-HARMONIC ANALYSIS FOR TRANSFORMER CONDITION ASSESSMENT AND TELEMETRY. www.eecs.ucf.edu/seniordesign/sp2019su2019/g06/assets/docs/Senior.Design1.paper.pdf.

[112] “Ethernet Tutorial – Part I: Networking Basics.” Lantronix, www.lantronix.com/resources/networking-tutorials/ethernet-tutorial-networking-basics/.

[113] Honsberg, Christiana, and Stuart Bowden. “The Sun's Position.” PVEducation, www.pveducation.org/pvcdrom/properties-of-sunlight/the-suns-position.

[114] *Power & Beyond*, 2020, www.power-and-beyond.com/.

[115] “U.S. Energy Information Administration - EIA - Independent Statistics and Analysis.” *Electricity in the U.S. - U.S. Energy Information Administration (EIA)*, 2020, www.eia.gov/energyexplained/electricity/electricity-in-the-us.php#:~:text=Most electricity is generated with,wind turbines, and solar photovoltaics.

[116] “Welcome to Python.org.” *Python.org*, 2020, www.python.org/.

[117] “Python Software Foundation.” *Python.org*, 2020, www.python.org/psf-landing/.

[118] “PEP 8 -- Style Guide for Python Code.” *Python.org*, 2020, www.python.org/dev/peps/pep-0008/.

[119] “NASA-STD-8739.2 (W/ CHANGE 2), NASA TECHNICAL STANDARD: WORKMANSHIP STANDARD FOR SURFACE MOUNT TECHNOLOGY (SMT) (29 MAR 2011).” *EverySpec Standards*, NASA, everyspec.com/NASA/NASA-NASA-STD/NASA-STD-8739x2_CHG-2_33215/.

[120] SEL. (n.d.). SEL-787 Transformer Protection Relay

[121] SEL. (n.d.). Instruction Manual. *SEL-787 Relay Transformer Protection Relay*

[122] RENOGY. *Installation Guide for Photovoltaic PV mpdules*. https://m.media-amazon.com/images/I/91JkFF2KKEL.pdf

[123] PranathiBaduguCheck out this Author's contributed articles., et al. “Software Engineering: Architectural Design.” *GeeksforGeeks*, 23 July 2018, www.geeksforgeeks.org/software-engineering-architectural-design/.

[124] anonymous007Check out this Author's contributed articles., et al. “Software Engineering: Software Design Process.” *GeeksforGeeks*, 24 May 2019, www.geeksforgeeks.org/software-engineering-software-design-process/.

[125] “Principles of Detailed Design.” *Software Engineering Design: Theory and Practice* , people.utm.my/noraini/files/2016/09/Chapter-5-Detailed-Design-Principles.pdf.

[126] Artmann, Casimir. “Example of a High Level Design.” *Disruptive Architecture*, Disruptive Architecture, 6 Sept. 2016, disruptivearchitecture.info/blog/2016/9/6/example-of-a-high-level-design.

[127] “Software Design Basics.” *Tutorialspoint*, www.tutorialspoint.com/software_engineering/software_design_basics.htm.

[128] “MSP Bootloader (BSL) Overview.” *TI Training*, 9 July 2020, training.ti.com/msp-bootloader-bsl-overview.

[129] Jones, D., (June, 29th 2004), PCB Design Tutorial, Revision A, Retrieved 12/5/2020: http://alternatezone.com/electronics/files/PCBDesignTutorialRevA.pdf

[130] PCBWay, (December, 30, 2013), Retrieved 12/5/2020: https://www.pcbway.com/blog/Engineering_Technical/How_to_Select_high_quality_PCB_Suppliers.html

[131] Chon, N., et al, (n.d.), Block Box, A Porch Package Protection System, Retrieved 12/5/2020: http://www.eecs.ucf.edu/seniordesign/sp2019su2019/g03/papers/BlackBoxSD2Report.pdf

[132] Foster KR. Is Wi-Fi a Health Threat in Schools? Sorting Fact from Fiction. Education Next. 2019;19(3):28-36. Accessed December 8, 2020. https://search.ebscohost.com/login.aspx?direct=true&db=eric&AN=EJ1218378&site=eds-live&scope=site

[133] Andrzej Magiera, Jolanta Solecka. Radiofrequency electromagnetic radiation from Wi-fi and its effects on human health, in particular children and adolescents. Review. Roczniki Panstwowego Zakladu Higieny. 2020;71(3):251-259. doi:10.32394/rpzh.2020.0125

[134] “Application of Single, Dual and Multi-Touch User Interfaces on Projected Capacitive Touch Screens.” *New Vision Display*, 20 Aug. 2019, newvisiondisplay.com/application-of-various-user-interfaces-on-projected-capacitive-touch-screens/.

[135] Inc., Apple. *Adaptivity and Layout - Visual Design - IOS - Human Interface Guidelines - Apple Developer*, developer.apple.com/design/human-interface-guidelines/ios/visual-design/adaptivity-and-layout/.

[136] LIsah01, et al. “Auto Drive 12 Volt 6’ Car Clip-On or Dash Mount Fan, Black.” *Walmart.com*, 14 July 2020, www.walmart.com/ip/Auto-Drive-12-Volt-6-Car-Clip-On-or-Dash-Mount-Fan-Black/52523639?wmlspartner=wmtlabs&selectedSellerId=0&wl13=1220&adid=22222222420449455996&wl0=&wl1=g&wl2=c&wl3=501107745824&wl4=pla-293946777986&wl5=9011785&wl6=&wl7=&wl8=&wl9=pla&wl10=8175035&wl11=local&wl12=52523639&veh=sem_LIA&gclid=CjwKCAjwmv-DBhAMEiwA7xYrd_XWnKY2BF2O4U6F9xbJ5hlkXdOBaZSaRHVJefXZxxaV1cgrjVfHlBoCTQEQAvD_BwE&gclsrc=aw.ds.

[137] “Insight Into ESP8266 NodeMCU Features & Using It With Arduino IDE.” *Https://Lastminuteengineers.com/*, lastminuteengineers.com/esp8266-nodemcu-arduino-tutorial/.

[138] Texas Instrument, TIDUCM3, *Voltage, Current, and Temperature Monitoring for Solar Module Level Power Electronics*

[139] *TUTORIAL: How to wire up and flash the ESP8266 12E properly! It works! (Arduino - Getting Started);* https://www.youtube.com/watch?v=YCeWpg_SqI8

[140] NodeMCU-DEVKIT-V1.0, https://github.com/nodemcu/nodemcu-devkit-v1.0/blob/master/NODEMCU_DEVKIT_V1.0.PDF

Appendix B: Email Requests

- OPAL-RT

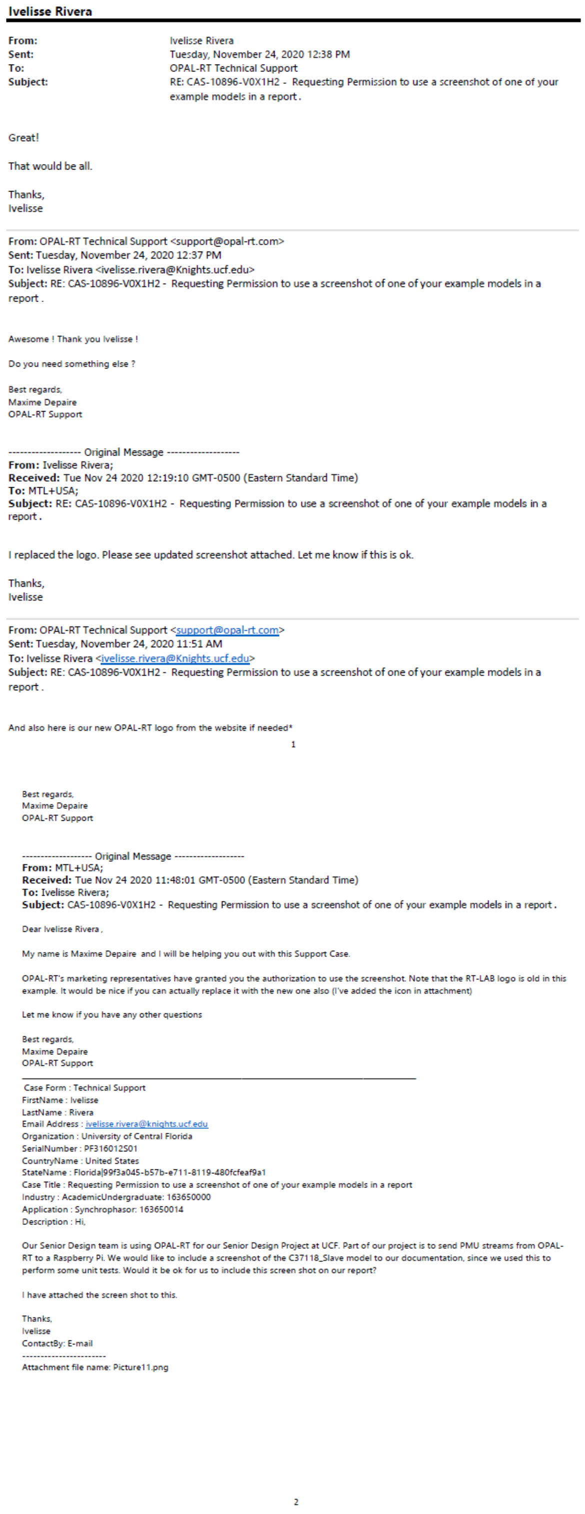

Ivelisse Rivera

From: Ivelisse Rivera
Sent: Tuesday, November 24, 2020 12:38 PM
To: OPAL-RT Technical Support
Subject: RE: CAS-10896-V0X1H2 - Requesting Permission to use a screenshot of one of your example models in a report .

Great!

That would be all.

Thanks,
Ivelisse

From: OPAL-RT Technical Support <support@opal-rt.com>
Sent: Tuesday, November 24, 2020 12:37 PM
To: Ivelisse Rivera <ivelisse.rivera@Knights.ucf.edu>
Subject: RE: CAS-10896-V0X1H2 - Requesting Permission to use a screenshot of one of your example models in a report .

Awesome ! Thank you Ivelisse !

Do you need something else ?

Best regards,
Maxime Depaire
OPAL-RT Support

------------------- Original Message -------------------
From: Ivelisse Rivera;
Received: Tue Nov 24 2020 12:19:10 GMT-0500 (Eastern Standard Time)
To: MTL+USA;
Subject: RE: CAS-10896-V0X1H2 - Requesting Permission to use a screenshot of one of your example models in a report **.**

I replaced the logo. Please see updated screenshot attached. Let me know if this is ok.

Thanks,
Ivelisse

From: OPAL-RT Technical Support <support@opal-rt.com>
Sent: Tuesday, November 24, 2020 11:51 AM
To: Ivelisse Rivera <ivelisse.rivera@Knights.ucf.edu>
Subject: RE: CAS-10896-V0X1H2 - Requesting Permission to use a screenshot of one of your example models in a report .

And also here is our new OPAL-RT logo from the website if needed*

Best regards,
Maxime Depaire
OPAL-RT Support

------------------- Original Message -------------------
From: MTL+USA;
Received: Tue Nov 24 2020 11:48:01 GMT-0500 (Eastern Standard Time)
To: Ivelisse Rivera;
Subject: CAS-10896-V0X1H2 - Requesting Permission to use a screenshot of one of your example models in a report **.**

Dear Ivelisse Rivera ,

My name is Maxime Depaire and I will be helping you out with this Support Case.

OPAL-RT's marketing representatives have granted you the authorization to use the screenshot. Note that the RT-LAB logo is old in this example. It would be nice if you can actually replace it with the new one also (I've added the icon in attachment)

Let me know if you have any other questions

Best regards,
Maxime Depaire
OPAL-RT Support

Case Form : Technical Support
FirstName : Ivelisse
LastName : Rivera
Email Address : ivelisse.rivera@knights.ucf.edu
Organization : University of Central Florida
SerialNumber : PF316012S01
CountryName : United States
StateName : Florida|99f3a045-b57b-e711-8119-480fcfeaf9a1
Case Title : Requesting Permission to use a screenshot of one of your example models in a report
Industry : AcademicUndergraduate: 163650000
Application : Synchrophasor: 163650014
Description : Hi,

Our Senior Design team is using OPAL-RT for our Senior Design Project at UCF. Part of our project is to send PMU streams from OPAL-RT to a Raspberry Pi. We would like to include a screenshot of the C37118_Slave model to our documentation, since we used this to perform some unit tests. Would it be ok for us to include this screen shot on our report?

I have attached the screen shot to this.

Thanks,
Ivelisse
ContactBy: E-mail

Attachment file name: Picture11.png

- Sunrom Electronics

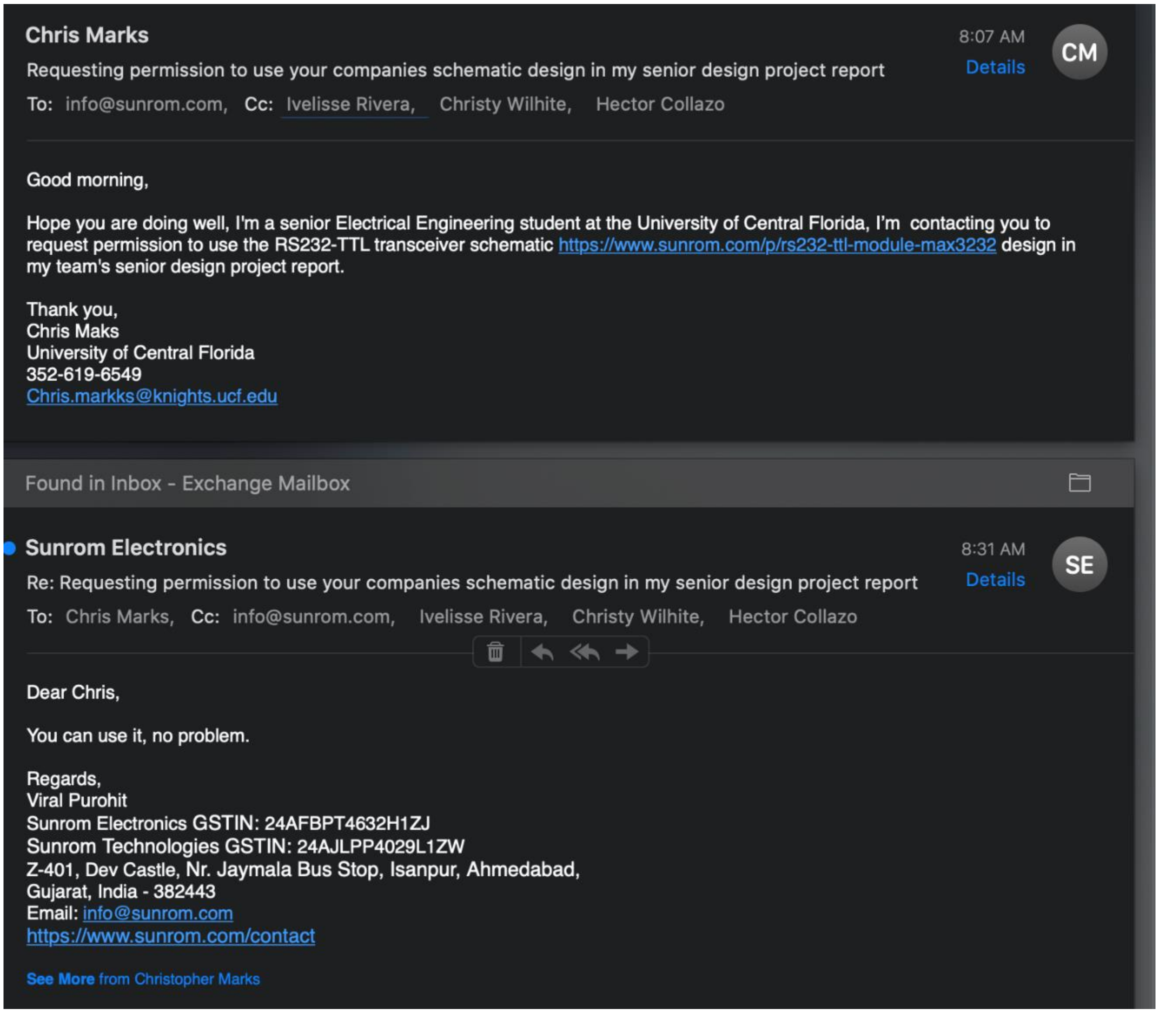

Chris Marks

Requesting permission to use your companies schematic design in my senior design project report

To: info@sunrom.com, Cc: Ivelisse Rivera, Christy Wilhite, Hector Collazo

Good morning,

Hope you are doing well, I'm a senior Electrical Engineering student at the University of Central Florida, I'm contacting you to request permission to use the RS232-TTL transceiver schematic https://www.sunrom.com/p/rs232-ttl-module-max3232 design in my team's senior design project report.

Thank you,
Chris Maks
University of Central Florida
352-619-6549
Chris.markks@knights.ucf.edu

Sunrom Electronics

Re: Requesting permission to use your companies schematic design in my senior design project report

To: Chris Marks, Cc: info@sunrom.com, Ivelisse Rivera, Christy Wilhite, Hector Collazo

Dear Chris,

You can use it, no problem.

Regards,
Viral Purohit
Sunrom Electronics GSTIN: 24AFBPT4632H1ZJ
Sunrom Technologies GSTIN: 24AJLPP4029L1ZW
Z-401, Dev Castle, Nr. Jaymala Bus Stop, Isanpur, Ahmedabad,
Gujarat, India - 382443
Email: info@sunrom.com
https://www.sunrom.com/contact